

## ***Supporting Information***

### **Bis(4-dialkylaminophenyl)heteroaryl amino donor chromophores exhibiting exceptional hyperpolarizabilities**

Huajun Xu,<sup>1</sup> Lewis E. Johnson,<sup>1,2\*</sup> Yovan de Coene,<sup>3</sup> Delwin L. Elder,<sup>1\*</sup> Scott R. Hammond,<sup>1,2</sup> Koen Clays,<sup>3</sup>  
Larry R. Dalton,<sup>1</sup> Bruce H. Robinson<sup>1</sup>

<sup>1</sup>Department of Chemistry, University of Washington, Seattle, Washington 98195-1700, United States

<sup>2</sup>Nonlinear Materials Corporation, Seattle WA 98109, USA

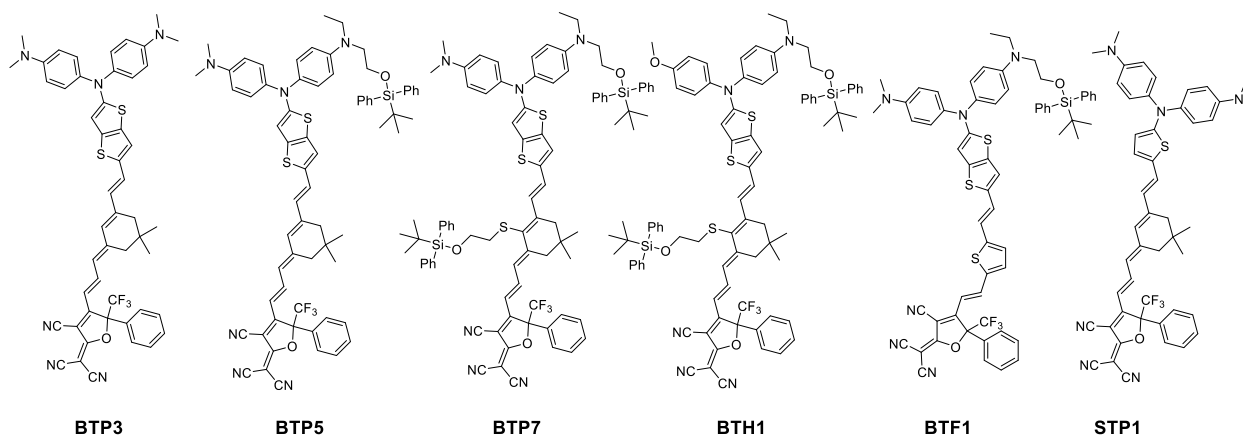
<sup>3</sup>Department of Chemistry, University of Leuven, Celestijnenlaan 200D, 3001 Leuven, Belgium

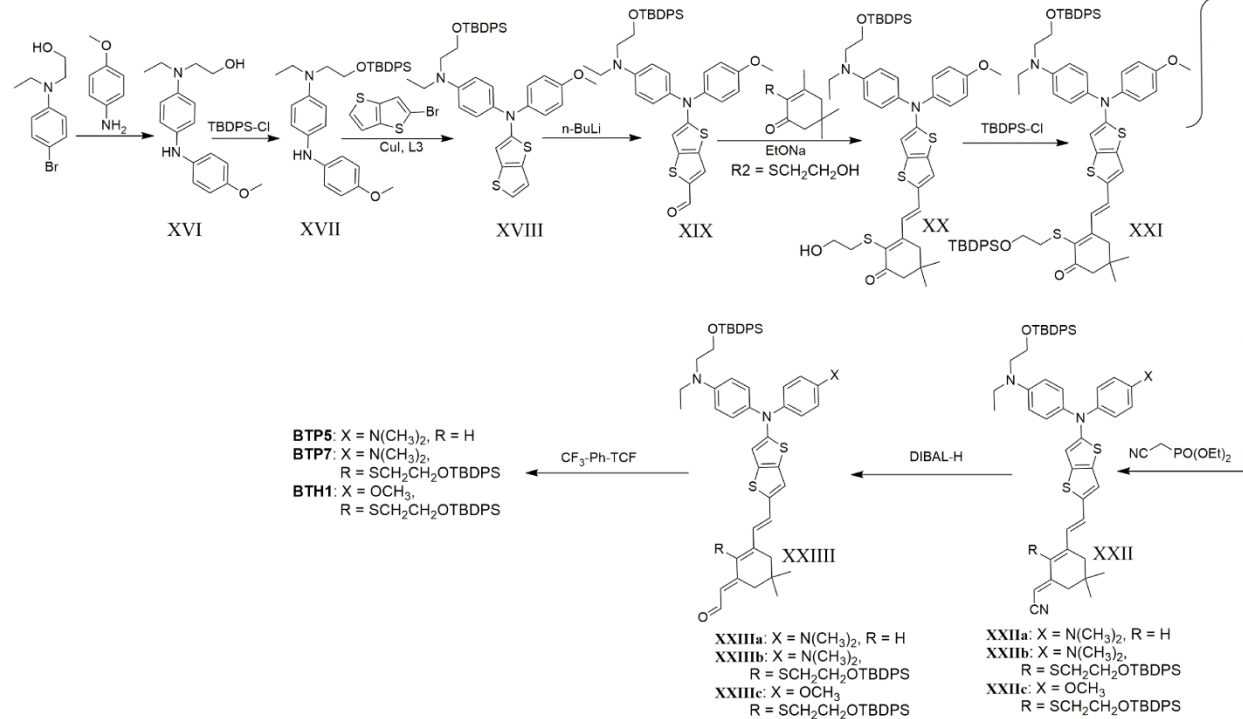
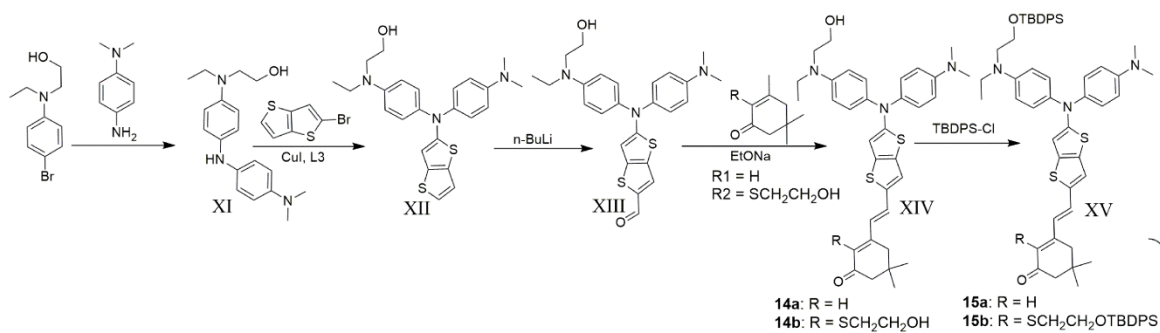
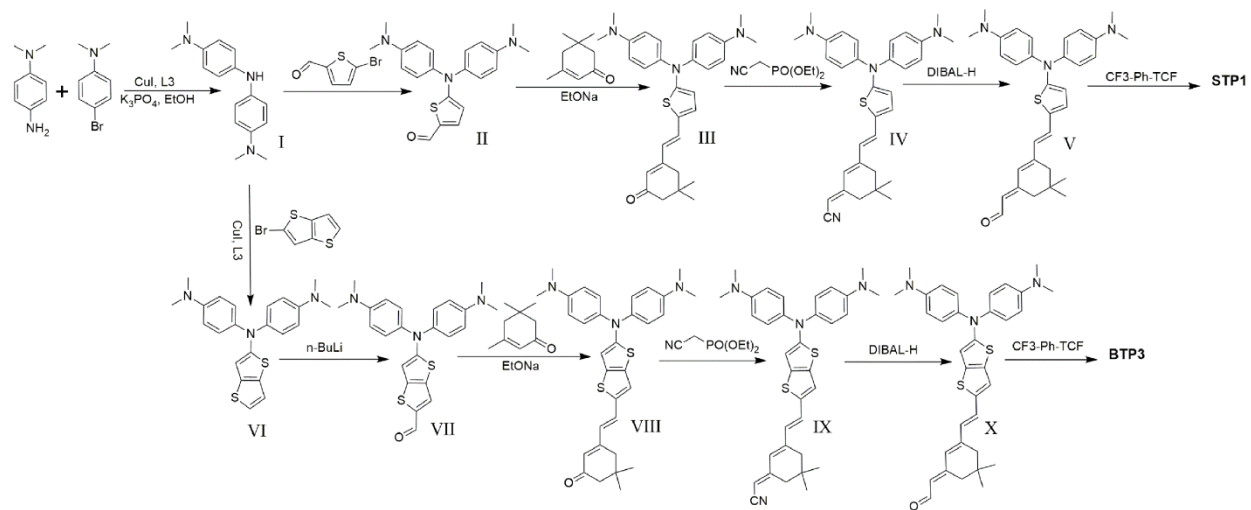
Corresponding Author. E-mail: lewisj@uw.edu (L.E.J.), elderdl@uw.edu (D.L.E.)

## 1 Experimental

### 1.1 Materials and instrumentation

All chemicals that are commercially available were purchased from Sigma-Aldrich, Acros, Alfa Aesar, or TCI and are used without further purification unless otherwise stated. Tetrahydrofuran (THF), dichloromethane, and toluene solvents were dried by passage through commercial solvent purification system columns (Glass Contour or Pure Process Technology). *N,N*-dimethylformamide (DMF) was purchased in anhydrous form and stored over molecular sieves (pore size 3Å). 1,1,2-Trichloroethane (TCE) was dried over CaCl<sub>2</sub> for several days then collected via vacuum distillation prior to use. The ligand **L3**<sup>1</sup> was prepared based on the literature method. ITO/glass slides were purchased from Thin Film Devices, Inc. TLC analyses were carried out on 0.25 mm thick precoated silica plates and spots were visualized under UV light. Chromatographic purification was carried out on technical grade silica gel (230-400 mesh). <sup>1</sup>H and <sup>13</sup>C NMR spectra were determined on an Avance Bruker (500 MHz) NMR spectrometer (tetramethylsilane as internal reference). Gas chromatography with mass spectrometry detection (GC/MS) was carried out on an Agilent 7980A or a Hewlett-Packard 6890 gas chromatograph with a quadrupole mass detector. Electrospray ionization mass spectrometry (ESI-MS) was carried out on a Bruker Esquire ion trap mass spectrometer. High-Resolution Mass Spectrometry (HRMS) was performed using a Waters Micromass Quattro Premier XW instrument using electrospray ionization. The UV-Vis spectra were performed on Cary 5000 spectrophotometer. Optical constants (*n* and *k*) were measured by variable angle spectroscopic ellipsometry (VASE) analysis of chromophore thin films on glass substrates using a J. A. Woollam M-2000 instrument. Data were acquired at 55°, 65° and 75°; and fitting was done using Woollam CompleteEASE software. The decomposition temperature (*T<sub>d</sub>*) was determined by TGA analysis, performed on a TA5000-2950TGA (TA Instruments) with a heating rate of 10 °C min<sup>-1</sup> under the protection of nitrogen. Glass transition temperature (*T<sub>g</sub>*) was measured by differential scanning calorimetry (DSC) with a heating rate of 10 °C min<sup>-1</sup> under the protection of nitrogen.





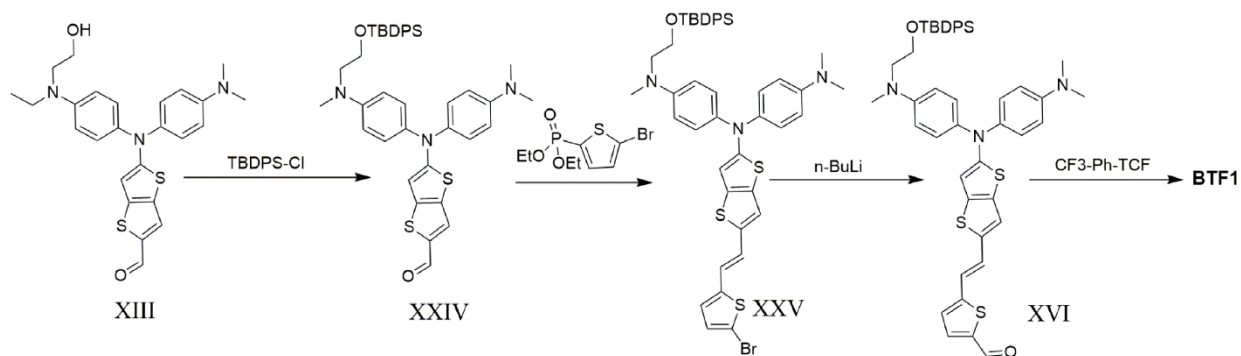


Figure S1. Synthesis routes. TBDPS = *tert*-butyldiphenylsilyl. CF<sub>3</sub>-Ph-TCF = (2-[3-cyano-4-methyl-5-phenyl-5-(trifluoromethyl)-2,5-dihydrofuran-2-ylidene]propanedinitrile)

## 1.2 Synthesis

### 1.2.1 Synthesis of N,N-Di(4-methylphenyl)amine (Compound I)

In a three-neck round bottom flask, 4-bromo-N,N-dimethylaniline (2.0 g, 10.0 mmol), N<sup>1</sup>,N<sup>1</sup>-dimethylbenzene-1,4-diamine (1.63 g, 12.0 mmol), CuI (9.5 mg, 0.05 mmol, 0.005 equiv), diamide ligand (12.5 mg, 0.05 mmol, 0.005 equiv) and K<sub>3</sub>PO<sub>4</sub> (4.23 g, 20 mmol, 2.0 equiv) were placed and evacuated and backfilled with nitrogen. The process was repeated for three times. After that, 10 mL EtOH was added and sealed the tube under positive nitrogen pressure. The reaction mixture was then placed in an oil bath maintaining temperature 80 °C and heating was continued for 24 h. The reaction mixture was then diluted with dichloromethane and filtered through Celite pad and washed it two times with dichloromethane. The filtrate was concentrated under vacuum and residual oil was purified by flash column chromatography (EtOAc: hexane = 1:8 to 1:4) on silica gel to afford the compound **I** blue powder in 71.4% (1.82 g, 7.14 mmol). MS and NMR please refer to Ref. 2.<sup>2</sup>

### 1.2.2 Synthesis of 5-(bis(4-(dimethylamino)phenyl)amino)thiophene-2-carbaldehyde (Compound II)

In a three-neck round bottom flask, 5-bromothiophene-2-carbaldehyde (3.82 g, 20.0 mmol), compound **I** (2.55 g, 10.0 mmol), CuI (9.5 mg, 0.05 mmol, 0.005 equiv), **L3** (12.5 mg, 0.05 mmol, 0.005 equiv) and K<sub>3</sub>PO<sub>4</sub> (4.23 g, 20 mmol, 2.0 equiv) were placed and evacuated and backfilled with nitrogen. The process was repeated for three times. After that, 10 mL EtOH was added and sealed the tube under positive nitrogen pressure. The reaction mixture was then placed in an oil bath maintaining temperature 80 °C and heating was continued for 24 h. The reaction mixture was then diluted with dichloromethane and filtered through Celite pad and washed it two times with dichloromethane. The filtrate was concentrated under vacuum and residual oil was purified by flash column chromatography (EtOAc: hexane = 1:8 to 1:4) on silica gel to afford the compound **II** orange powder in 21%. MS (ESI) (M<sup>+</sup>, C<sub>21</sub>H<sub>23</sub>N<sub>3</sub>OS): calcd: 365.17; found: 365.20. <sup>1</sup>H NMR (500 MHz, CDCl<sub>3</sub>) δ 9.52 (s, 1H), 7.41 (s, 1H), 7.22 (s, 4H), 6.71 (s, 4H), 6.15 (s, 1H), 2.98 (s, 12H). <sup>13</sup>C NMR (126 MHz, CDCl<sub>3</sub>) δ 180.40, 167.65, 149.13, 139.03, 135.45, 126.85, 113.14, 107.96, 40.52.

### 1.2.3 Synthesis of (E)-3-(2-(5-(bis(4-(dimethylamino)phenyl)amino)thiophen-2-yl)vinyl)-5,5-dimethylcyclohex-2-en-1-one (Compound III)

To a solution of compound **II** (1.30 g, 3.60 mmol) and isophorone (2.13 mL, 14.40 mmol) in 10 mL of 0.5M EtONa/EtOH fresh solution. The reaction mixture was allowed to stir at 65 °C for overnight. After cooling to

room temperature, adding a few drops of water quenched the reaction, and all the solvent was removed under reduced pressure by roto-evaporator. Flash chromatography of the crude (Hexane: DCM = 1: 1) over SiO<sub>2</sub> gave a red solid in 75% yield. MS (ESI) (M<sup>+</sup>, C<sub>30</sub>H<sub>35</sub>N<sub>3</sub>OS): calcd: 485.25; found: 485.15. <sup>1</sup>H NMR (500 MHz, CDCl<sub>3</sub>) δ 7.17 (s, 4H), 7.02 (d, *J* = 14.8 Hz, 1H), 6.82 (s, 1H), 6.69 (s, 4H), 6.28 (d, *J* = 14.8 Hz, 1H), 6.12 (s, 1H), 5.90 (s, 1H), 2.96 (s, 12H), 2.39 (s, 2H), 2.28 (s, 2H), 1.09 (s, 6H). <sup>13</sup>C NMR (126 MHz, CDCl<sub>3</sub>) δ 199.32, 158.65, 155.42, 148.31, 136.77, 130.59, 129.39, 128.01, 126.21, 124.07, 123.35, 113.21, 109.82, 60.26, 51.46, 40.67, 39.23, 33.20, 28.42, 20.91, 14.23.

#### 1.2.4 Synthesis of (E)-2-(3-((E)-2-(5-(bis(4-(dimethylamino)phenyl)amino)thiophen-2-yl)vinyl)-5,5-dimethylcyclohex-2-en-1-ylidene)acetonitrile (Compound IV)

Under a nitrogen atmosphere, diethyl(cyanomethyl)phosphonate (1 mL, 1.10g, 6.2 mmol) was slowly added to a two-necked flask charged with NaH (in oil, 0.27 g, 6.2 mmol) in dry 8 mL THF. The solution was stirred for 10 min in ice bath. Compound III (0.75 g, 1.5 mmol) dissolved in THF (3 mL) was added to the mixture then directly heated to 70 °C for 18 h. The reaction was then cooled, quenched with 20 mL water. The resulting mixture is extracted with 3 x 50 mL ethyl acetate. The resulting organic layer was dried using magnesium sulfate and roto-evaporated to dry without further purification for the next use.

#### 1.2.5 Synthesis of (E)-2-(3-((E)-2-(5-(bis(4-(dimethylamino)phenyl)amino)thiophen-2-yl)vinyl)-5,5-dimethylcyclohex-2-en-1-ylidene)acetaldehyde (Compound V)

In a 50 mL round bottom flask were added IV (1.30 g, 2.56 mmol), and backfilled with nitrogen. To this was added 15 mL dry, degassed toluene. After dissolved and cooled to -78 °C, to the solution was added 4.3 mL diisobutylaluminum hydride (1.2 M in toluene) dropwise. The solution became dark red immediately. The solution was stirred at -78° C under nitrogen for 2h. Hydrolysis is then accomplished by the addition of damp silica (3 g, about 10% water by mass), which is added to the reaction mixture and the reaction is allowed to return to room temperature while being stirred 2h. The resulting mixture is then diluted with hexane/EtOAc, dried with magnesium sulfate, then the cold bath was removed and the solution stirred a further 4 hours. The solution was filtered to remove the silica gel and MgSO<sub>4</sub>, and stripped of solvent by rotary evaporator. Flash chromatography of the crude (acetone: hexane = 1:10) over SiO<sub>2</sub> gave a red solid in 81% yields. MS (ESI) (M<sup>+</sup>, C<sub>32</sub>H<sub>37</sub>N<sub>3</sub>OS) calcd: 511.26; found: 511.24. <sup>1</sup>H NMR (500 MHz, CDCl<sub>3</sub>) δ 10.18 (s, 0.3H), 10.05 (s, 0.7H), 7.18 (s, 4H), 6.86 (s, 1H), 6.77 (s, 1H), 6.71 (s, 4H), 6.34 (t, *J* = 19.0 Hz, 1H), 6.15 (s, 2H), 5.89 (s, 0.7H), 5.68 (d, *J* = 19.1 Hz, 0.3H) 2.97 (s, 12H), 2.67 (s, 3H), 2.29 (s, 3H), 1.06 (s, 7H). <sup>13</sup>C NMR (126 MHz, CDCl<sub>3</sub>) δ 190.40, 156.83, 148.10, 146.41, 136.95, 129.22, 127.30, 126.08, 125.80, 113.20, 40.83, 39.14, 31.08, 28.41.

#### 1.2.6 Synthesis of STP1

Compound 5 (0.20 g, 0.40 mmol) and acceptor CF<sub>3</sub>PhTCF (0.15 g, 0.48mmol) were mixed with anhydrous ethanol (5 mL). The mixture was allowed to stir at 50 °C for 0.5h. TLC trace. The solvent was removed under vacuum and the residual mixture was recrystallized in ethanol to afford chromophore STP1 as a dark powder in 64 % yield. HRMS (ESI) (M<sup>+</sup>, C<sub>48</sub>H<sub>43</sub>F<sub>3</sub>N<sub>6</sub>OS): calcd: 808.3171; found: 808.3182. <sup>1</sup>H NMR (500 MHz, CD<sub>3</sub>CN, one drop CF<sub>3</sub>COOH was added to increase solubility) δ 7.75 (s, 1H, CH), 7.60 (dt, *J* = 8.6, 5.5 Hz, 5H, Ar-H), 7.52 (d, *J* = 9.0 Hz, 4H, Ar-H), 7.31 (d, *J* = 8.7 Hz, 4H, Ar-H), 7.11 (d, *J* = 13.3 Hz, 1H, CH), 7.08 (s, 1H), 6.74 (d, *J* = 3.9 Hz, 1H, CH), 6.67 (d, *J* = 15.5 Hz, 1H, CH), 6.57 (d, *J* = 13.6 Hz, 1H, CH), 6.44 (s, 2H, CH), 3.24 (s,

12H, CH<sub>3</sub>), 2.36 (s, 2H, CH<sub>2</sub>), 2.27 (d, 2H, CH<sub>2</sub>), 0.99 (s, 3H, CH<sub>3</sub>), 0.90 (s, 3H, CH<sub>3</sub>). <sup>13</sup>C NMR (126 MHz, CDCl<sub>3</sub>) δ 176.28, 164.07, 160.44, 155.46, 155.12, 149.99, 149.62, 147.92, 138.84, 137.76, 131.72, 129.89, 128.75, 126.86, 125.08, 124.34, 123.73, 122.06, 116.68, 114.39, 112.11, 111.06, 57.83, 47.23, 46.88, 39.70, 31.51, 28.38, 27.70, 14.02.

### 1.2.7 Synthesis of N1-(4-(dimethylamino)phenyl)-N4,N4-dimethyl-N1-(thieno[3,2-b]thiophen-2-yl)benzene-1,4-diamine (Compound VI)

In a three-neck round bottom flask, N,N-Di(4-methylphenyl)amine (2.55 g, 10.0 mmol), 2-bromothiopheno[3,2-b]thiophene (2.63 g, 12.0 mmol), CuI (9.5 mg, 0.05 mmol, 0.005 equiv), diamide ligand (12.5 mg, 0.05 mmol, 0.005 equiv) and K<sub>3</sub>PO<sub>4</sub> (4.23 g, 20 mmol, 2.0 equiv) were placed and evacuated and backfilled with nitrogen. The reaction mixture was heated to 80°C and allowed to reflux for 24 h before cooling, diluted with dichloromethane and filtered through Celite pad and washed it two times with dichloromethane. The filtrate was concentrated under vacuum and residual oil was purified by flash column chromatography (ethyl acetate: hexane = 1:9 to 1:5) on silica gel to afford the compound VI green solid in 23% (0.84 g, 2.30 mmol). MS (ESI) (M<sup>+</sup>, C<sub>23</sub>H<sub>23</sub>N<sub>3</sub>OS<sub>2</sub>): calcd: 393.13; found: 393.21. <sup>1</sup>H NMR (500 MHz, CDCl<sub>3</sub>) δ 7.20 (t, 6H), 6.75 (s, 5H), 3.01 (s, broad, 12H). <sup>13</sup>C NMR (126 MHz, CDCl<sub>3</sub>) δ 147.44, 138.52, 124.85, 122.99, 119.82, 113.57, 41.04.

### 1.2.8 Synthesis of 5-(bis(4-(dimethylamino)phenyl)amino)thieno[3,2-b]thiophene-2-carbaldehyde (Compound VII)

To a solution of VI (0.51 g, 1.3 mmol) in THF (10 mL) at -78°C was added a solution of n-butyllithium (1.33 mL, 1.3 mmol) over 3 minutes. Following 10 minutes of stirring at -78°C, then added dry DMF (0.82 mL, 10.6 mmol). Solution was gradually warmed to room temperature over 3 h before being quenched (H<sub>2</sub>O, 5 mL), extracted with ethyl acetate (3 x 50 mL), dried (Na<sub>2</sub>SO<sub>4</sub>), and concentrated in vacuo to give a crude brown oil. Flash chromatography of the crude (ethyl acetate: Hexane = 1: 8) over SiO<sub>2</sub> gave an orange solid in 92% yield (0.50 g, 1.1 mmol). MS (ESI) (M<sup>+</sup>, C<sub>23</sub>H<sub>23</sub>N<sub>3</sub>OS<sub>2</sub>): calcd: 421.12; found: 421.25. <sup>1</sup>H NMR (500 MHz, CDCl<sub>3</sub>) δ 9.71 (s, 1H), 7.58 (s, 1H), 7.22 (s, 4H), 6.71 (s, 4H), 6.31 (s, 1H), 2.98 (s, 12H). <sup>13</sup>C NMR (126 MHz, CDCl<sub>3</sub>) δ 181.08, 165.05, 148.88, 138.88, 135.86, 129.69, 126.76, 113.18, 100.02, 40.57.

### 1.2.9 Synthesis of (E)-3-(2-(5-(bis(4-(dimethylamino)phenyl)amino)thieno[3,2-b]thiophen-2-yl)vinyl)-5,5-dimethylcyclohex-2-en-1-one (Compound VIII)

To a solution of compound VII (5.05 g, 12.0 mmol) and isophorone (1.66 g, 12.0 mmol) in 20 mL of 1M EtONa/EtOH fresh solution. The reaction mixture was allowed to stir at 65 °C for overnight. After cooling to room temperature, adding a few drops of water quenched the reaction, and all the solvent was removed under reduced pressure by roto-evaporator. The crude product was purified by flash chromatography (ethyl acetate: hexane = 1:2) to afford compound VIII as red solid. (5.39 g, 83%). Flash chromatography of the crude (ethyl acetate: DCM = 1: 10) over SiO<sub>2</sub> gave a red solid in 76.1% yield. MS (ESI) (M<sup>+</sup>, C<sub>32</sub>H<sub>35</sub>N<sub>3</sub>OS<sub>2</sub>): calcd: 541.22; found: 541.25. <sup>1</sup>H NMR (500 MHz, CDCl<sub>3</sub>) δ 7.17 (s, 4H), 7.11 (s, 1H), 7.04 (s, 1H), 6.69 (s, 4H), 6.56 (d, J = 15.5 Hz, 1H), 6.39 (s, 1H), 6.01 (s, 1H), 2.95 (s, 12H), 2.30 (s, 2H), 2.18 (s, 2H), 1.11 (s, 6H). <sup>13</sup>C NMR (126 MHz, CDCl<sub>3</sub>) δ 199.60, 160.01, 154.92, 148.14, 140.42, 138.32, 136.94, 129.08, 125.98, 125.64, 125.25, 124.63, 122.12, 113.26, 51.46, 40.77, 39.11, 33.28, 30.89, 28.58.

### 1.2.10 Synthesis of (E)-2-(3-((E)-2-(5-(bis(4-(dimethylamino)phenyl)amino)thieno[3,2-b]thiophen-2-yl)vinyl)-5,5-dimethylcyclohex-2-en-1-ylidene)acetonitrile (Compound IX)

Under a nitrogen atmosphere, diethyl(cyanomethyl)phosphonate (1.81 mL, 1.99g, 11.2 mmol) was slowly added to a two-necked flask charged with NaH (0.27 g, 11.2 mmol) in dry 12 mL THF. The solution was stirred for 10 min in ice bath. Compound VIII (1.51 g, 2.80 mmol) dissolved in THF (3 mL) was added to the mixture then directly heated to 70 °C for 18 h. The reaction was then cooled, quenched with 20 mL water. The resulting mixture is extracted with 3 x 50 mL ethyl acetate. The resulting organic layer was dried using magnesium sulfate and roto-evaporated to dry. Flash chromatography of the crude (ethyl acetate: DCM = 1: 15) over SiO<sub>2</sub> gave a red solid in 52.3% yield. MS (ESI) (M<sup>+</sup>, C<sub>34</sub>H<sub>36</sub>N<sub>4</sub>S<sub>2</sub>): calcd: 564.23; found: 564.31. <sup>1</sup>H NMR (500 MHz, CDCl<sub>3</sub>) δ 7.16 (d, *J* = 8.1 Hz, 1H), 7.12 (d, *J* = 6.1 Hz, 1H), 6.98 (d, *J* = 3.8 Hz, 1H), 6.94 (dd, *J* = 15.7, 6.0 Hz, 1H), 6.69 (d, *J* = 9.1 Hz, 2H), 6.58 (d, *J* = 15.7 Hz, 1H), 6.41 (s, 1H), 6.19 (s, 1H), 2.95 (s, 12H), 2.26 (s, 2H), 2.20 (d, *J* = 5.1 Hz, 2H), 1.05 (s, 3H), 1.01 (s, 3H). <sup>13</sup>C NMR (126 MHz, CDCl<sub>3</sub>) δ 160.29, 147.97, 125.79, 118.64, 113.36, 113.19, 60.41, 42.08, 38.84, 31.07, 28.21, 24.58, 21.11, 14.35.

### 1.2.11 Synthesis of (E)-2-(3-((E)-2-(5-(bis(4-(dimethylamino)phenyl)amino)thieno[3,2-b]thiophen-2-yl)vinyl)-5,5-dimethylcyclohex-2-en-1-ylidene)acetaldehyde (Compound X)

The procedure for compound V was followed to prepare compound X as a dark red solid (91.1%). Prior the reduction a 50 mL round bottom flask containing IX (1.41 g, 2.50 mmol) was kept under high vacuum for 2 h. The flask was back filled with N<sub>2</sub> followed by addition of dry toluene (15 mL). The solution was then cooled to -78 °C (dry ice/acetone bath). diisobutyl aluminium hydride (5.0 mL, 1.0 M solution in toluene) was added dropwise. Color changed to dark red. The mixture was stirred at -78 °C for 2.0 h when wet silica (3.00 g) in diethyl ether was added. The mixture was allowed to warm to room temperature and was then run through a silica plug. Flash chromatography of the crude (acetone: DCM = 1: 30) over SiO<sub>2</sub> gave a dark red solid in 76.1% yield. MS (ESI) (M<sup>+</sup>, C<sub>34</sub>H<sub>36</sub>N<sub>4</sub>S<sub>2</sub>): calcd: 567.23; found: 567.31. <sup>1</sup>H NMR (500 MHz, CDCl<sub>3</sub>) δ 10.22 (d, *J* = 7.9 Hz, 0.3H), 10.08 (d, *J* = 8.2 Hz, 0.7H), 7.17 (d, *J* = 9.0 Hz, 4H), 7.12 (d, *J* = 7.4 Hz, 1H), 6.99 (d, *J* = 2.4 Hz, 1H), 6.98 – 6.92 (m, 1H), 6.71 – 6.67 (m, 4H), 6.59 (d, *J* = 15.6 Hz, 1H), 6.42 (s, 1H), 5.94 (d, *J* = 8.3 Hz, 0.7H), 5.74 (d, *J* = 7.9 Hz, 0.3H), 2.95 (s, 12H), 2.19 (s, 2H), 2.08 (s, 2H), 1.08 (s, 3H), 1.05 (s, 3H). <sup>13</sup>C NMR (126 MHz, CDCl<sub>3</sub>) δ 190.39, 171.05, 156.53, 148.00, 145.83, 139.37, 137.13, 128.59, 127.14, 126.46, 125.84, 124.49, 121.02, 113.52, 113.29, 60.40, 53.60, 46.19, 40.84, 39.10, 31.08, 28.45, 21.10, 14.33.

### 1.2.12 Synthesis of 2-(4-((1E,3E)-3-(3-((E)-2-(5-(bis(4-(dimethylamino)phenyl)amino)thieno[3,2-b]thiophen-2-yl)vinyl)-5,5-dimethylcyclohex-2-en-1-ylidene)prop-1-en-1-yl)-3-cyano-5-phenyl-5-(trifluoromethyl)furan-2(5H)-ylidene)malononitrile (BTP3)

Compound 10 (0.23 g, 0.40 mmol) and acceptor CF<sub>3</sub>PhTCF (0.15 g, 0.48mmol) were mixed with anhydrous ethanol (5 mL). The mixture was allowed to stir at 50 °C for 0.5h. TLC trace. The solvent was removed under vacuum and the residual mixture was purified by flash chromatography on silica gel (ethyl acetate/DCM (1:50 to 1:20)) to afford chromophore BTP3 as a black powder in 31.8 % yield (0.11 g, 0.13 mmol). HRMS (ESI) (M<sup>+</sup>, C<sub>50</sub>H<sub>43</sub>F<sub>3</sub>N<sub>6</sub>OS<sub>2</sub>): calcd: 864.2892; found: 864.2888. <sup>1</sup>H NMR (500 MHz, Acetone) δ 7.94 (s, 1H, CH), 7.74 – 7.69 (m, 2H, Ar-H), 7.66 (d, *J* = 14.6 Hz, 1H, CH), 7.60 (dd, *J* = 5.9, 3.1 Hz, 4H, CH, Ar-H), 7.28 (d, *J* = 9.0 Hz, 4H, Ar-H), 6.82 (d, *J* = 9.0 Hz, 4H, Ar-H), 6.72 (d, *J* = 14.4 Hz, 1H, CH), 6.60 (s, 1H, CH), 6.52 (s, 1H, CH), 6.47 (s, 1H, CH), 6.31 (d, *J* = 12.9 Hz, 1H, CH), 3.01 (s, 12H, CH<sub>3</sub>), 2.11 (s, 2H, CH<sub>2</sub>), 2.10 (s, 2H, CH<sub>2</sub>), 1.04

(s, 3H, CH<sub>3</sub>), 0.98 (s, 3H, CH<sub>3</sub>). <sup>13</sup>C NMR (126 MHz, CDCl<sub>3</sub>) δ 175.94, 148.69, 131.02, 129.47, 126.74, 123.45, 121.16, 113.04, 68.19, 60.42, 40.70, 39.66, 31.65, 28.53, 28.12, 21.08, 14.24 (CF<sub>3</sub> carbon too weak to observe).

### 1.2.13 Synthesis of 2-((4-((4-(dimethylamino)phenyl)amino)phenyl)(ethyl)amino)ethan-1-ol (Compound XI)

The procedure for compound **I** was followed to prepare **XI**. Flash chromatography of the crude (acetone: hexane = 1:10 to 1:5) over SiO<sub>2</sub> gave a red solid in 89% yields. MS (ESI) (M<sup>+</sup>, C<sub>18</sub>H<sub>25</sub>N<sub>3</sub>O): calcd: 299.20; found: 299.21. <sup>1</sup>H NMR (500 MHz, CDCl<sub>3</sub>) δ 6.98 (br, 4H), 6.83 (br, 4H), 3.76 (t, *J* = 5.9 Hz, 2H), 3.38 (br, 2H), 2.99 (br, 8H), 1.18 (t, *J* = 7.0 Hz, 3H). <sup>13</sup>C NMR (126 MHz, CDCl<sub>3</sub>) δ 170.24, 146.04, 142.96, 119.43, 116.61, 114.98, 64.11, 53.71, 41.78, 11.04.

### 1.2.14 Synthesis of 2-((4-((4-(dimethylamino)phenyl)(thieno[3,2-b]thiophen-2-yl)amino)phenyl)(ethyl)amino)ethan-1-ol (Compound XII)

The procedure for compound **6** was followed to prepare **XII**. Flash chromatography of the crude (DCM: ethyl acetate = 20:1 to 10:1) over SiO<sub>2</sub> gave a red solid in 23% yields. MS (ESI) (M<sup>+</sup>, C<sub>24</sub>H<sub>27</sub>N<sub>3</sub>OS<sub>2</sub>): calcd: 437.16; found: 437.10. <sup>1</sup>H NMR (500 MHz, CDCl<sub>3</sub>) δ 7.13 (m, 6H), 6.75 (m, 5H), 3.80 (t, *J* = 5.5 Hz, 2H), 3.65 – 2.64 (br, 10H), 1.21 (t, *J* = 7.0 Hz, 3H). <sup>13</sup>C NMR (126 MHz, CDCl<sub>3</sub>) δ 147.53, 131.04, 128.91, 124.71, 114.41, 113.61, 68.27, 60.53, 41.08, 38.83, 31.01, 29.03, 23.87, 23.10, 14.33, 11.11.

### 1.2.15 Synthesis of 5-((4-(dimethylamino)phenyl)(4-(ethyl(2-hydroxyethyl)amino)phenyl)amino)thieno[3,2-b]thiophene-2-carbaldehyde (Compound XIII)

The procedure for compound **VII** was followed to prepare **XIII**. Flash chromatography of the crude (DCM: ethyl acetate = 10:1) over SiO<sub>2</sub> gave a red solid in 87% yields. MS (ESI) (M<sup>+</sup>, C<sub>25</sub>H<sub>27</sub>N<sub>3</sub>O<sub>2</sub>S<sub>2</sub>): calcd: 465.15; found: 465.10. <sup>1</sup>H NMR (500 MHz, CDCl<sub>3</sub>) δ 9.72 (s, 1H), 7.61 (s, 1H), 7.20 (s, 4H), 6.72 (d, *J* = 9.0 Hz, 4H), 6.30 (s, 1H), 3.82 (s, 2H), 3.46 (br, 2H), 2.99 (br, 8H), 1.20 (t, *J* = 7.0 Hz, 3H). <sup>13</sup>C NMR (126 MHz, CDCl<sub>3</sub>) δ 181.33, 148.87, 138.72, 135.71, 129.95, 126.89, 113.10, 99.99, 68.20, 60.20, 52.69, 45.73, 40.63, 38.78, 30.93, 30.40, 29.30, 28.95, 23.79, 23.00, 14.06, 10.99.

### 1.2.16 Synthesis of (E)-3-(2-(5-((4-(dimethylamino)phenyl)(4-(ethyl(2-hydroxyethyl)amino)phenyl)amino)thieno[3,2-b]thiophen-2-yl)vinyl)-5,5-dimethylcyclohex-2-en-1-one (Compound XIVa) and (E)-3-(2-(5-((4-(dimethylamino)phenyl)(4-(ethyl(2-hydroxyethyl)amino)phenyl)amino)thieno[3,2-b]thiophen-2-yl)vinyl)-2-((2-hydroxyethyl)thio)-5,5-dimethylcyclohex-2-en-1-one (Compound XIVb)

The procedure for compound **8** was followed to prepare **XIVa** and **XIVb**. Flash chromatography of the crude (**XIVa**: acetone: hexane = 1:5 to 1:2; **XIVb**: acetone: hexane = 1:1) over SiO<sub>2</sub> gave a red solid in 67.8% and 55.6% yields. **XIVa** MS (ESI) (M<sup>+</sup>, C<sub>34</sub>H<sub>39</sub>N<sub>3</sub>O<sub>2</sub>S<sub>2</sub>): calcd: 585.25; found: 585.26. <sup>1</sup>H NMR (500 MHz, CDCl<sub>3</sub>) δ 7.21 – 7.13 (m, 4H), 7.12 (s, 1H), 7.07 (s, 1H), 6.72 (m, 4H), 6.57 (d, *J* = 15.5 Hz, 1H), 6.41 (s, 1H), 6.02 (s, 1H), 3.80 (t, *J* = 5.9 Hz, 2H), 3.45 (s, 2H), 2.97 (s, 6H), 2.44 (s, 2H), 2.31 (s, 2H), 1.19 (t, *J* = 7.0 Hz, 3H), 1.12 (s, 6H). <sup>13</sup>C NMR (126 MHz, CDCl<sub>3</sub>) δ 199.95, 170.26, 155.16, 148.14, 125.95, 125.26, 113.72, 113.25, 60.38, 51.41, 48.16, 40.81, 39.08, 38.02, 33.33, 32.68, 30.96, 28.57, 28.13, 24.56.

**XIVb** MS (ESI) (M<sup>+</sup>, C<sub>36</sub>H<sub>43</sub>N<sub>3</sub>O<sub>3</sub>S<sub>3</sub>): calcd: 661.25; found: 661.25. <sup>1</sup>H NMR (500 MHz, CDCl<sub>3</sub>) <sup>1</sup>H NMR (500

MHz, CDCl<sub>3</sub>) δ 7.70 (s, 1H), 7.24 (d, *J* = 8.1 Hz, 1H), 7.12 (br, 5H), 6.68 (br, 5H), 6.36 (s, 1H), 3.80 – 3.76 (m, 2H), 3.58 – 3.51 (m, 2H), 3.42 (m, 2H), 2.95 (s, 6H), 2.82 (d, *J* = 4.5 Hz, 2H), 2.60 (s, 2H), 2.44 (s, 2H), 2.17 (s, 2H), 1.18 – 1.14 (m, 3H), 1.08 (s, 6H). <sup>13</sup>C NMR (126 MHz, CDCl<sub>3</sub>) δ 197.09, 162.56, 159.46, 148.31, 126.11, 113.16, 60.26, 51.62, 41.24, 40.74, 39.01, 32.34, 30.93, 28.37, 11.96.

**1.2.17 Synthesis of (E)-3-(2-(5-((4-((tert-butylidiphenylsilyl)oxy)ethyl)(ethyl)amino)phenyl)(4-(dimethylamino)phenyl)amino)thieno[3,2-b]thiophen-2-yl)vinyl)-5,5-dimethylcyclohex-2-en-1-one (Compound XVa) and (E)-3-(2-(5-((4-((tert-butylidiphenylsilyl)oxy)ethyl)(ethyl)amino)phenyl)(4-(dimethylamino)phenyl)amino)thieno[3,2-b]thiophen-2-yl)vinyl)-2-((2-((tert-butylidiphenylsilyl)oxy)ethyl)thio)-5,5-dimethylcyclohex-2-en-1-one (Compound XVb)**

In a 50 mL round bottom flask were combined **XIV** (5.00 mmol), imidazole (**XIVa**: 6.0 mmol; **XIVb**: 12.0 mmol), and dry DMF (20 mL). After solids dissolved TBDPS-Cl (**XIVa**: 6.0 mmol; **XIVb**: 12 mmol) was added. The solution was stirred for 12 h at room temperature. 200 mL water was added to the solution. The mixture was then extracted by 3 x 50 mL ethyl acetate. The organic layers were combined, then washed with brine, dried over MgSO<sub>4</sub>. Solvent was removed under reduced pressure. The crude material was purified using silica gel chromatography ( ) to afford 2.67 g of orange solid. Yield: 87%. Flash chromatography of the crude (ethyl acetate: hexane = 1:8 to 1:5) over SiO<sub>2</sub> gave a red solid in 91.4%, 87.1% and 88.4% yields. **XVa** MS (ESI) (M<sup>+</sup>, C<sub>50</sub>H<sub>57</sub>N<sub>3</sub>O<sub>2</sub>S<sub>2</sub>Si): calcd: 823.37; found: 823.31. <sup>1</sup>H NMR (500 MHz, CDCl<sub>3</sub>) δ 7.57 (d, *J* = 7.5 Hz, 4H), 7.33 – 7.23 (m, 6H), 7.05 (d, *J* = 7.8 Hz, 2H), 6.98 (s, 1H), 6.93 (d, *J* = 8.4 Hz, 2H), 6.72 (s, 1H), 6.57 (d, *J* = 7.8 Hz, 2H), 6.43 (d, *J* = 15.8 Hz, 1H), 6.37 (d, *J* = 8.0 Hz, 2H), 6.22 (s, 1H), 5.89 (s, 1H), 3.69 (t, *J* = 5.7 Hz, 2H), 3.32 (s, 2H), 3.21 (s, 2H), 2.83 (s, 6H), 2.30 (s, 2H), 2.18 (s, 2H), 1.13 (t, *J* = 7.0 Hz, 3H), 1.02 – 0.90 (m, 15H). <sup>13</sup>C NMR (126 MHz, CDCl<sub>3</sub>) δ 199.88, 148.13, 145.59, 135.67, 133.52, 129.80, 127.81, 126.50, 125.97, 113.27, 112.16, 58.38, 51.46, 40.84, 39.11, 35.72, 33.34, 32.06, 30.98, 28.62, 26.95, 19.18, 18.53.

**XVb** MS (ESI) (M<sup>+</sup>, C<sub>68</sub>H<sub>79</sub>N<sub>3</sub>O<sub>3</sub>S<sub>3</sub>Si<sub>2</sub>): calcd: 1137.48; found: 1137.25. <sup>1</sup>H NMR (500 MHz, CDCl<sub>3</sub>) δ 7.67 – 7.61 (m, 8H), 7.60 (d, *J* = 1.5 Hz, 1H), 7.43 – 7.28 (m, 15H), 7.05 (br, 4H), 6.68 (b, 2H), 6.47 (br, 2H), 3.82 – 3.66 (m, 4H), 3.41 (s, 2H), 2.93 (s, 6H), 2.32 (s, 2H), 2.14 (s, 2H), 2.12 – 1.99 (m, 2H), 1.12 – 1.09 (m, 3H), 1.06 – 0.99 (m, 24H), 0.83 (s, 3H), 0.73 (s, 3H). <sup>13</sup>C NMR (126 MHz, CDCl<sub>3</sub>) δ 170.19, 147.96, 145.43, 135.50, 133.46, 129.70, 127.69, 113.19, 112.06, 63.19, 60.36, 52.12, 45.41, 43.28, 41.40, 40.80, 37.45, 30.59, 30.07, 27.97, 26.83, 21.03, 19.10, 14.20.

**1.2.18 Synthesis of 2-(ethyl(4-((4-methoxyphenyl)amino)phenyl)amino)ethan-1-ol (Compound XVI)**

The procedure for compound **1** was followed to prepare **XVI**. Flash chromatography of the crude (ethyl acetate: hexane = 1:6 to 1:3) over SiO<sub>2</sub> gave a brown solid in 73% yields. MS (ESI) (M<sup>+</sup>, C<sub>17</sub>H<sub>22</sub>N<sub>2</sub>O<sub>2</sub>): calcd: 286.17; found: 286.16. <sup>1</sup>H NMR (500 MHz, Pyr) δ 7.29 – 7.25 (m, 2H), 7.24 – 7.21 (m, 2H), 6.99 (dd, *J* = 8.7, 1.9 Hz, 2H), 6.89 (dd, *J* = 8.7, 1.9 Hz, 2H), 4.02 (t, *J* = 5.6 Hz, 2H), 3.68 (s, 3H), 3.60 (t, *J* = 5.6 Hz, 2H), 3.42 – 3.35 (q, *J* = 7.0 Hz, 2H), 1.09 (t, *J* = 7.0 Hz, 3H). <sup>13</sup>C NMR (126 MHz, CDCl<sub>3</sub>) δ 170.25, 167.28, 166.55, 107.47, 102.63, 99.09, 96.64, 92.81, 86.31, 85.05, 64.10, 55.69, 43.59, 30.93, 29.04, 11.03.

**1.2.19 Synthesis of N<sup>1</sup>-(2-((tert-butylidiphenylsilyl)oxy)ethyl)-N<sup>1</sup>-ethyl-N<sup>4</sup>-(4-methoxyphenyl)benzene-1,4-diamine (Compound XVII)**

The procedure for **XV** was followed to prepare **XVII**. Flash chromatography of the crude (ethyl acetate: hexane = 1:10 to 1:5) over SiO<sub>2</sub> gave a brown oil in 74.1% yields. MS (ESI) (M<sup>+</sup>, C<sub>33</sub>H<sub>40</sub>N<sub>2</sub>O<sub>2</sub>Si): calcd: 524.29; found: 524.28. <sup>1</sup>H NMR (500 MHz, Pyr) δ 7.86 (d, *J* = 5.5 Hz, 4H), 7.51 – 7.46 (m, 6H), 7.26 (t, *J* = 7.9 Hz, 4H), 7.02 (d, *J* = 10.7 Hz, 2H), 6.74 (d, *J* = 8.6 Hz, 2H), 3.93 (t, *J* = 6.4 Hz, 2H), 3.69 (s, 3H), 3.52 (t, *J* = 6.0 Hz, 2H), 3.34 (q, *J* = 6.7 Hz, 2H), 1.15 (d, *J* = 1.9 Hz, 2H), 1.09 – 1.05 (m, 1H). <sup>13</sup>C NMR (126 MHz, CDCl<sub>3</sub>) δ 170.20, 135.63, 134.80, 133.60, 129.68, 127.69, 55.71, 26.86, 19.12, 0.00.

#### 1.2.20 Synthesis of N<sup>1</sup>-(2-((tert-butyldiphenylsilyloxy)ethyl)-N<sup>1</sup>-ethyl-N<sup>4</sup>-(4-methoxyphenyl)-N<sup>4</sup>-(thieno[3,2-b]thiophen-2-yl)benzene-1,4-diamine (Compound XVIII)

The procedure for **VI** was followed to prepare **XVIII**. Flash chromatography of the crude (ethyl acetate: hexane = 1:10) over SiO<sub>2</sub> gave a brown solid in 24.1% yields. MS (ESI) (M<sup>+</sup>, C<sub>39</sub>H<sub>42</sub>N<sub>2</sub>O<sub>2</sub>S<sub>2</sub>Si): calcd: 662.25; found: 662.23. <sup>1</sup>H NMR (500 MHz, CDCl<sub>3</sub>) δ 7.65 (s, 4H), 7.42 – 7.30 (m, 6H), 7.15 (s, 1H), 7.07 (s, 3H), 6.97 (s, 2H), 6.78 (s, 2H), 6.64 (s, 1H), 6.44 (s, 2H), 3.81 – 3.73 (m, 5H), 3.40 (s, 2H), 3.30 (s, 2H), 1.08 (d, *J* = 7.2 Hz, 3H), 1.04 (d, *J* = 7.9 Hz, 9H). <sup>13</sup>C NMR (126 MHz, CDCl<sub>3</sub>) δ 135.61, 133.49, 129.71, 127.71, 126.00, 123.36, 119.80, 114.35, 112.19, 61.40, 55.53, 52.22, 45.55, 26.85, 19.10, 12.34.

#### 1.2.21 Synthesis of 5-((4-((2-((tert-butyldiphenylsilyloxy)ethyl)(ethylamino)phenyl)(4-methoxyphenyl)amino)thieno[3,2-b]thiophene-2-carbaldehyde (Compound XIX)

The procedure for **VII** was followed to prepare **XIX**. Flash chromatography of the crude (ethyl acetate: hexane = 1:8) over SiO<sub>2</sub> gave an orange solid in 84.4% yields. MS (ESI) (M<sup>+</sup>, C<sub>40</sub>H<sub>42</sub>N<sub>2</sub>O<sub>3</sub>S<sub>2</sub>Si): calcd: 690.24; found: 690.23. <sup>1</sup>H NMR (500 MHz, CDCl<sub>3</sub>) δ 9.70 (dd, *J* = 8.2, 4.9 Hz, 1H), 7.66 (d, *J* = 5.4 Hz, 4H), 7.57 (d, *J* = 2.4 Hz, 1H), 7.41 – 7.31 (m, 6H), 7.23 (dd, *J* = 9.0, 2.6 Hz, 2H), 7.05 (dd, *J* = 8.9, 2.5 Hz, 3H), 6.86 (dd, *J* = 9.0, 2.6 Hz, 2H), 6.49 (d, *J* = 6.5 Hz, 2H), 6.29 (d, *J* = 2.4 Hz, 1H), 3.79 (t, *J* = 5.2 Hz, 5H), 3.44 (t, *J* = 5.2 Hz, 2H), 3.36 – 3.30 (m, 2H), 1.11 (t, *J* = 7.0, 3H), 1.05 (s, 9H). <sup>13</sup>C NMR (126 MHz, CDCl<sub>3</sub>) δ 181.34, 164.36, 157.29, 148.48, 146.40, 139.52, 139.11, 135.58, 134.39, 133.37, 129.72, 127.72, 127.30, 126.42, 114.76, 112.09, 100.67, 61.21, 60.33, 55.47, 51.98, 45.38, 26.83, 21.00, 19.07, 14.19, 12.11.

#### 1.2.22 Synthesis of (E)-3-(2-(5-((4-((2-((tert-butyldiphenylsilyloxy)ethyl)(ethylamino)phenyl)(4-methoxyphenyl)amino)thieno[3,2-b]thiophen-2-yl)vinyl)-2-((2-hydroxyethyl)thio)-5,5-dimethylcyclohex-2-en-1-one (Compound XX)

The procedure for **VIII** was followed to prepare **XX**. Flash chromatography of the crude (acetone: hexane = 1:5) over SiO<sub>2</sub> gave a red solid in 64.5% yields. MS (ESI) (M<sup>+</sup>, C<sub>51</sub>H<sub>58</sub>N<sub>2</sub>O<sub>4</sub>S<sub>3</sub>Si): calcd: 886.33; found: 886.23. <sup>1</sup>H NMR (500 MHz, CDCl<sub>3</sub>) δ 7.74 (d, *J* = 15.7 Hz, 1H), 7.65 (m, 4H), 7.42 – 7.29 (m, 6H), 7.25 (d, *J* = 15.7 Hz, 1H), 7.13 (m, 4H), 7.07 – 6.99 (m, 3H), 6.98 – 6.92 (m, 2H), 6.86 – 6.81 (m, 2H), 6.77 (d, *J* = 7.2 Hz, 2H), 6.51 – 6.41 (m, 3H), 6.38 (s, 1H), 3.82 – 3.70 (m, 2H), 3.55 (s, 3H), 3.42 (m, 2H), 3.36 – 3.25 (m, 2H), 2.78 (t, *J* = 4.8 Hz, 2H), 2.41 (s, 2H), 2.37 (s, 2H), 1.11 – 1.06 (m, 3H), 1.05 (s, 6H), 1.02 (s, 9H). <sup>13</sup>C NMR (126 MHz, CDCl<sub>3</sub>) δ 196.73, 166.74, 135.52, 133.34, 129.67, 128.62, 127.67, 126.77, 125.35, 114.57, 114.57, 112.18, 112.07, 55.46, 51.49, 48.01, 37.66, 32.56, 28.03, 26.81, 24.48, 19.03, 14.16.

#### 1.2.23 Synthesis of (E)-3-(2-(5-((4-((2-((tert-butyldiphenylsilyloxy)ethyl)(ethylamino)phenyl)(4-methoxyphenyl)amino)thieno[3,2-b]thiophen-2-yl)vinyl)-2-((2-((tert-butyldiphenylsilyloxy)ethyl)thio)-

### 5,5-dimethylcyclohex-2-en-1-one (Compound XXI)

The procedure for **XV** was followed to prepare **XXI**. Flash chromatography of the crude (ethyl acetate: hexane = 1:5) over SiO<sub>2</sub> gave a red solid in 85% yields. MS (ESI) (M<sup>+</sup>, C<sub>67</sub>H<sub>76</sub>N<sub>2</sub>O<sub>4</sub>S<sub>3</sub>Si<sub>2</sub>): calcd: 1124.45; found: 1124.45. <sup>1</sup>H NMR (500 MHz, CDCl<sub>3</sub>) δ 7.73 – 7.68 (d, 1H), 7.68 – 7.59 (m, 8H), 7.41 – 7.28 (m, 12H), 7.19 – 7.14 (m, 2H), 7.14 – 7.06 (m, 2H), 7.02 (dd, *J* = 8.3, 6.2 Hz, 2H), 6.98 – 6.92 (m, 1H), 6.86 – 6.80 (m, 2H), 6.78 (dd, *J* = 6.8, 2.2 Hz, 1H), 6.50 – 6.42 (m, 3H), 6.40 (t, *J* = 3.1 Hz, 1H), 3.71 (t, *J* = 6.8 Hz, 2H), 3.43 (s, 3H), 3.34 – 3.28 (m, 2H), 2.96 (t, *J* = 6.9 Hz, 2H), 2.92 – 2.87 (m, 2H), 2.48 (s, 2H), 2.32 (s, 2H), 2.14 (d, *J* = 5.2 Hz, 2H). <sup>13</sup>C NMR (126 MHz, CDCl<sub>3</sub>) δ 195.41, 159.43, 156.34, 145.74, 140.79, 139.53, 135.54, 133.57, 129.71, 129.52, 127.65, 126.68, 125.12, 123.43, 122.12, 114.54, 112.10, 104.44, 63.63, 61.26, 60.31, 55.46, 52.05, 45.39, 41.10, 36.19, 32.52, 32.17, 31.55, 28.31, 27.43, 26.83, 25.49, 22.62, 20.99, 19.13, 14.15, 12.16.

### 1.2.24 Synthesis of (E)-2-(3-((E)-2-(5-((4-((2-((tert-butylidiphenylsilyloxy)ethyl)(ethyl)amino)phenyl)(4-(dimethylamino)phenyl)amino)thieno[3,2-b]thiophen-2-yl)vinyl)-5,5-dimethylcyclohex-2-en-1-ylidene)acetonitrile (Compound XXIIa), (E)-2-(3-((E)-2-(5-((4-((2-((tert-butylidiphenylsilyloxy)ethyl)(ethyl)amino)phenyl)(4-(dimethylamino)phenyl)amino)thieno[3,2-b]thiophen-2-yl)vinyl)-2-((2-((tert-butylidiphenylsilyloxy)ethyl)thio)-5,5-dimethylcyclohex-2-en-1-ylidene)acetonitrile (Compound XXIIb) and (E)-2-(3-((E)-2-(5-((4-((2-((tert-butylidiphenylsilyloxy)ethyl)(ethyl)amino)phenyl)(4-methoxyphenyl)amino)thieno[3,2-b]thiophen-2-yl)vinyl)-2-((2-((tert-butylidiphenylsilyloxy)ethyl)thio)-5,5-dimethylcyclohex-2-en-1-ylidene)acetonitrile (Compound XXIIc)

The procedure for compound **9** was followed to prepare **XXIIa**, **XXIIb** and **XXIIc**. Flash chromatography of the crude (ethyl acetate: hexane = 1:8 to 1:6) over SiO<sub>2</sub> gave a red solid in 84.5% and 81.4% and 73.2% yields. **XXIIa** MS (ESI) (M<sup>+</sup>, C<sub>52</sub>H<sub>58</sub>N<sub>4</sub>O<sub>2</sub>S<sub>2</sub>Si): calcd: 846.38; found: 846.40. <sup>1</sup>H NMR (500 MHz, CDCl<sub>3</sub>) δ 7.53 – 7.49 (m, 4H), 7.25 (m, 2H), 7.22 – 7.17 (m, 4H), 7.00 – 6.96 (m, 2H), 6.93 – 6.89 (m, 1H), 6.87 (dd, *J* = 9.0, 1.9 Hz, 2H), 6.82 (d, *J* = 9.3 Hz, 1H), 6.80 (d, *J* = 4.0 Hz, 1H), 6.54 – 6.48 (m, 3H), 6.30 (t, *J* = 8.6 Hz, 3H), 6.20 (d, *J* = 7.9 Hz, 1H), 3.66 – 3.60 (m, 2H), 3.26 (q, *J* = 6.6 Hz, 2H), 3.19 – 3.13 (m, 2H), 2.77 (s, 6H), 2.74 (d, *J* = 2.6 Hz, 2H), 2.08 (d, *J* = 5.2 Hz, 2H), 0.94 (t, *J* = 6.5 Hz, 3H), 0.91 (s, 9H), 0.86 (s, 6H). <sup>13</sup>C NMR (126 MHz, CDCl<sub>3</sub>) δ 147.95, 145.40, 135.63, 133.55, 129.72, 127.73, 113.30, 112.20, 44.69, 42.08, 38.94, 34.69, 31.59, 31.22, 29.70, 28.12, 26.88, 25.30, 22.65, 19.12, 14.10.

**XXIIb** MS (ESI) (M<sup>+</sup>, C<sub>70</sub>H<sub>80</sub>N<sub>4</sub>O<sub>2</sub>S<sub>3</sub>Si<sub>2</sub>): calcd: 1160.50; found: 1160.55. <sup>1</sup>H NMR (500 MHz, CDCl<sub>3</sub>) δ 7.68 – 7.58 (m, 10H), 7.45 – 7.30 (m, 16H), 7.13 (br, 4H), 6.68 (s, 2H), 6.46 (s, 2H), 6.32 – 6.04 (br, 1H), 3.78 (t, *J* = 6.5 Hz, 2H), 3.71 (t, *J* = 7.0 Hz, 2H), 3.34 (br, 4H), 2.95 (br, 6H), 2.69 (t, *J* = 7.0 Hz, 2H), 2.46 (s, 2H), 1.09 (t, *J* = 6.9 Hz, 3H), 1.06 – 1.02 (m, 18H), 0.95 (s, 6H). <sup>13</sup>C NMR (126 MHz, CDCl<sub>3</sub>) δ 170.19, 147.96, 145.43, 135.50, 133.46, 129.70, 127.69, 113.19, 112.06, 63.19, 60.36, 43.28, 41.40, 40.80, 37.45, 30.07, 27.97, 26.84, 21.03, 19.17, 14.20.

**XXIIc** MS (ESI) (M<sup>+</sup>, C<sub>69</sub>H<sub>77</sub>N<sub>3</sub>O<sub>3</sub>S<sub>3</sub>Si<sub>2</sub>): calcd: 1147.47; found: 1147.48. <sup>1</sup>H NMR (500 MHz, CDCl<sub>3</sub>) δ 7.63 (m, 8H), 7.44 – 7.27 (m, 12H), 7.16 (d, *J* = 8.7 Hz, 2H), 7.00 (dd, *J* = 14.6, 11.4 Hz, 3H), 6.93 (d, *J* = 12.5 Hz, 1H), 6.83 (d, *J* = 8.7 Hz, 2H), 6.48 (d, *J* = 8.7 Hz, 2H), 6.40 (d, *J* = 12.0 Hz, 1H), 6.18 (d, *J* = 12.0 Hz, 1H), 3.79 (s, 2H), 3.77 (s, 3H), 3.71 (d, *J* = 6.6 Hz, 2H), 3.42 (d, *J* = 5.9 Hz, 2H), 3.36 – 3.24 (m, 2H), 2.73 – 2.63 (m, 2H), 2.46 (s, 2H), 2.32 (s, 2H), 1.10 (t, *J* = 5.9 Hz, 3H), 1.06 – 0.99 (m, 18H), 0.94 (s, 3H), 0.92 (s, 3H). <sup>13</sup>C NMR (126 MHz, CDCl<sub>3</sub>) δ 158.70, 156.19, 148.01, 145.67, 140.85, 140.16, 139.71, 135.60, 133.46, 129.72, 127.71,

126.60, 124.88, 121.12, 114.54, 112.11, 104.94, 95.19, 63.19, 61.30, 55.53, 52.08, 45.42, 43.27, 41.39, 37.50, 30.08, 27.98, 26.84, 19.17, 12.19.

**1.2.25 Synthesis of (E)-2-(3-((E)-2-(5-((4-((2-((tert-butyl)diphenylsilyloxy)ethyl)(ethyl)amino)phenyl)(4-(dimethylamino)phenyl)amino)thieno[3,2-b]thiophen-2-yl)vinyl)-5,5-dimethylcyclohex-2-en-1-ylidene)acetaldehyde (Compound XXIIIa), (E)-2-(3-((E)-2-(5-((4-((2-((tert-butyl)diphenylsilyloxy)ethyl)(ethyl)amino)phenyl)(4-(dimethylamino)phenyl)amino)thieno[3,2-b]thiophen-2-yl)vinyl)-2-((2-((tert-butyl)diphenylsilyloxy)ethyl)thio)-5,5-dimethylcyclohex-2-en-1-ylidene)acetaldehyde (Compound XXIIIb) and (E)-2-(3-((E)-2-(5-((4-((2-((tert-butyl)diphenylsilyloxy)ethyl)(ethyl)amino)phenyl)(4-methoxyphenyl)amino)thieno[3,2-b]thiophen-2-yl)vinyl)-2-((2-((tert-butyl)diphenylsilyloxy)ethyl)thio)-5,5-dimethylcyclohex-2-en-1-ylidene)acetaldehyde (Compound XXIIIc)**

The procedure for compound X was followed to prepare **XXIIIa**, **XXIIIb** and **XXIIIc**. Flash chromatography of the crude (ethyl acetate: hexane = 1:5) over SiO<sub>2</sub> gave a red solid in 87.5%, 81.4% and 76.5% yields. **XXIIIa** MS (ESI) (M<sup>+</sup>, C<sub>52</sub>H<sub>59</sub>N<sub>3</sub>O<sub>2</sub>S<sub>2</sub>Si): calcd: 849.38; found: 849.43. <sup>1</sup>H NMR (500 MHz, CDCl<sub>3</sub>) δ 10.23 (d, *J* = 8.0 Hz, 0.4H), 10.07 (d, *J* = 8.2 Hz, 0.6H), 7.69 (d, *J* = 6.8 Hz, 4H), 7.42 (m, 6H), 7.16 (s, 2H), 7.05 (d, *J* = 7.1 Hz, 2H), 7.02 – 6.90 (m, 2H), 6.71 (d, *J* = 8.3 Hz, 2H), 6.59 (d, *J* = 16.7 Hz, 2H), 6.49 (d, *J* = 8.2 Hz, 2H), 6.34 (d, 2H), 5.93 (s, 1H), 3.81 (t, *J* = 6.4 Hz, 2H), 3.45 (s, 2H), 3.35 (d, *J* = 6.4 Hz, 2H), 2.97 (s, 6H), 2.33 (s, 2H), 2.08 (s, 2H), 1.29 (t, *J* = 7.1 Hz, 3H), 1.15 – 1.04 (m, 15H). <sup>13</sup>C NMR (126 MHz, CDCl<sub>3</sub>) δ 190.54, 147.96, 145.43, 135.65, 133.52, 129.75, 127.75, 113.27, 112.14, 60.41, 39.12, 38.88, 31.10, 29.73, 28.42, 28.28, 26.89, 19.14, 14.15.

**XXIIIb** MS (ESI) (M<sup>+</sup>, C<sub>70</sub>H<sub>81</sub>N<sub>3</sub>O<sub>3</sub>S<sub>3</sub>Si<sub>2</sub>): calcd: 1163.50; found: 1163.47. <sup>1</sup>H NMR (500 MHz, CDCl<sub>3</sub>) δ 10.09 (d, *J* = 8.0 Hz) 7.72 (d, *J* = 15.7 Hz, 1H), 7.68 – 7.57 (m, 8H), 7.43 – 7.27 (m, 12H), 7.15 (d, *J* = 8.9 Hz, 2H), 7.04 (d, *J* = 8.9 Hz, 2H), 7.01 (s, 1H), 6.98 – 6.91 (m, 2H), 6.68 (d, *J* = 9.0 Hz, 2H), 6.47 (d, *J* = 9.0 Hz, 2H), 6.34 (s, 1H), 3.79 (t, *J* = 6.6 Hz, 2H), 3.73 (t, *J* = 7.2 Hz, 2H), 3.42 (t, *J* = 6.6 Hz, 2H), 3.32 (q, *J* = 6.8 Hz, 2H), 2.94 (s, 6H), 2.72 (t, *J* = 7.2 Hz, 2H), 2.61 (s, 2H), 2.35 (s, 2H), 1.13 – 1.08 (m, 3H), 1.05 (s, 9H), 1.02 (s, 9H), 0.95 (s, 6H). <sup>13</sup>C NMR (126 MHz, CDCl<sub>3</sub>) δ 191.40, 156.10, 149.07, 147.96, 145.42, 135.51, 133.51, 129.71, 127.72, 126.27, 125.71, 113.20, 112.07, 63.46, 61.29, 52.12, 45.43, 41.41, 40.82, 39.74, 37.16, 34.66, 31.58, 29.95, 28.26, 26.85, 25.27, 22.64, 19.10, 14.12, 12.20.

**XXIIIc** MS (ESI) (M<sup>+</sup>, C<sub>69</sub>H<sub>78</sub>N<sub>2</sub>O<sub>4</sub>S<sub>3</sub>Si<sub>2</sub>): calcd: 1150.47; found: 1150.52. <sup>1</sup>H NMR (500 MHz, CDCl<sub>3</sub>) δ 10.11 – 10.05 (m, 1H), 7.74 (dd, *J* = 15.8, 5.3 Hz, 1H), 7.69 – 7.57 (m, 8H), 7.34 (m, 12H), 7.16 (dd, *J* = 8.6, 6.0 Hz, 2H), 7.04 – 6.99 (m, 3H), 6.98 – 6.91 (m, 2H), 6.86 – 6.79 (m, 2H), 6.50 – 6.44 (m, 2H), 6.42 (d, *J* = 5.6 Hz, 1H), 3.79 (d, *J* = 5.9 Hz, 5H), 3.76 – 3.69 (m, 2H), 3.42 (d, *J* = 5.9 Hz, 2H), 3.36 – 3.27 (m, 2H), 2.75 – 2.68 (m, 2H), 2.61 (s, 2H), 2.35 (s, 2H), 1.03 (m, 18H), 0.96 (t, *J* = 5.9 Hz, 6H). <sup>13</sup>C NMR (126 MHz, CDCl<sub>3</sub>) δ 191.42, 158.63, 156.17, 148.91, 145.66, 140.39, 135.60, 133.50, 129.72, 127.72, 126.58, 124.85, 114.52, 112.11, 105.03, 63.44, 61.28, 55.52, 52.08, 45.41, 41.41, 39.72, 37.18, 31.58, 29.96, 28.26, 26.84, 19.10, 14.12, 12.18.

**1.2.26 Synthesis of 2-(4-((1E,3E)-3-(3-((E)-2-(5-((4-((2-((tert-butyl)diphenylsilyloxy)ethyl)(ethyl)amino)phenyl)(4-(dimethylamino)phenyl)amino)thieno[3,2-b]thiophen-2-yl)vinyl)-5,5-dimethylcyclohex-2-en-1-ylidene)prop-1-en-1-yl)-3-cyano-5-phenyl-5-(trifluoromethyl)furan-2(5H)-ylidene)malononitrile (BTP5), 2-(4-((1E,3E)-3-(3-((E)-2-(5-((4-((2-((tert-**

butyldiphenylsilyloxy)ethyl)(ethyl)amino)phenyl)(4-(dimethylamino)phenyl)amino)thieno[3,2-b]thiophen-2-yl)vinyl)-2-((2-((tert-butylidiphenylsilyloxy)ethyl)thio)-5,5-dimethylcyclohex-2-en-1-ylidene)prop-1-en-1-yl)-3-cyano-5-phenyl-5-(trifluoromethyl)furan-2(5H)-ylidene)malononitrile (**BTP7**) and 2-(4-((1E,3E)-3-(3-((E)-2-(5-((4-((2-((tert-butylidiphenylsilyloxy)ethyl)(ethyl)amino)phenyl)(4-methoxyphenyl)amino)thieno[3,2-b]thiophen-2-yl)vinyl)-2-((2-((tert-butylidiphenylsilyloxy)ethyl)thio)-5,5-dimethylcyclohex-2-en-1-ylidene)prop-1-en-1-yl)-3-cyano-5-phenyl-5-(trifluoromethyl)furan-2(5H)-ylidene)malononitrile (**BTH1**)

The procedure for compound **BTP3** was followed to prepare **BTP5**, **BTP7** and **BTH1**. Flash chromatography of the crude (ethyl acetate: hexane = 1:8 to 1:4) over SiO<sub>2</sub> gave a black solid in 52.3%, 41.4% and 39.3% yields. **BTP5** HRMS (ESI) (M<sup>+</sup>, C<sub>52</sub>H<sub>59</sub>N<sub>3</sub>O<sub>2</sub>S<sub>2</sub>Si): calcd: 1146.4332; found: 1146.4337. <sup>1</sup>H NMR (500 MHz, THF) δ 7.99 (s, 1H, CH), 7.60 – 7.54 (m, 4H, Ar-H), 7.51 (d, *J* = 1.3 Hz, 2H, Ar-H), 7.47 – 7.40 (m, 3H, Ar-H), 7.29 (t, *J* = 6.7 Hz, 2H, Ar-H), 7.24 (t, *J* = 7.0 Hz, 4H, Ar-H), 7.17 (d, *J* = 15.3 Hz, 1H, CH), 7.11 (s, 1H, CH), 7.02 (d, *J* = 8.9 Hz, 2H, Ar-H), 6.94 (d, *J* = 8.9 Hz, 2H, Ar-H), 6.60 (d, *J* = 8.9 Hz, 2H, Ar-H), 6.54 (d, *J* = 15.4 Hz, 1H, CH), 6.46 (d, *J* = 9.0 Hz, 2H, Ar-H), 6.37 (s, 1H, CH), 6.31 (s, 1H, CH), 6.28 (s, 1H, CH), 6.17 (s, 1H, CH), 3.70 (t, *J* = 6.3 Hz, 2H, OCH<sub>2</sub>), 3.43 – 3.35 (m, 2H, NH<sub>2</sub>), 3.34 – 3.25 (m, 2H, NH<sub>2</sub>), 2.83 (s, 6H, NCH<sub>3</sub>), 2.31 (s, 2H, CH<sub>2</sub>), 2.20 (m, 2H, CH<sub>2</sub>), 1.00 (t, *J* = 7.0 Hz, 3H, CH<sub>3</sub>), 0.94 (s, 9H, CH<sub>3</sub>), 0.90 (s, 3H, CH<sub>3</sub>), 0.85 (s, 3H, CH<sub>3</sub>). <sup>13</sup>C NMR (126 MHz, THF) δ 175.53, 166.84, 149.01, 146.37, 143.80, 135.53, 133.33, 132.75, 131.42, 130.79, 129.69, 129.38, 127.68, 126.71, 126.31, 123.90, 121.62, 100.00, 61.35, 54.82, 51.94, 45.31, 39.83, 39.28, 38.94, 31.29, 30.47, 29.00, 27.86, 27.36, 26.41, 22.97, 18.82, 13.57, 11.59, 10.51 (CF<sub>3</sub> carbon too weak to observe).

**BTP7** HRMS (ESI) (M<sup>+</sup>, C<sub>86</sub>H<sub>87</sub>F<sub>3</sub>N<sub>6</sub>O<sub>3</sub>S<sub>3</sub>Si<sub>2</sub>): calcd: 1460.5492; found: 1460.5479. <sup>1</sup>H NMR (500 MHz, THF) δ 7.98 (t, *J* = 12.9 Hz, 1H, CH), 7.67 (d, *J* = 16.4 Hz, 1H, CH), 7.59 – 7.55 (m, 4H, Ar-H), 7.52 (d, *J* = 6.4 Hz, 2H, Ar-H), 7.48 (d, *J* = 7.0 Hz, 4H, Ar-H), 7.42 (d, *J* = 6.8 Hz, 3H, Ar-H), 7.37 (d, *J* = 12.3 Hz, 1H), 7.28 (t, *J* = 7.3 Hz, 2H, CH), 7.23 (t, *J* = 7.2 Hz, 6H, Ar-H), 7.16 (m, 6H, Ar-H), 7.04 (d, *J* = 7.7 Hz, 2H, Ar-H), 6.95 (d, *J* = 7.5 Hz, 2H, Ar-H), 6.61 (d, *J* = 8.8 Hz, 2H, Ar-H), 6.47 (d, *J* = 8.7 Hz, 2H, Ar-H), 6.42 (d, *J* = 14.5 Hz, 1H, CH), 6.18 (s, 1H, CH), 3.71 (t, *J* = 6.2 Hz, 2H, OCH<sub>2</sub>), 3.63 (t, *J* = 7.0 Hz, 2H, OCH<sub>2</sub>), 3.39 (s, 2H, NH<sub>2</sub>), 3.30 (s, 2H, NH<sub>2</sub>), 2.83 (s, 6H, NCH<sub>3</sub>), 2.63 (t, *J* = 7.0 Hz, 2H, SCH<sub>2</sub>), 2.40 (s, 2H, CH<sub>2</sub>), 2.18 (m, 2H, CH<sub>2</sub>), 1.00 (t, *J* = 6.9 Hz, 3H, CH<sub>3</sub>), 0.94 (s, 9H, CH<sub>3</sub>), 0.89 (s, 9H, CH<sub>3</sub>), 0.82 (s, 3H, CH<sub>3</sub>), 0.74 (s, 3H, CH<sub>3</sub>). <sup>13</sup>C NMR (126 MHz, THF) δ 175.39, 148.83, 146.09, 135.50, 135.36, 133.32, 130.96, 129.60, 129.48, 127.61, 127.54, 126.76, 112.88, 112.03, 63.31, 41.08, 40.79, 39.73, 39.00, 37.71, 29.95, 29.13, 27.65, 27.07, 26.30, 18.84, 18.76, 13.62, 10.56 (CF<sub>3</sub> carbon too weak to observe).

**BTH1** HRMS (ESI) (M<sup>+</sup>, C<sub>85</sub>H<sub>84</sub>F<sub>3</sub>N<sub>5</sub>O<sub>4</sub>S<sub>3</sub>Si<sub>2</sub>): calcd: 1447.5176; found: 1447.5183. <sup>1</sup>H NMR (500 MHz, THF) δ 7.96 (t, *J* = 13.2 Hz, 1H, CH), 7.69 (d, *J* = 15.5 Hz, 1H, CH), 7.59 – 7.55 (m, 4H, Ar-H), 7.52 (d, *J* = 7.7 Hz, 2H, Ar-H), 7.50 – 7.46 (m, 4H, Ar-H), 7.43 (t, *J* = 5.5 Hz, 3H, Ar-H), 7.38 (d, *J* = 12.4 Hz, 1H, CH), 7.30 – 7.26 (m, 2H), 7.26 – 7.21 (m, 6H, Ar-H), 7.20 – 7.12 (m, 6H, Ar-H), 7.09 (d, *J* = 8.9 Hz, 2H, Ar-H), 6.93 (d, *J* = 8.9 Hz, 2H, Ar-H), 6.77 (d, *J* = 9.0 Hz, 2H, Ar-H), 6.51 – 6.43 (m, 3H, CH + Ar-H), 6.26 (s, 1H, CH), 3.71 (t, *J* = 6.3 Hz, 2H, OCH<sub>2</sub>), 3.66 (s, 3H, OCH<sub>3</sub>), 3.63 (t, *J* = 7.0 Hz, 2H, OCH<sub>2</sub>), 3.39 (t, *J* = 5.8 Hz, 2H, NH<sub>2</sub>), 3.29 (d, *J* = 6.1 Hz, 2H, NH<sub>2</sub>), 2.63 (t, *J* = 7.0 Hz, 2H, SCH<sub>2</sub>), 2.40 (s, 2H, CH<sub>2</sub>), 2.16 (m, 2H, CH<sub>2</sub>), 1.00 (t, *J* = 6.9 Hz, 3H, CH<sub>3</sub>), 0.94 (s, 9H, CH<sub>3</sub>), 0.89 (s, 9H, CH<sub>3</sub>), 0.82 (s, 3H, CH<sub>3</sub>), 0.73 (s, 3H, CH<sub>3</sub>). <sup>13</sup>C NMR (126 MHz, THF) δ 175.32, 161.59, 161.17, 157.22, 156.35, 152.56, 146.36, 146.17, 142.71, 140.46, 140.15, 135.50, 135.36, 135.17, 133.32, 131.07, 130.82, 130.49, 130.39, 130.26, 129.61, 128.44, 127.61, 127.54, 126.84, 125.72, 125.59,

123.37, 116.88, 114.45, 112.12, 111.26, 110.87, 110.37, 63.30, 61.35, 54.73, 51.88, 45.22, 41.07, 40.73, 29.94, 27.66, 27.05, 26.30, 18.80, 11.48 (CF<sub>3</sub> carbon too weak to observe).

### 1.2.27 Synthesis of 5-((4-((tert-butylidiphenylsilyloxy)ethyl)(methylamino)phenyl)(4-(dimethylamino)phenyl)amino)thieno[3,2-b]thiophene-2-carbaldehyde (Compound XXIV)

The procedure for compound **XV** was followed to prepare **XXIV**. Flash chromatography of the crude (ethyl acetate: hexane = 1:8 to 1:4) over SiO<sub>2</sub> gave a red solid in 88% yields. MS (ESI) (M<sup>+</sup>, C<sub>40</sub>H<sub>43</sub>N<sub>3</sub>O<sub>2</sub>S<sub>2</sub>Si): calcd: 689.26; found: 689.20. <sup>1</sup>H NMR (500 MHz, CDCl<sub>3</sub>) δ 9.74 (s, 1H), 7.76 (dd, *J* = 7.9, 1.4 Hz, 4H), 7.59 (s, 1H), 7.50 – 7.41 (m, 6H), 7.28 – 7.25 (m, 2H), 7.16 (d, *J* = 9.0 Hz, 2H), 6.74 (t, *J* = 6.2 Hz, 2H), 6.57 (d, *J* = 9.1 Hz, 2H), 6.31 (s, 1H), 3.88 (t, *J* = 6.4 Hz, 2H), 3.52 (t, *J* = 6.4 Hz, 2H), 3.41 (q, *J* = 7.0 Hz, 2H), 3.00 (s, 6H), 1.19 (t, *J* = 7.0 Hz, 4H), 1.15 (s, 9H). <sup>13</sup>C NMR (126 MHz, CDCl<sub>3</sub>) δ 181.19, 171.07, 165.35, 148.85, 146.30, 138.57, 135.70, 134.69, 133.49, 129.86, 127.86, 126.85, 113.13, 112.19, 99.46, 61.37, 60.42, 52.13, 45.54, 40.68, 26.98, 21.11, 19.20, 14.33, 12.29.

### 1.2.28 Synthesis of (E)-N1-(5-(2-(5-bromothiophen-2-yl)vinyl)thieno[3,2-b]thiophen-2-yl)-N4-(2-((tert-butylidiphenylsilyloxy)ethyl)-N1-(4-(dimethylamino)phenyl)-N4-methylbenzene-1,4-diamine (Compound XXV)

To a stirring solution of **XXIV** (4.01 g, 5.9 mmol) and diethyl (5-bromothiophen-2-yl)phosphonate (1.76 g, 5.9 mmol) was added NaH (0.17 g, 7.1 mmol) by portions. After allowing the mixture to warm to rt over 12 h, the reaction was quenched (H<sub>2</sub>O, 50 mL), extracted with ethyl acetate (3 x 75 ml), dried (Na<sub>2</sub>SO<sub>4</sub>), and concentrated in vacuo to give a crude orange solid. Flash column chromatography (ethyl acetate: hexane = 1:15) over SiO<sub>2</sub> gave a pure orange solid in 91.8% yield (4.6 g, 5.4 mmol). MS (ESI) (M<sup>+</sup>, C<sub>45</sub>H<sub>46</sub>BrN<sub>3</sub>OS<sub>3</sub>Si): calcd: 847.18; found: 847.16. <sup>1</sup>H NMR (500 MHz, CDCl<sub>3</sub>) δ 7.69 (d, *J* = 6.3 Hz, 5H), 7.49 – 7.42 (m, 3H), 7.39 (t, *J* = 7.1 Hz, 6H), 7.01 (br, 6H), 6.71 (br, 2H), 6.50 (br, 2H), 3.82 (s, 2H), 3.37 (s, 2H), 3.00 (s, 6H), 1.13 (d, *J* = 3.6 Hz, 3H), 1.08 (s, 9H). <sup>13</sup>C NMR (126 MHz, CDCl<sub>3</sub>) δ 156.35, 155.09, 143.89, 140.02, 137.55, 130.38, 126.83, 124.55, 122.86, 116.57, 115.75, 62.67, 60.29, 47.41, 46.90, 40.21, 36.62, 32.81, 31.14, 30.32, 26.09, 18.55, 14.26.

### 1.2.29 Synthesis of (E)-5-(2-(5-((4-((tert-butylidiphenylsilyloxy)ethyl)(methylamino)phenyl)(4-(dimethylamino)phenyl)amino)thieno[3,2-b]thiophen-2-yl)vinyl)thiophene-2-carbaldehyde (Compound XXVI)

The procedure for compound **VII** was followed to prepare **XXVI**. Flash chromatography of the crude (ethyl acetate: hexane = 1:6) over SiO<sub>2</sub> gave a red solid in 87.6% yields. MS (ESI) (M<sup>+</sup>, C<sub>46</sub>H<sub>47</sub>N<sub>3</sub>O<sub>2</sub>S<sub>3</sub>Si): calcd: 797.26; found: 797.26. <sup>1</sup>H NMR (500 MHz, CDCl<sub>3</sub>) δ 9.84 (d, *J* = 4.1 Hz, 1H), 7.74 (d, *J* = 6.7 Hz, 4H), 7.65 (td, *J* = 7.1, 3.4 Hz, 1H), 7.50 (d, *J* = 12.6 Hz, 1H), 7.48 – 7.38 (m, 6H), 7.37 – 7.32 (m, 1H), 7.32 – 7.26 (m, 1H), 7.25 – 7.17 (m, 2H), 7.11 (dd, *J* = 12.3, 6.6 Hz, 2H), 7.06 (d, *J* = 2.8 Hz, 1H), 6.74 (d, *J* = 8.2 Hz, 2H), 6.53 (d, *J* = 8.7 Hz, 2H), 6.46 – 6.26 (m, 1H), 3.86 (t, *J* = 6.3 Hz, 2H), 3.49 (s, 2H), 3.39 (s, 2H), 3.00 (s, 6H), 1.17 (t, *J* = 7.1 Hz, 3H), 1.12 (s, 9H). <sup>13</sup>C NMR (126 MHz, CDCl<sub>3</sub>) δ 182.32, 182.13, 171.06, 145.83, 141.63, 136.92, 135.65, 133.57, 129.76, 127.77, 126.56, 126.10, 124.90, 113.25, 112.24, 60.38, 52.20, 45.63, 40.78, 26.92, 21.03, 19.15, 14.24, 12.38.

### 1.2.30 Synthesis of 2-(4-((E)-2-(5-((E)-2-(5-((4-((tert-

**butyldiphenylsilyloxy)ethyl(methylamino)phenyl)(4-(dimethylamino)phenyl)amino)thieno[3,2-b]thiophen-2-yl)vinyl)thiophen-2-yl)vinyl)-3-cyano-5-phenyl-5-(trifluoromethyl)furan-2(5H)-ylidene)malononitrile (BTF1)**

The procedure for **BTP3** was followed to prepare **BTF1**. Flash chromatography of the crude (ethyl acetate: hexane = 1:6 to 1:3) over SiO<sub>2</sub> gave a red solid in 37.5% yields. HRMS (ESI) (M<sup>+</sup>, C<sub>62</sub>H<sub>53</sub>F<sub>3</sub>N<sub>6</sub>O<sub>2</sub>S<sub>3</sub>Si): calcd: 1108.3270; found: 1108.3261. <sup>1</sup>H NMR (500 MHz, CDCl<sub>3</sub>) δ 7.74 – 7.64 (m, 1H, CH), 7.58 (d, *J* = 7.1 Hz, 4H, Ar-H), 7.50 – 7.40 (m, 6H, CH + Ar-H), 7.37 – 7.32 (m, 2H, Ar-H), 7.29 (t, *J* = 7.4 Hz, 5H, CH + Ar-H), 7.22 (s, 1H, CH), 7.18 (s, 1H, CH), 7.10 (d, *J* = 6.8 Hz, 2H, Ar-H), 6.98 (s, 2H, Ar-H), 6.90 (s, 1H, CH), 6.61 (d, *J* = 6.9 Hz, 2H, Ar-H), 6.53 (d, *J* = 15.6 Hz, 1H, CH), 6.40 (d, *J* = 7.6 Hz, 2H, Ar-H), 6.22 (s, 1H, CH), 3.71 (t, *J* = 6.9 Hz, 2H, OCH<sub>2</sub>), 3.36 (d, *J* = 7.8 Hz, 2H, NCH<sub>2</sub>), 3.26 (s, 2H, NCH<sub>2</sub>), 2.93 (s, 6H, NCH<sub>3</sub>), 1.03 (t, *J* = 6.9 Hz, 3H, CH<sub>3</sub>), 0.98 (s, 9H, CH<sub>3</sub>). <sup>13</sup>C NMR (126 MHz, THF) δ 174.99, 174.86, 170.26, 166.76, 140.48, 135.50, 133.33, 132.74, 131.30, 130.65, 130.02, 129.62, 128.64, 127.62, 126.95, 112.92, 112.06, 110.73, 38.97, 30.44, 28.98, 26.33, 22.93, 18.77, 13.48, 10.42.

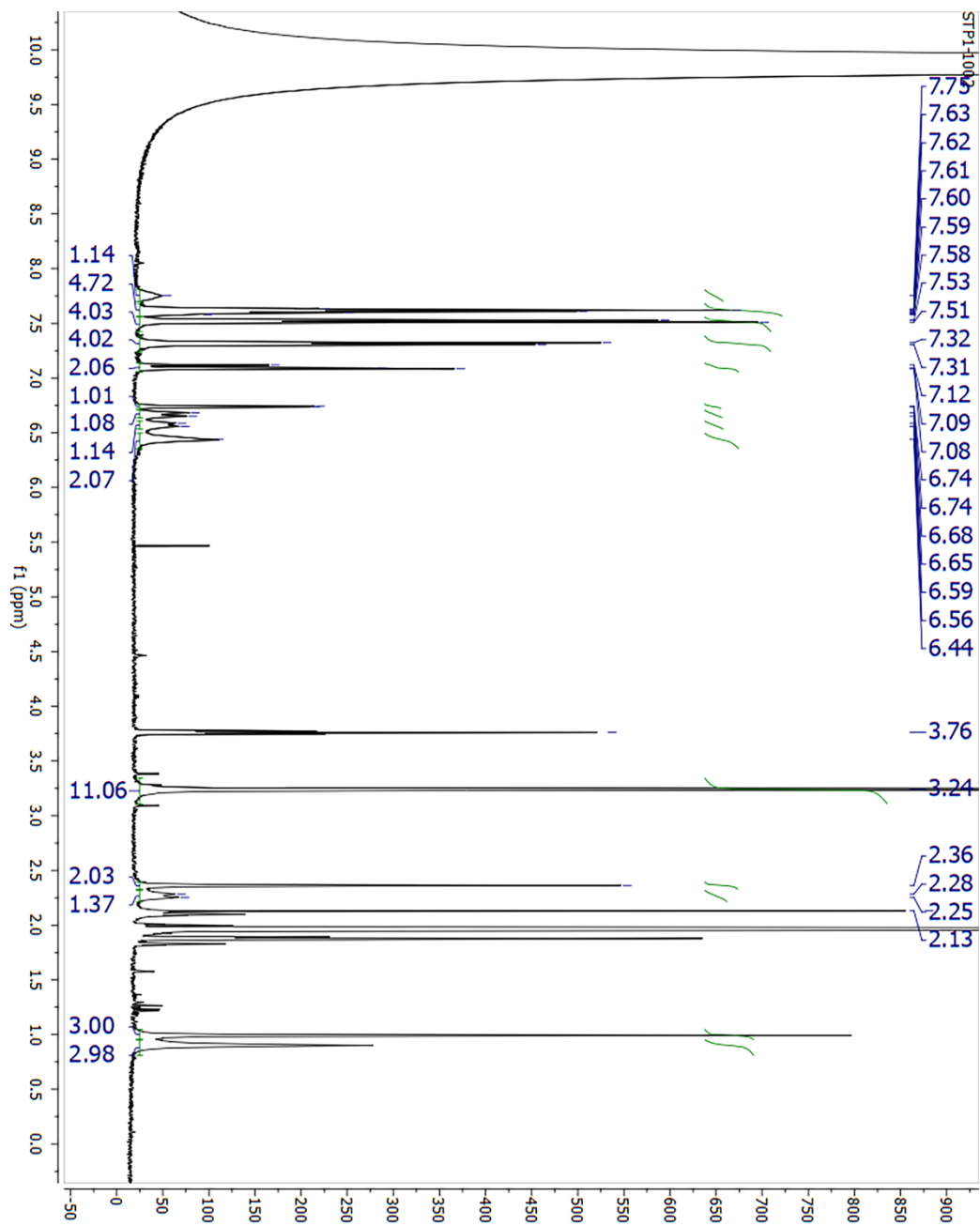


Figure S2. <sup>1</sup>H NMR spectrum of STP1

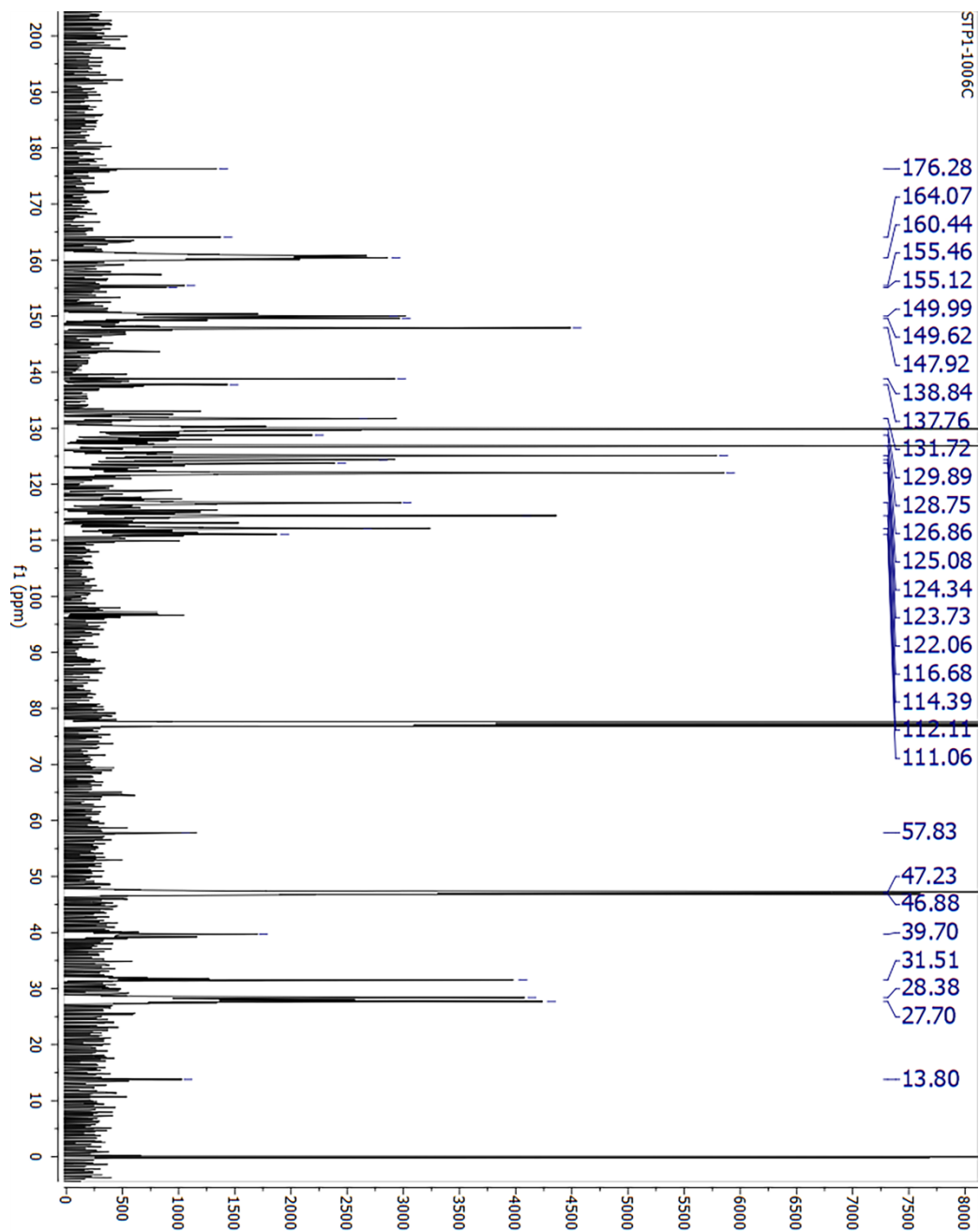


Figure S3.  $^{13}\text{C}$  NMR spectrum of STP1

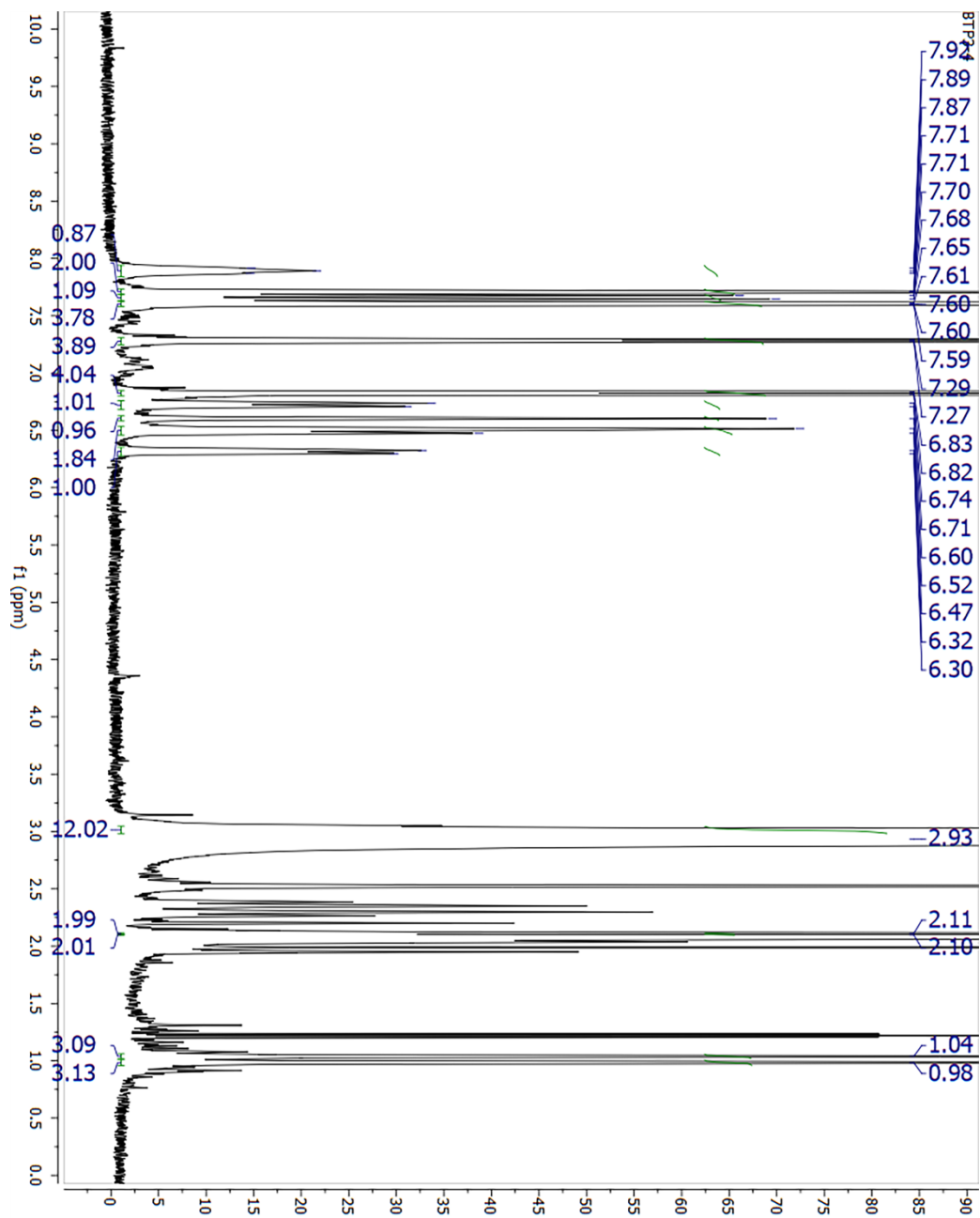


Figure S4.  $^1\text{H}$  NMR spectrum of BTP3.

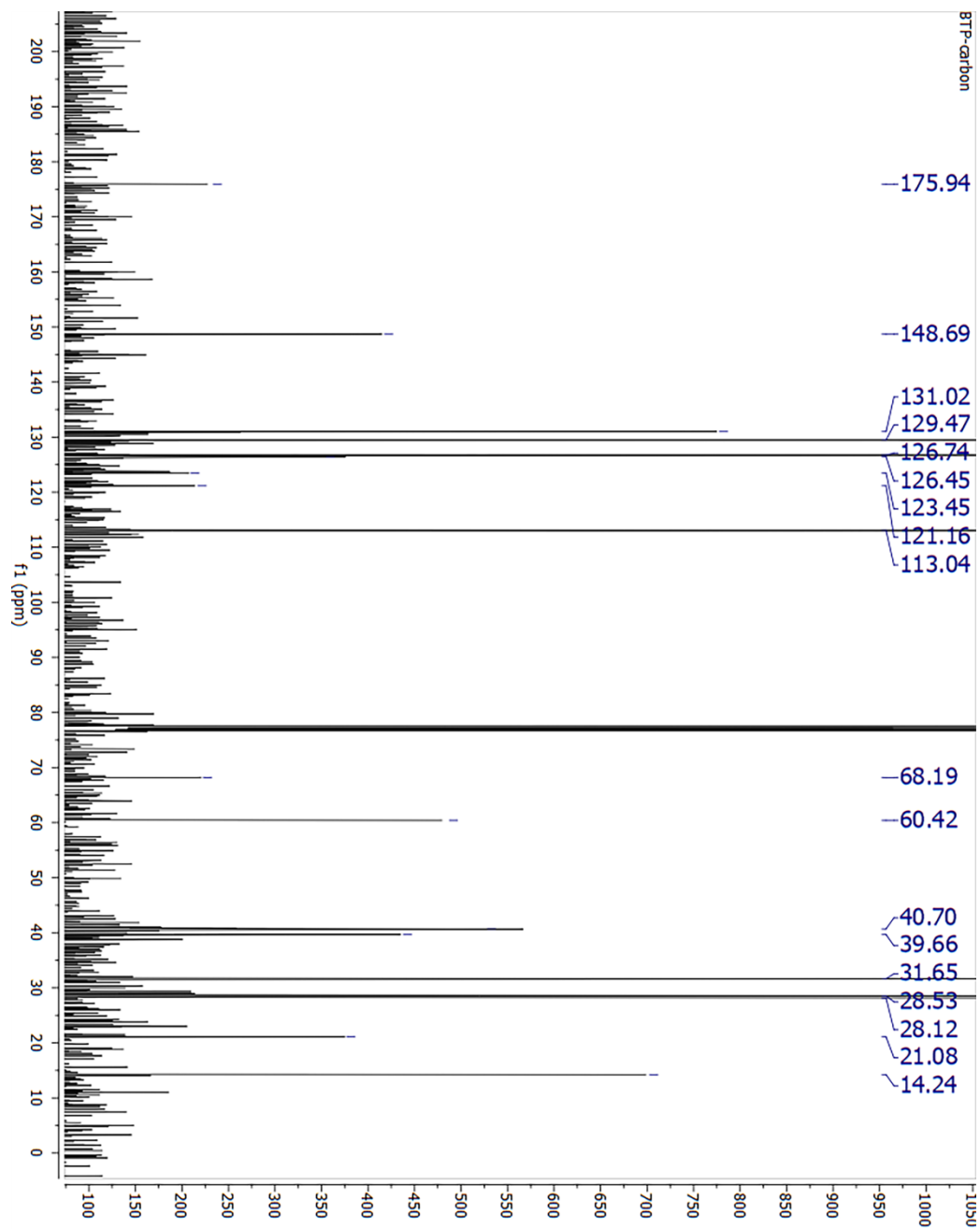


Figure S5.  $^{13}\text{C}$  NMR spectrum of BTP3.

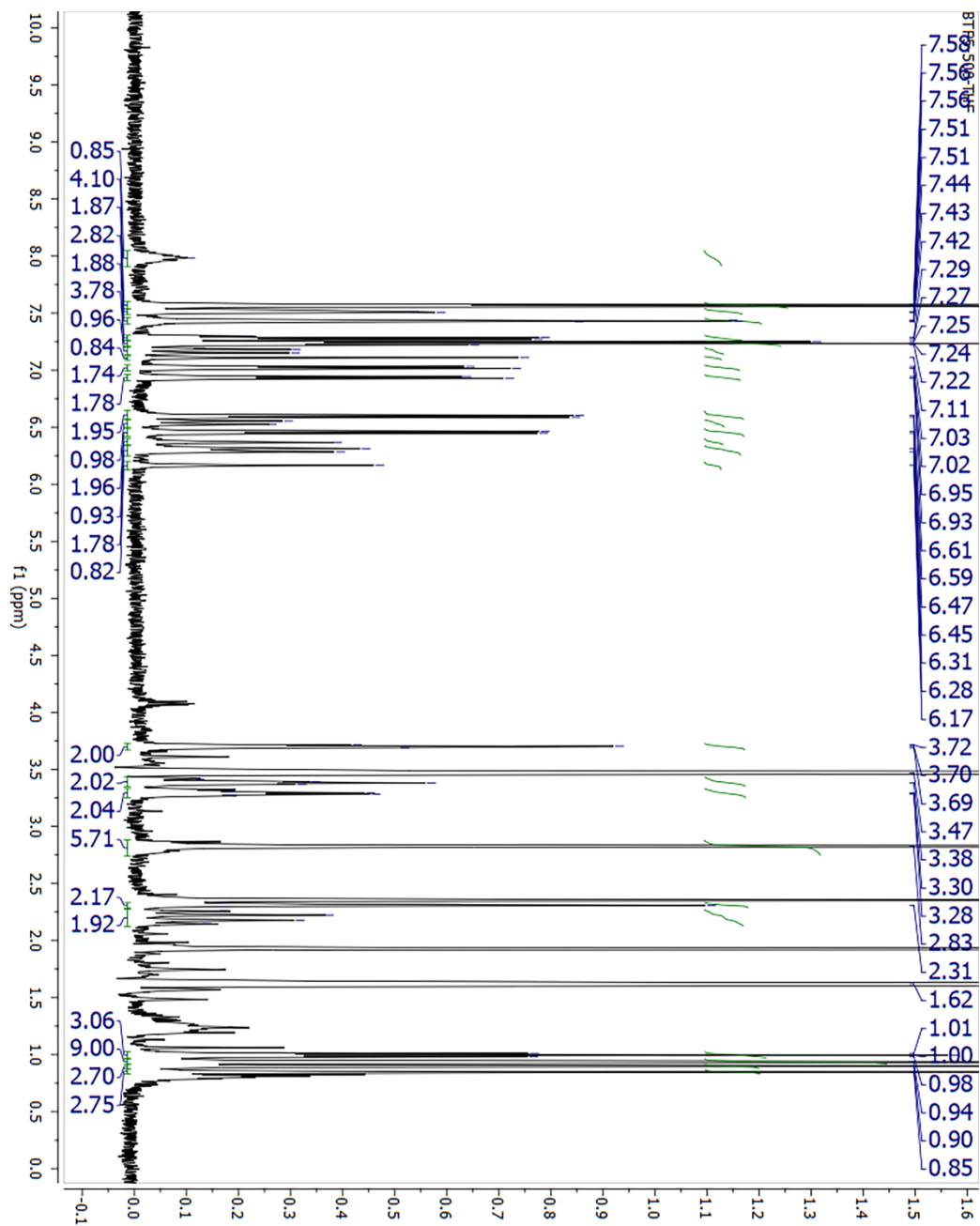


Figure S6.  $^1\text{H}$  NMR spectrum of BTP5.

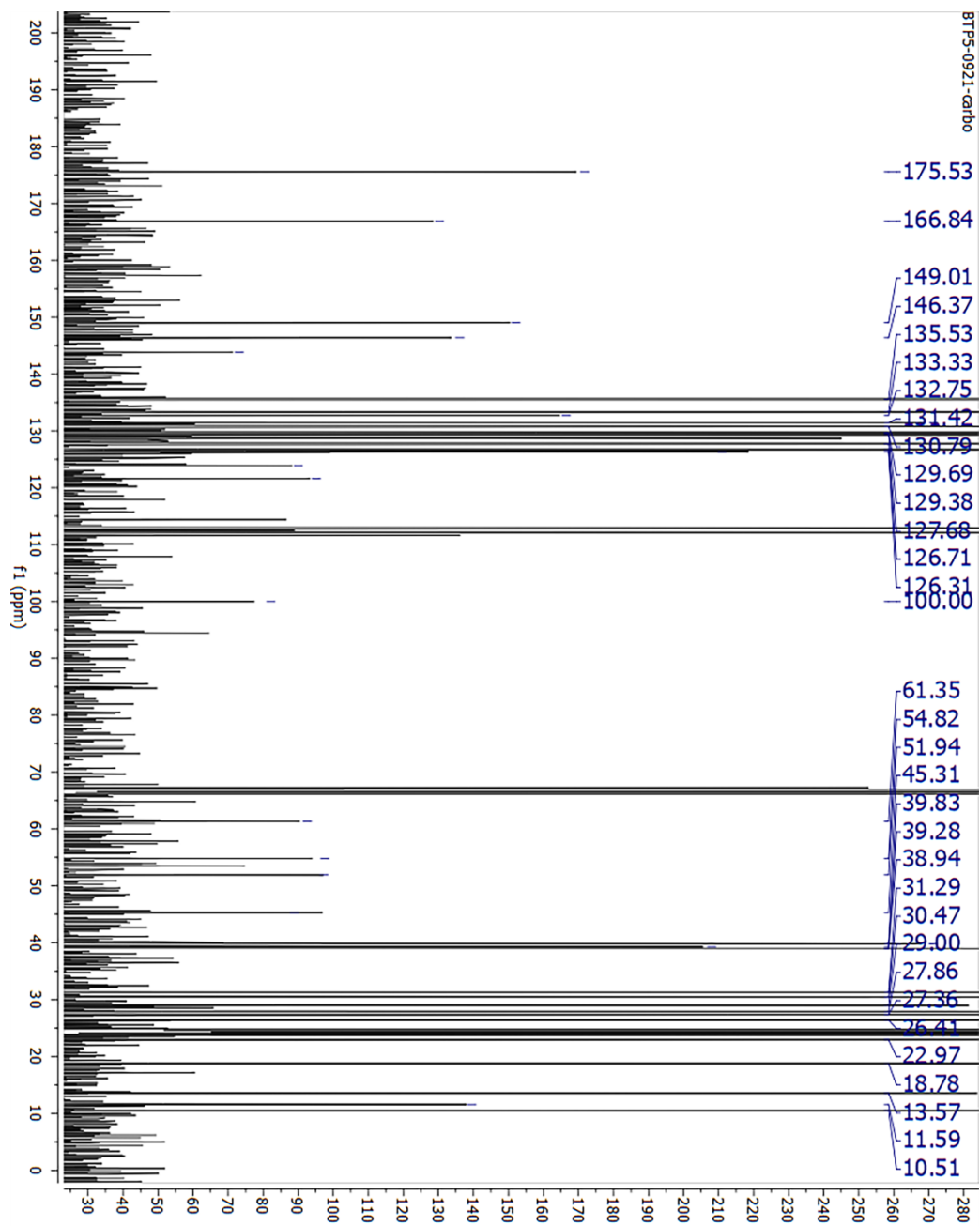


Figure S7.  $^{13}\text{C}$  NMR spectrum of BTP5.

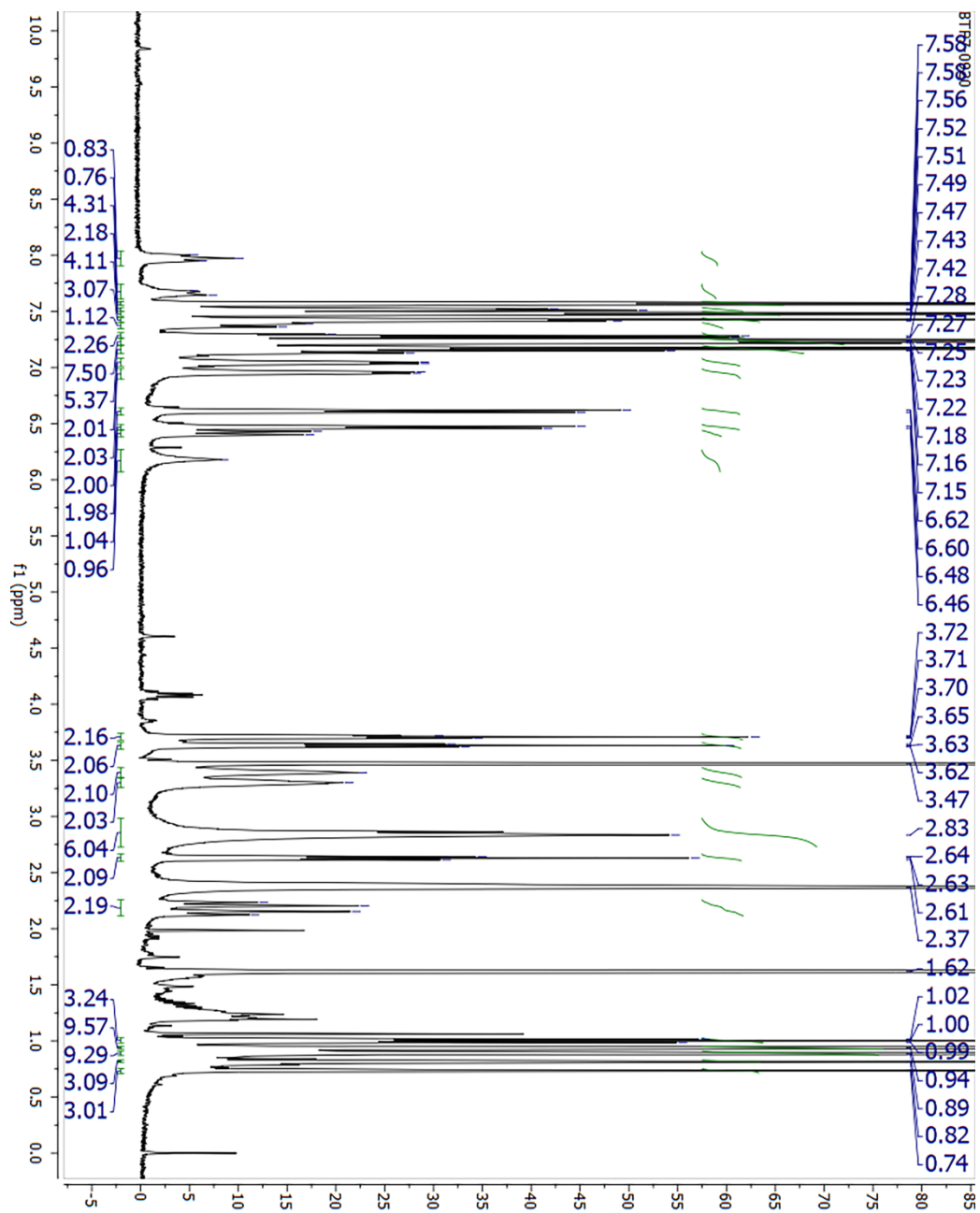


Figure S8.  $^1\text{H}$  NMR spectrum of BTP7.

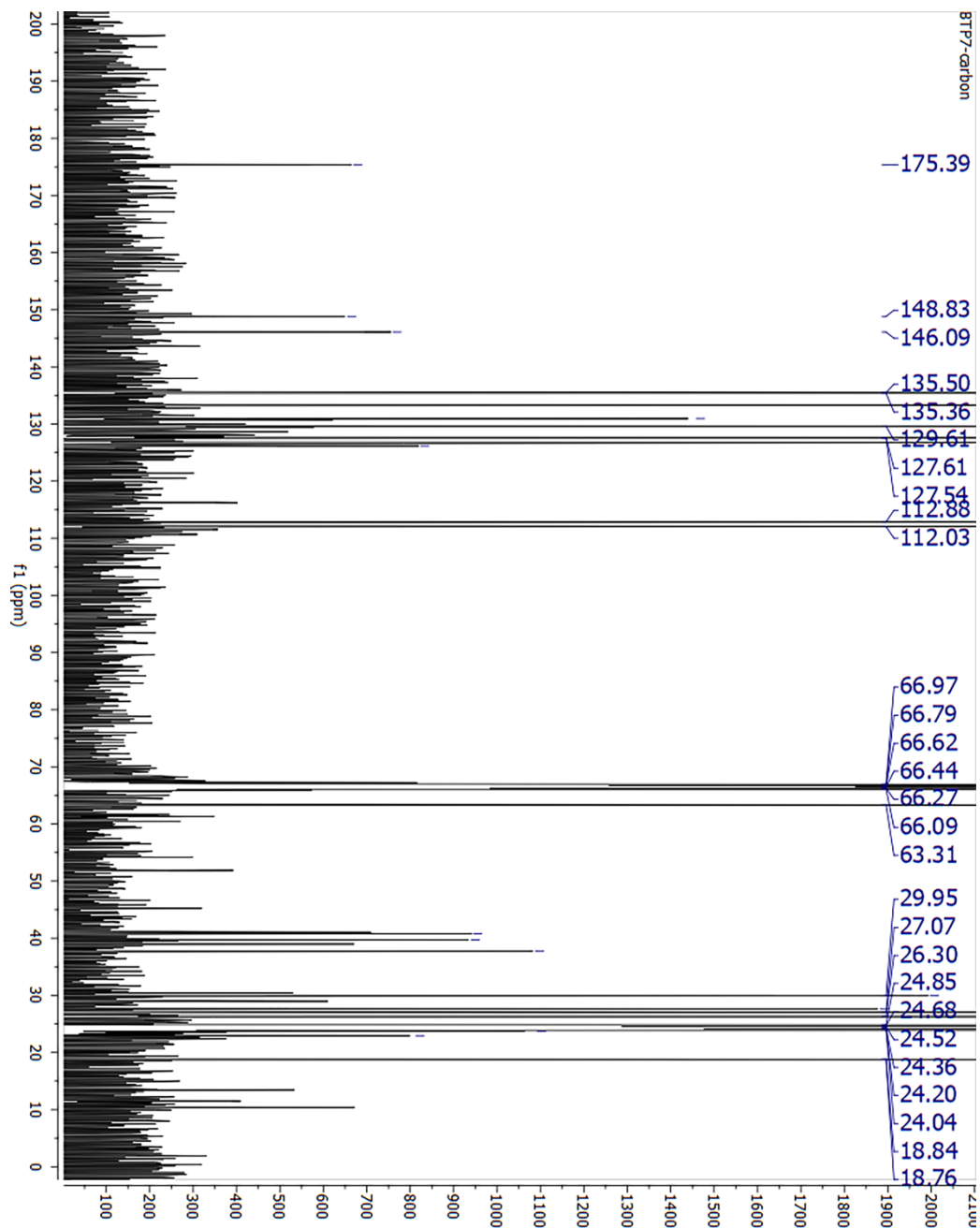


Figure S9.  $^{13}\text{C}$  NMR spectrum of BTP7.

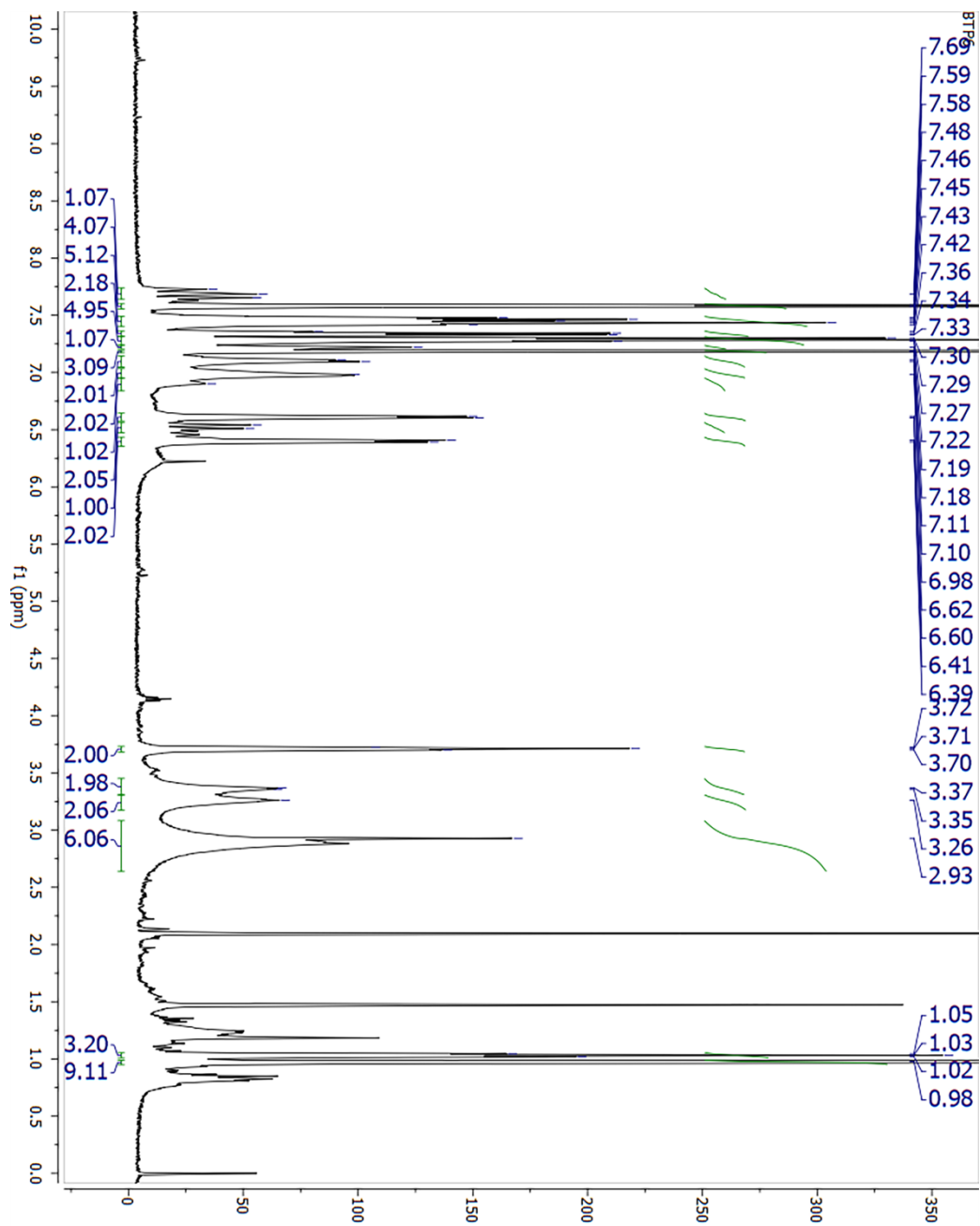


Figure S10.  $^1\text{H}$  NMR spectrum of BTF1.

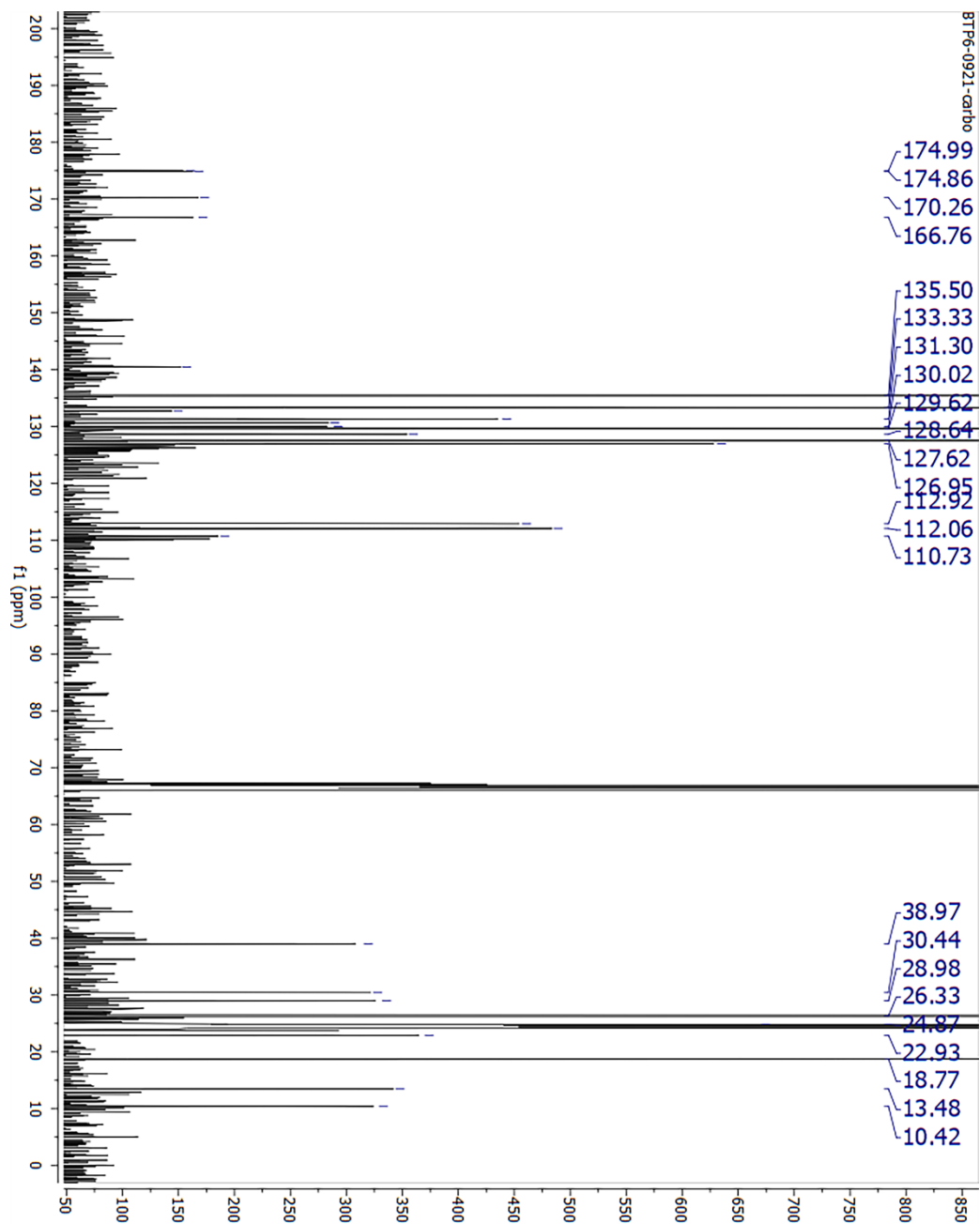


Figure S11.  $^{13}\text{C}$  NMR spectrum of BTF1.

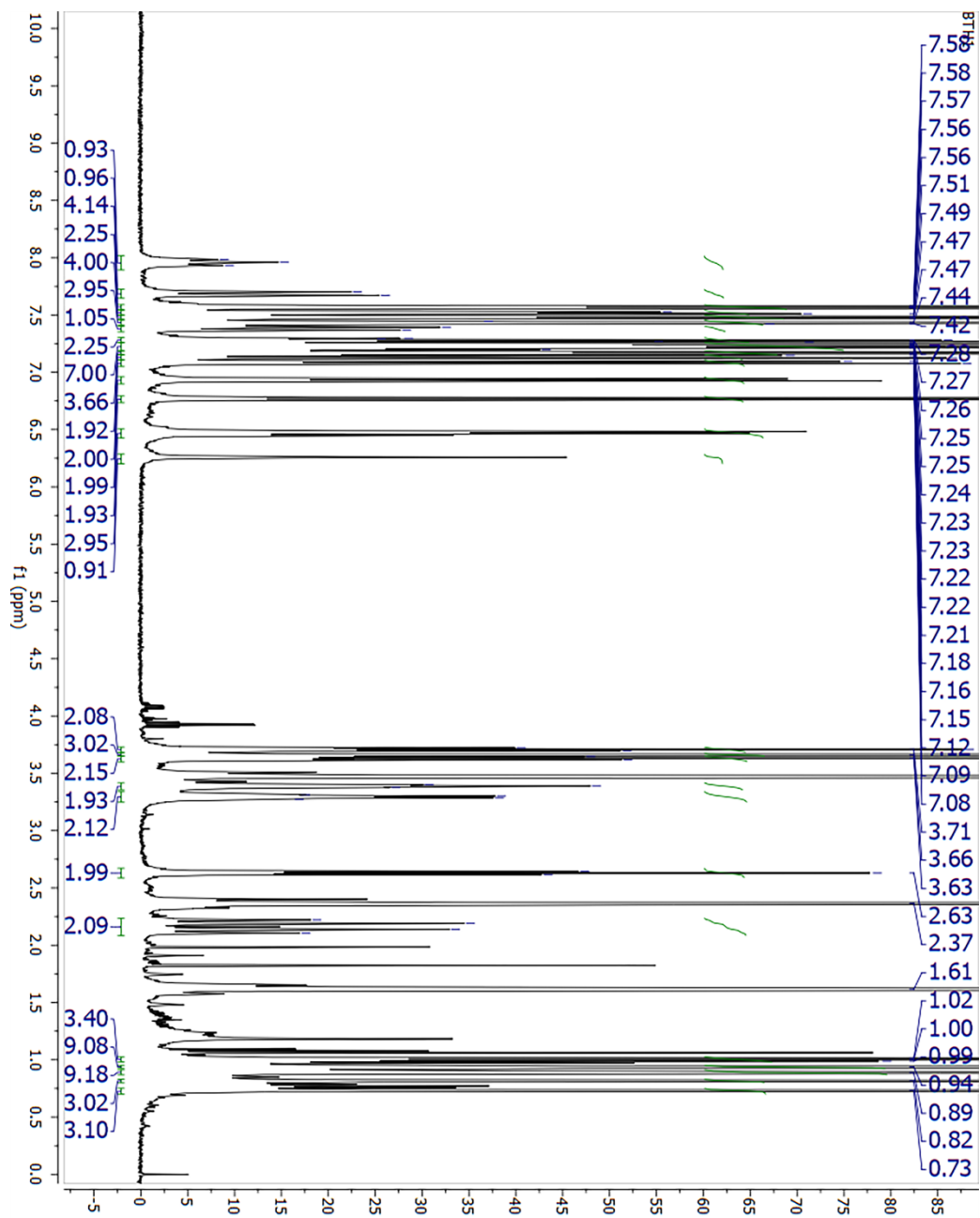
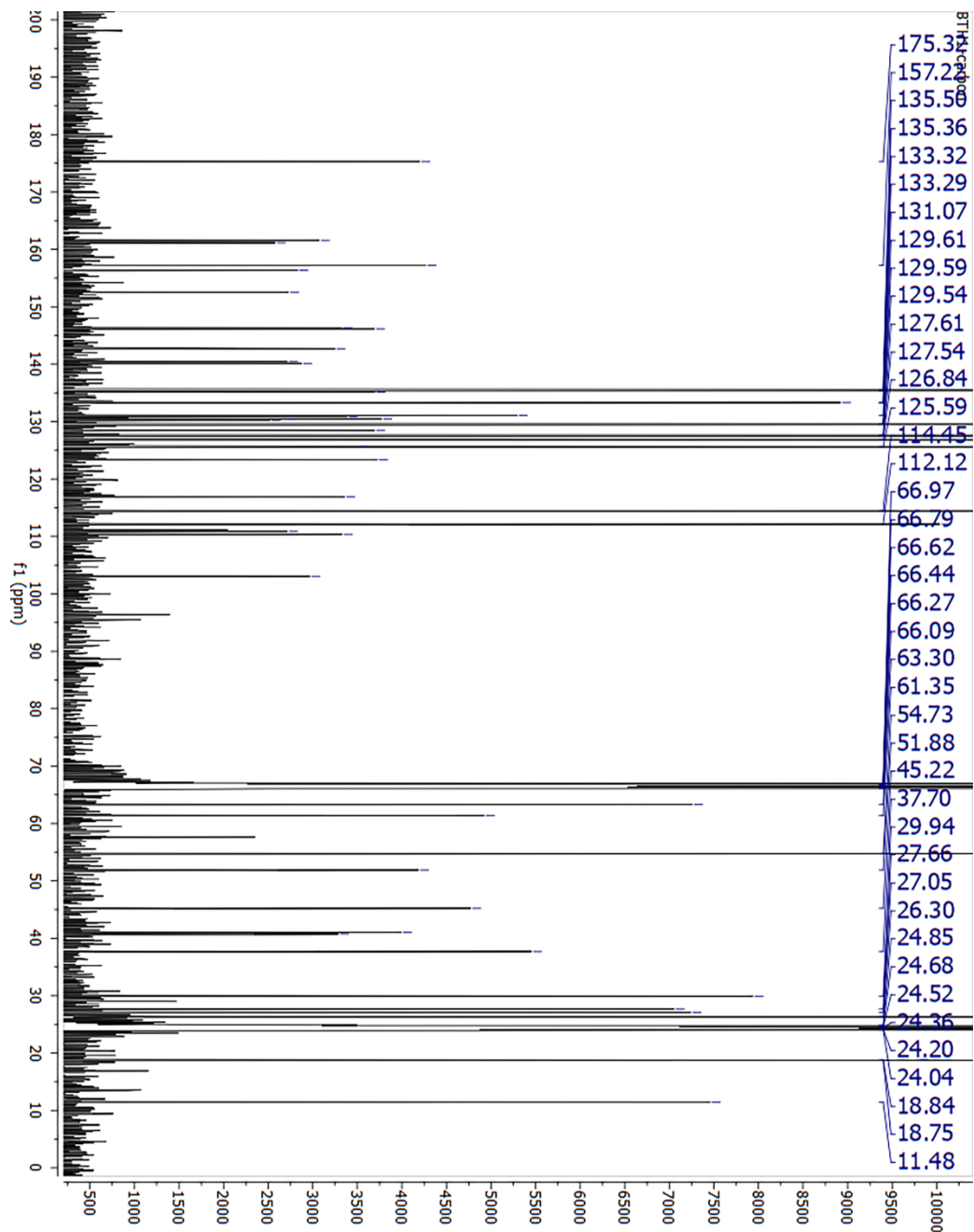


Figure S12.  $^1\text{H}$  NMR spectrum of BTH1.



**Figure S13.**  $^{13}\text{C}$  NMR spectrum of **BTH1**.

## 2. Device Fabrication and Testing.

Solutions of 8-10% w/w EO material in TCE were prepared and sonicated for 15 min to dissolve, filtered through a  $0.2\ \mu\text{m}$  PTFE filter, and spin cast onto ITO/glass substrates. Chromophore in polymer solutions were prepared by combining EO material, poly(methylmethacrylate), and TCE in a vial and rotating for  $\sim 12$  hr to dissolve, filtered through a  $0.2\ \mu\text{m}$  PTFE filter, and spin cast onto ITO/glass substrates EO films were spin cast in three stages, 500 rpm for 5 seconds, 850 rpm for 30 seconds, followed immediately by 1500 rpm for 30 seconds. The

films were then dried either in a vacuum oven at room temperature overnight or at 65 °C for a specific period of time (usually 6-12 hr). The thickness of the EO film was then measured to be around 1-2  $\mu\text{m}$  via optical profilometry. Finally, patterned gold electrodes were deposited on top of the films by sputter coating through a shadow mask, thus completing a device. Electric field poling is conducted by applying a desired electric field (in the range of 10 to 100  $\text{V}/\mu\text{m}$ ) at room temperature, heating the sample to above  $T_g$  (115 °C) and holding at that temperature for a few minutes (5~10) until molecular orientation is complete, cooling to room temperature, and then removing the electric field. During poling, current, voltage, temperature, and relative  $r_{33}$  were measured real-time. After poling and cooling to near room temperature,  $r_{33}$  for the poled films were measured using the Teng–Man technique<sup>3,4</sup> on a custom apparatus at 1310 nm using the index of refraction values reported in Table S2. At high poling fields, there is risk of device damage resulting in  $r_{33}$  measurements that are unreliable due to dielectric breakdown or arcing, or in rare cases, device failure. Therefore, we did not include any of the unreliable measurements in the data of Figure S19 or Table 2. This is not unique to chromophores or device structures in this paper, but is a general limitation for electric field poling. All of our  $r_{33}$  measurements are shown in Figure S19. Each data point is from a separate device and poling experiment. Standard error in  $r_{33}$  and poling efficiency were calculated as in Ref. 5.<sup>5</sup>

Leakage current for neat BTP-type chromophore films was too high to allow effective poling as neat materials. there is quite a bit of literature on charge barrier layers for reducing leakage current during electric field poling. The best barrier material we have evaluated is a benzocyclobutene polymer, which reduces the leakage current with neat JRD1 by an order of magnitude.<sup>5</sup> However, this barrier layer does not significantly reduce the leakage current with novel BTP-type chromophores reported here, presumably due to their smaller band gaps.

### 3. UV-Vis absorption spectra

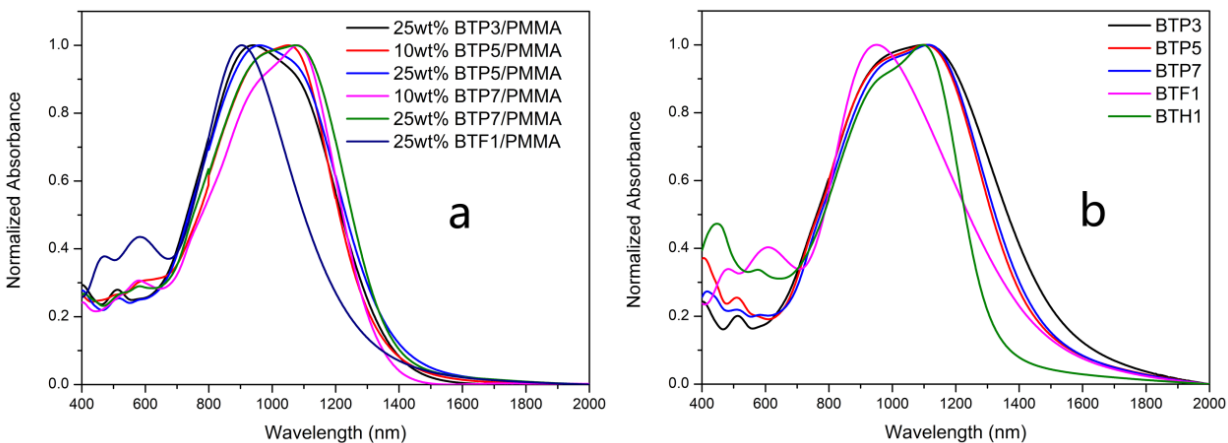


**Figure S14.** Normalized UV-Vis absorption spectra of neat blending with PMMA films.

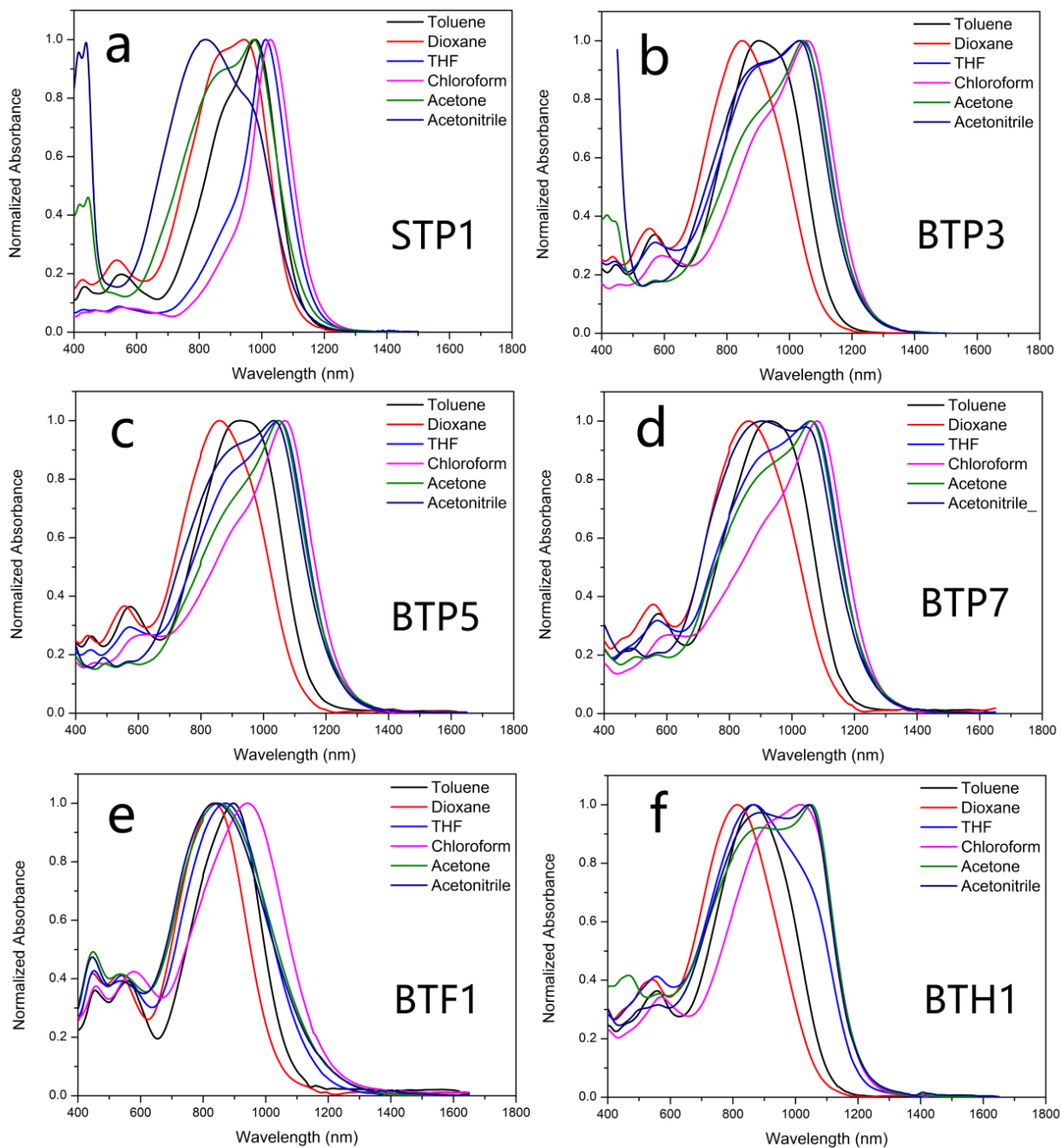


**Figure S15.** Normalized UV-Vis absorption spectra of chromophores in six aprotic solvents with varying dielectric constants ( $\epsilon$ ).

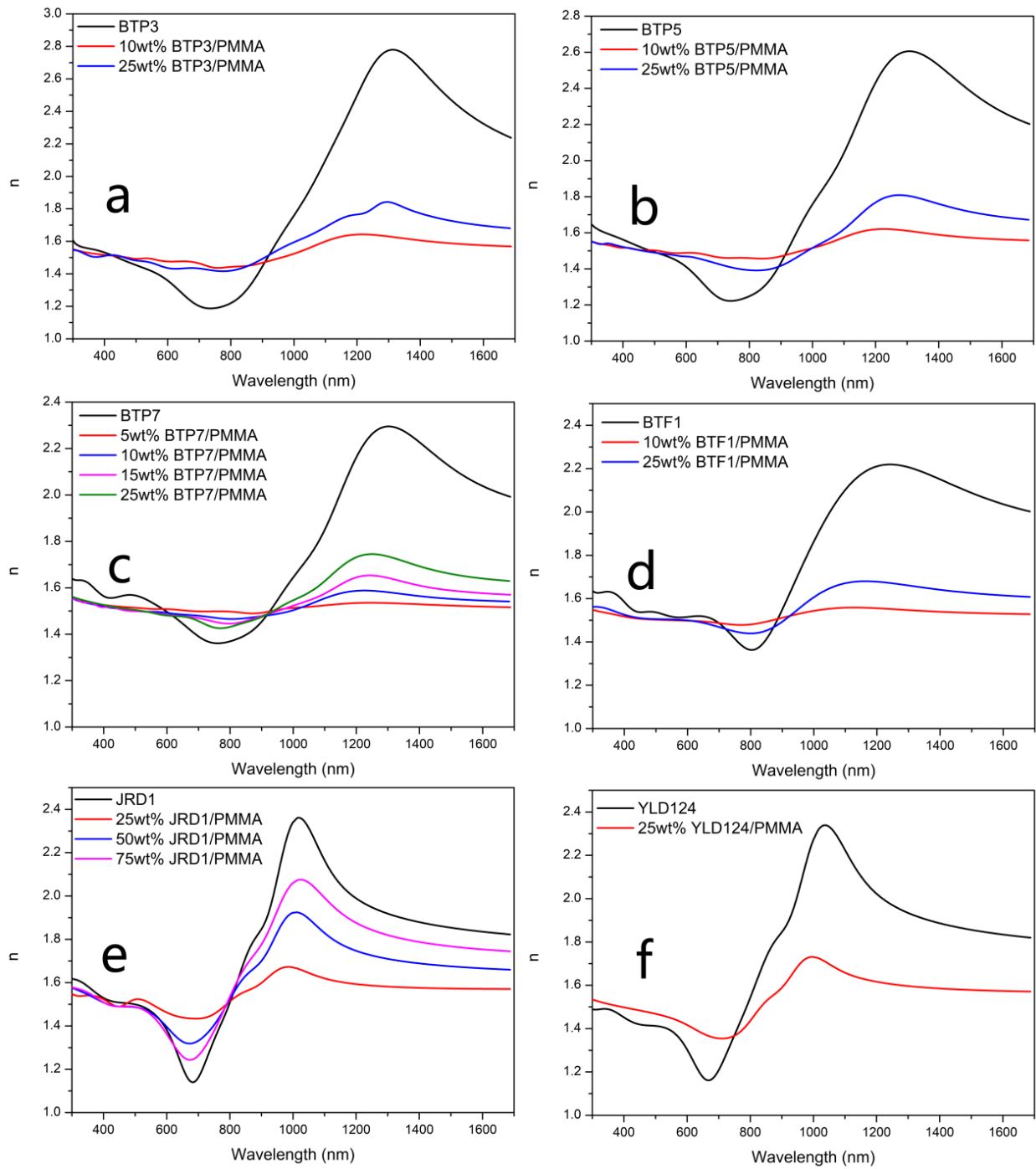
**Table S1.** UV-Vis data of chromophores in various solvents, as neat thin films, and thin films in PMMA.

	1,4-dioxane (nm)	Toluene (nm)	THF (nm)	Acetone (nm)	Chloroform (nm)	Acetonitrile (nm)	Film (nm)	25%wt in PMMA (nm)
<b>STP1</b>	944	980	1012	974	1028	821	-	-
<b>BTP3</b>	848	903	1037	1047	1058	1031	1105	941
<b>BTP5</b>	859	927	1049	1050	1068	1033	1103	963
<b>BTF1</b>	834	897	872	852	943	839	951	904
<b>BTP7</b>	863	928	1061	1062	1081	1045	1114	1072
<b>BTH1</b>	814	865	867	1050	1020	1043	1097	-
<b>JRD1</b>	725	751	767	777	784	782	800	792
$\epsilon$	2.209	2.379	7.6	20.7	4.806	37.5	-	-
$(\epsilon-$ <b>1)/(</b> $\epsilon+$ <b>2)</b>	0.287	0.3145	0.688	0.868	0.559	0.924	-	-

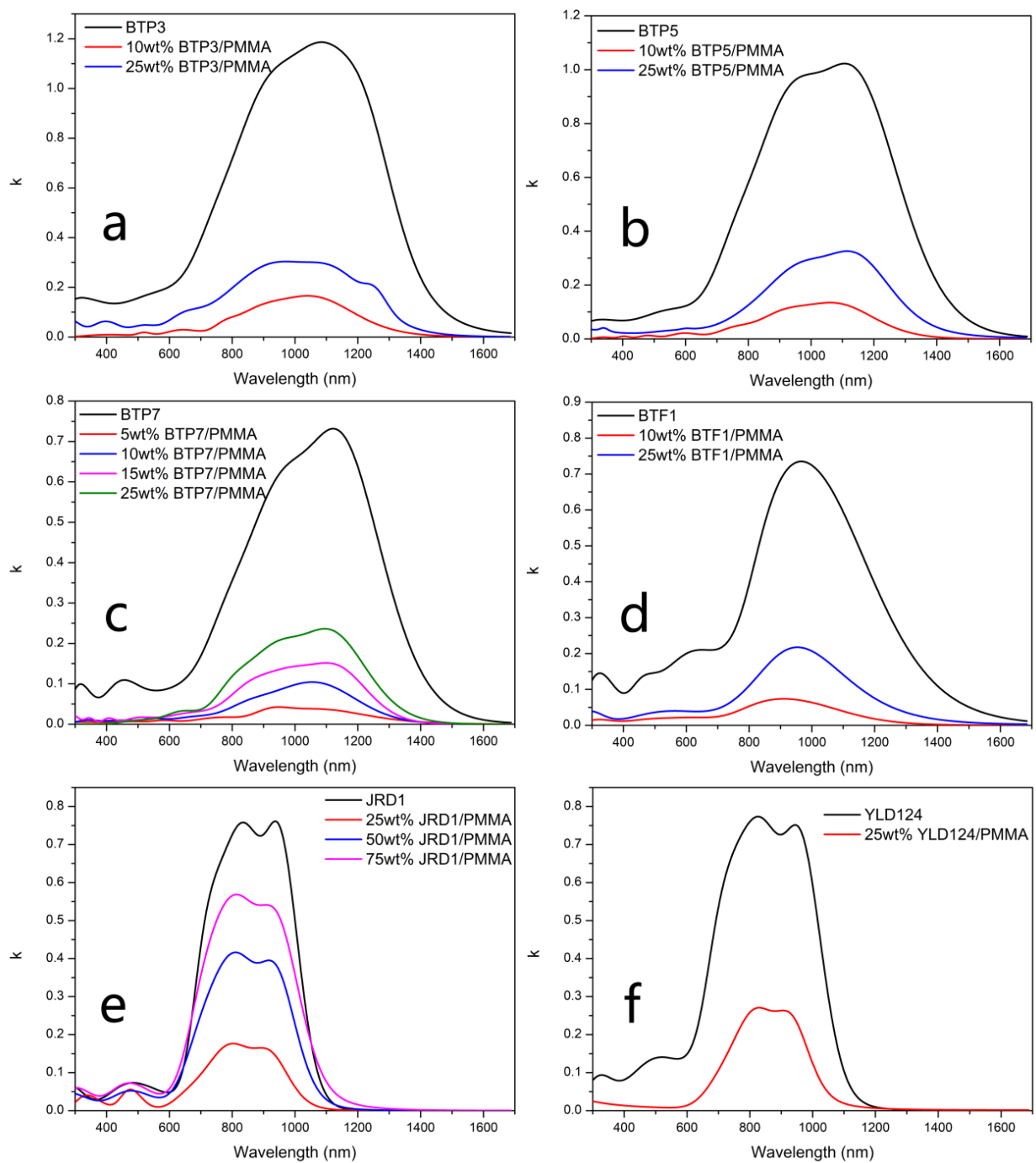
**4. Optical constants from VASE measurements****Table S2.** Optical constants and number density of films.

	$\rho_N(\times 10^{20} \text{ molecules/cm}^3)^a$	$n_{1310}$	$n_{1550}$	$k_{1310}$	$k_{1550}$
<b>BTP3</b>	6.96	2.78	2.39	0.588154	0.048217
10wt% <b>BTP3/PMMA</b>	0.696	1.63	1.58	0.030475	0.001706
<b>BTP5</b>	5.25	2.61	2.32	0.472277	0.039715
10wt% <b>BTP5/PMMA</b>	0.525	1.61	1.57	0.024863	0.000634
25wt% <b>BTP5/PMMA</b>	1.31	1.80	1.70	0.113637	0.010428
<b>BTP7</b>	4.12	2.29	2.07	0.323548	0.020612
5wt% <b>BTP7/PMMA</b>	0.206	1.53	1.52	0.012412	0.001323
10wt% <b>BTP7/PMMA</b>	0.412	1.58	1.55	0.018901	0.000462
15wt% <b>BTP7/PMMA</b>	0.618	1.64	1.58	0.029253	0.000242
25wt% <b>BTP7/PMMA</b>	1.03	1.73	1.65	0.056604	0.001094
<b>BTF1</b>	5.44	2.20	2.06	0.206878	0.034085
10wt% <b>BTF1/PMMA</b>	0.544	1.55	1.53	0.006146	0.000431
25wt% <b>BTF1/PMMA</b>	1.36	1.66	1.62	0.033203	0.005979
<b>JRD1</b>	5.33	1.91	1.84	0.000103	0.000018
25wt% <b>JRD1/PMMA</b>	1.33	1.58	1.57	0.000065	0.000001
50wt% <b>JRD1/PMMA</b>	2.66	1.71	1.67	0.000789	0.000063
75wt% <b>JRD1/PMMA</b>	4.00	1.82	1.76	0.004617	0.000472
<b>YLD124</b>	6.83	1.93	1.84	0.002319	0.000787
25wt% <b>YLD124/PMMA</b>	1.71	1.60	1.58	0.003136	0.001626

<sup>a</sup>Number density (assumes mass density of 1 g/cm<sup>3</sup>).



**Figure S16.** Refractive index ( $k$ ) of films of neat chromophores and their blends.

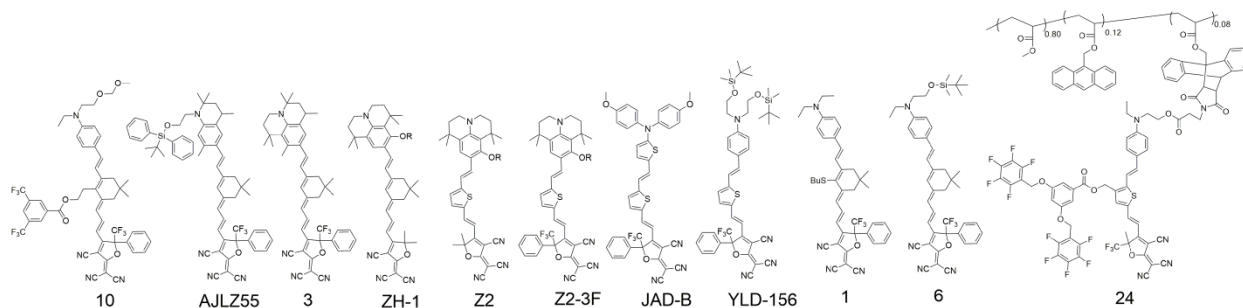


**Figure S17.** Extinction Absorption coefficient ( $k$ ) of films of neat chromophores and their blends.

**Table S3.** Summary comparison of optical properties

Name	Comp <sup>b</sup> .	$\lambda_{\max}$ (nm)	Band edge	$\lambda_{\max}$ (nm)	Band edge	$n_{1310}$	$n_{1550}$
	$\beta_0/\beta_{0,\text{JRD1}}$	CHCl <sub>3</sub>	(nm), in CHCl <sub>3</sub>	Film	(nm), Film		
JRD1	1	790	976	800	1138	1.91	1.85
EZFTC	0.59	676	810	678	950	1.95	1.91
BTP3	2.16	1055	1224	1105	1524	2.78	2.39
BTP5	2.19	1070	1240	1103	1440	2.61	2.32
BTF1	1.85	950	1178	951	1452	2.20	2.06
BTP7	2.32	1081	1256	1114	1460	2.29	2.07
STP1	1.97	1030	1166	-	1362*	-	-
BTH1	1.76	1020	1196	1097	1304	2.09	1.89
ZH-1	1.24	763	1025	-	-	-	-
Molec. 3	1.03	980	1075	1250	-	-	-
JAD-B	1.23	857	1008	856	1234	-	-
YLD-156	0.81	758	892	-	994	-	-

\* The thin film optical band gap (long wavelength band edge) was estimated by using the long wavelength band edge of the main charge transfer absorbance in chloroform and the plot of calculated  $\beta_0/\beta_{0,\text{JRD1}}$  vs. band edge in chloroform (Figure S15) to calculate  $\beta_0/\beta_{0,\text{JRD1}}$ , then use this  $\beta_0/\beta_{0,\text{JRD1}}$  value and the calibration curve of  $\beta_0/\beta_{0,\text{JRD1}}$  vs. thin film band edge (Figure S14) to evaluate the thin film band edge.

**Figure S18.**<sup>6-12</sup> Structures of some other high-performance chromophores

## 5. Electric field poling and EO performances.

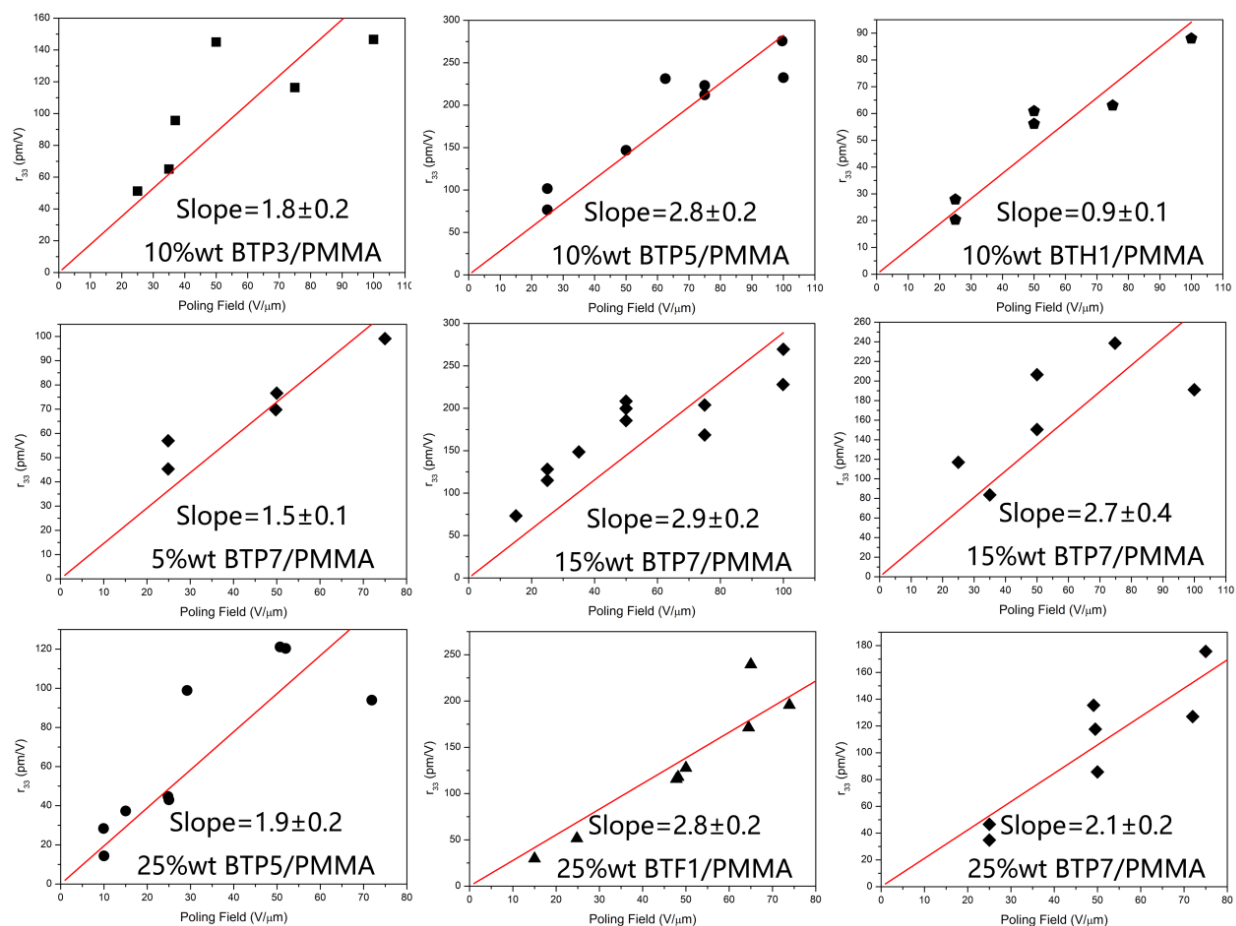


**Figure S19.** Poling curves (plots of  $r_{33}$  vs poling field). Average  $r_{33}/E_p \pm$  standard errors are shown. The statistical analysis for  $r_{33}$  and  $E_p$  was according to previously published method.<sup>5</sup>

## 6. Thermal properties of chromophores

Glass transition temperatures of chromophores were characterized by differential scanning calorimetry (DSC) and decomposition temperatures of chromophores were characterized by thermogravimetric analysis (TGA). Results are summarized in Table S4; TGA and DSC curves are shown in figures S20 and S21, respectively.

**Table S4.** Summary of DSC and TGA data

Name	DSC $T_g$ (°C)	TGA $T_d$ (°C)
JRD1	82	226
BTP3	-	182
BTP5	109	205
BTP7	83	199
BTF1	104	251
STP1	-	201

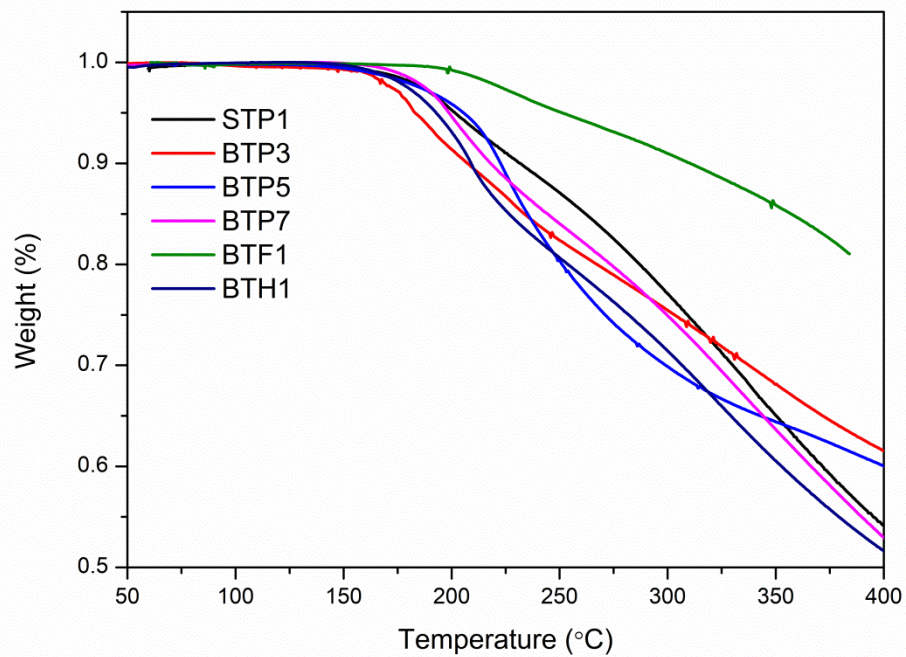


**Figure S20.** TGA curves of chromophores (powders) with a heating rate of  $10\text{ }^{\circ}\text{C min}^{-1}$  in a nitrogen atmosphere.

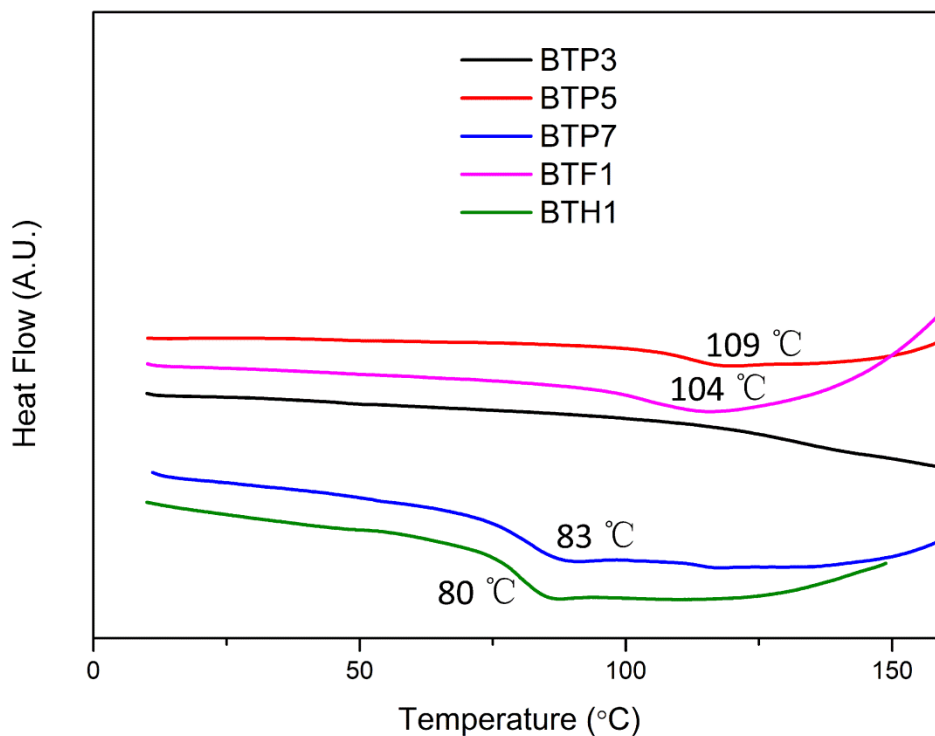


**Figure S21.** DSC curves of chromophores

## 8. Hyper-Rayleigh Scattering

Femtosecond Hyper-Rayleigh scattering<sup>13</sup> (HRS) measurements were performed in chloroform solution using a custom-built setup at KU Leuven. Measurements were performed using a fundamental wavelength of 1300 nm and a repetition rate of 80 MHz. HRS intensity was extrapolated to zero concentration using a Beer-Lambert correction at the second harmonic wavelength. Resonance effects were approximated using the damped two-level model (Equation) and a linewidth ( $\gamma$ ) of 0.1 eV.<sup>14</sup>  $\omega_{\max}$  is the energy corresponding to  $\lambda_{\max}$ .

$$\beta(0) = \frac{\beta(-2\omega; \omega, \omega)}{F(\omega_{laser}, \omega_{max}, \gamma)}$$

$$F(\omega_{laser}, \omega_{max}, \gamma) = \frac{\omega_{max}^2}{3} \left[ \frac{1}{(\omega_{max} + 2\omega_{laser} + i\gamma)(\omega_{max} + \omega_{laser} + i\gamma)} + \frac{1}{(\omega_{max} + \omega_{laser} + i\gamma)(\omega_{max} - \omega_{laser} - i\gamma)} + \frac{1}{(\omega_{max} - \omega_{laser} + i\gamma)(\omega_{max} - 2\omega_{laser} + i\gamma)} \right] \quad (S1)$$

The chloroform solvent was used as the reference for the measurements, based on a  $\beta_{zzz,0}$  value of  $0.44 \times 10^{-30}$  esu<sup>13</sup> and assuming dipolar symmetry and a single dominant tensor component such that

$$\beta_{zzz,0} \approx \sqrt{35/6} \cdot \beta_{HRS,0} \quad (S2)$$

Measurements were performed currently with those previously reported for the JRD1 and HLD chromophores; detailed HRS methods are available in Ref. 8.<sup>15</sup> HRS data is summarized in table S5:

**Table S5. HRS data summary**

Name	$\lambda_{max}$ (nm) CHCl <sub>3</sub>	Two-level factor (TLF)	$\beta_{zzz}$ (1300 nm) (10 <sup>-30</sup> esu)	$\beta_{zzz,0}$ (10 <sup>-30</sup> esu)	$\beta_{zzz,0}/\beta_{zzz,0,JRD1}$
JRD1	790	3.13	3330 ± 50	1060 ± 20	1 ± 0.02
EZFTC	676	9.86	3600 ± 900	360 ± 90	0.34 ± 0.09
BTP3	1055	1.61	4880 ± 170	3030 ± 100	2.85 ± 0.10
BTP5	1070	1.61	4410 ± 70	2740 ± 40	2.60 ± 0.04
BTF1	950	1.79	4750 ± 20	2650 ± 10	2.52 ± 0.01
BTP7	1081	1.61	5700 ± 100	3550 ± 80	3.37 ± 0.08
STP1	1030	1.60	2000 ± 200	1250 ± 130	1.18 ± 0.12
BTH1	1020	1.64	4900 ± 300	3000 ± 200	2.83 ± 0.17

HRS can be performed using a wide variety of different reference standards, wavelengths, and solvents, which can make comparisons between datasets difficult.<sup>16</sup> However, literature data can be directly compared if studies have a chromophore in common. The chromophores with the highest prior reported hyperpolarizabilities in the literature all were from studies containing the (EZ)FTC chromophore, which allows it to be used as a common reference with hyperpolarizabilities renormalized to the EZ-FTC hyperpolarizability value for the present study ( $360 \pm 90 \times 10^{-30}$  esu). A comparison is shown in Table S6; BTP7 exhibits  $2.13 \pm 0.6$  the hyperpolarizability of prior leader AJY2.

**Table S6. Renormalization of literature HRS data**

Chromophore	HRS $\lambda$ (nm)	Reported $\beta$ (10 <sup>-30</sup> )	$\beta/\beta_{FTC}$	$\lambda_{max}$ (nm)	TLF	$\beta_0/\beta_{0,FTC}$	Renorm. $\beta_{zzz,0}$
-------------	-----------------------	--	---------------------	----------------------	-----	-------------------------	----------------------------

		esu)					
B1 (Bu-FTC) <sup>8</sup>	1900	1498	1	685	2.33	1	360
A3 <sup>8</sup>	1900	10203	6.8	821	4.32	3.7	1300
EZ-FTC <sup>17</sup>	1907	1360	1	676	2.24	1	360
YLD124 <sup>6, 18</sup>	1907	7600	5.2 ± 0.2	786	3.51	3.3 ± 0.1	1200 ± 100
B <sup>17, 19</sup>	1907	8160	6 ± 0.5	857	5.33	2.5 ± 0.2	910 ± 120
AJY2 (1) <sup>7, 17</sup>	1907	10200	7.5 ± 1.3	793	3.63	4.6 ± 0.8	1670 ± 290
B3 <sup>6, 17</sup>	1907	7077	5.2 ± 0.5	772	3.27	3.6 ± 0.4	1280 ± 160

Dielectric effects on hyperpolarizability were also examined by HRS experiments on the BTP5 chromophore in a low-polarity environment (toluene) and a high-polarity environment (acetonitrile). Hyperpolarizability was enhanced in the toluene environment, suggesting that the BTP5 chromophore is starting to approach the cyanine limit in a chloroform environment.<sup>20</sup> As hyperpolarizability in acetonitrile is also larger than in chloroform, the BTP5 chromophore is on the zwitterionic side of the cyanine limit in an acetonitrile environment. The change in hyperpolarizability is consistent with the observed solvatochromism trend. Data is shown in Figure S22 and Table S7.

**Table S7.** HRS data for BTP5 in different solvent environments

Solvent	( $\epsilon-1$ )/ ( $\epsilon+2$ )	$\lambda_{\max}$ (nm) CHCl <sub>3</sub>	Two-level factor (TLF)	$\beta_{zzz}$ (1300 nm) (10 <sup>-30</sup> esu)	$\beta_{zzz,0}$ (10 <sup>-30</sup> esu)
Toluene	0.31	927	1.82	6750 ± 730	3700 ± 400
Chloroform	0.55	1070	1.61	4410 ± 70	2740 ± 40
Acetonitrile	0.92	1033	1.62	5030 ± 170	3100 ± 100

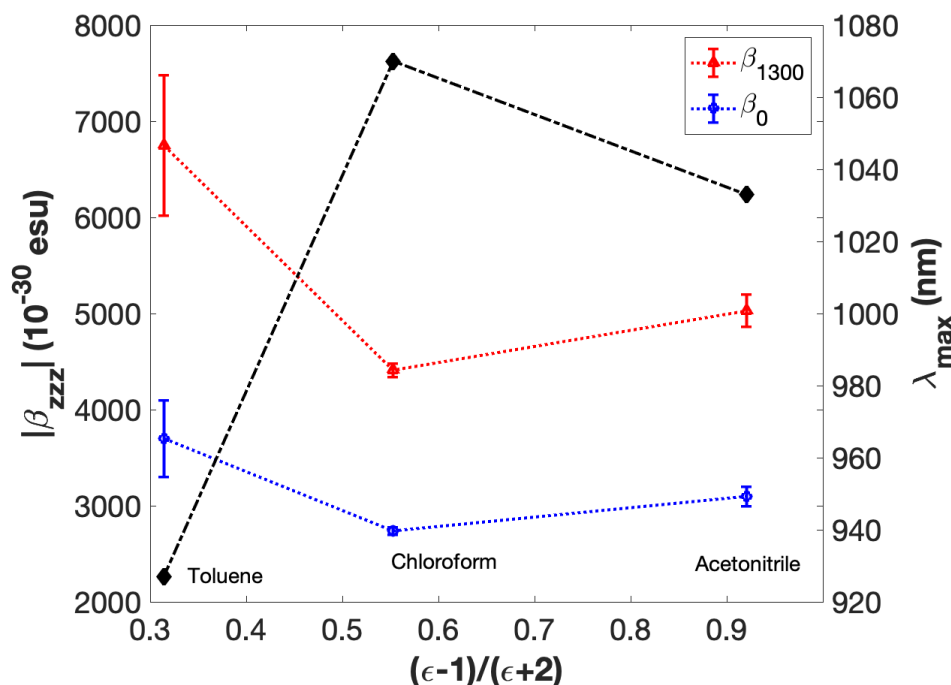


**Figure S22.** Solvatochromism and dielectric dependence of hyperpolarizability for the BTP5 chromophore.

### 9. DFT calculations

Closed shell density functional theory (DFT) calculations were performed using Gaussian 09<sup>21</sup> and the M062X functional<sup>22</sup> with a 6-31+G(d) basis set in a chloroform implicit solvent environment using default (IEF-PCM) parameters. Structures were optimized in the chloroform environment to RMS force  $< 4 \times 10^{-5}$  Hartrees/bohr and maximum force  $< 6 \times 10^{-5}$  Hartrees/bohr. Hyperpolarizabilities and vibrational frequencies were calculated via analytic differentiation (CPHF/KS). Calibration of the hyperpolarizability calculation protocol<sup>23</sup> is discussed in Ref. 12. A SCF convergence criterion of  $< 10^{-10}$  a.u. RMS in the density matrix was used for all properties calculations. Excitation energies were calculated at the TD-M062X/6-31+G(d) level of theory, calculations were configured to find the six lowest-lying singlet excited states. Data are summarized in Table S8. A subset of calculations were also performed in other PCM solvent environments (toluene, acetone, and acetonitrile) and are reported in Tables S9-11. The trends in calculated hyperpolarizability as a function of dielectric constant are shown in Figure S23. STP1 shows a clear reversal in sign of hyperpolarizability (indicative of a zwitterionic state); calculations for BTP3 do not show this reversal, likely due to the calculations underestimating the reaction field strength.

**Table S8.** Calculations in chloroform

	$\mu$ (D)	$\beta_{zzz,0}$ ( $10^{-30}$ esu)	$\beta_{zzz,0}/\beta_{zzz,0}$ JRD1	$\lambda_{\max}$ (nm)	HOMO (eV)	LUMO (eV)
EZFTC	25.9	830	0.58	564	-6.2839	-2.7111
JRD1	31	1418	1	642	-6.2695	-2.9669

BTP3	34.6	3068	2.16	726	-5.8159	-3.0055
BTP5	34.1	3105	2.19	731	-5.8042	-3.0079
BTP7	34.9	3285	2.32	720	-5.8379	-3.0096
BTF1	30.7	2627	1.85	690	-5.817	-2.9761
BTH1	33.3	2603	1.84	690	-5.9389	-3.0199
STP1	42.1	2799	1.97	769	-5.866	-2.9644
ZH1	32.2	1762	1.23	679	-6.1196	-2.9568
Molec3	29.7	1426	1.01	654	-6.1672	-2.9701
JAD-B	28.8	1742	1.23	661	-6.0986	-2.9644

**Table S9.** Calculations in toluene

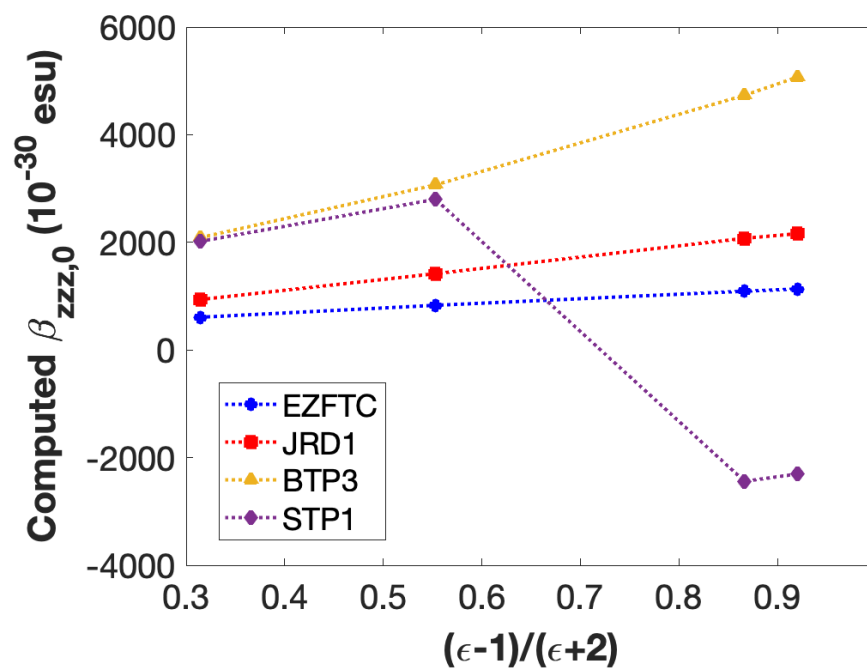
	$\mu$ (D)	$\beta_{zzz,0}$ ( $10^{-30}$ esu)	$\beta_{zzz,0}/\beta_{zzz,0 \text{ in } \text{CHCl}_3}$ JRD1	$\lambda_{\text{max}}$ (nm)	HOMO (eV)	LUMO (eV)
EZFTC	24	608	0.43	554	-6.3468	-2.7198
JRD1	27.5	937	0.66	619	-6.3204	-2.9342
BTP3	31	2088	1.47	703	-5.8156	-2.9601
STP1	34.9	2018	1.42	730	-5.8564	-2.904

**Table S10.** Calculations in acetone

	$\mu$ (D)	$\beta_{zzz,0}$ ( $10^{-30}$ esu)	$\beta_{zzz,0}/$ JRD1 $\beta_{zzz,0}$ in CHCl <sub>3</sub>	$\lambda_{\max}$ (nm)	HOMO (eV)	LUMO (eV)
EZFTC	27.7	1092	0.77	567	-6.236	-2.7005
JRD1	36.1	2075	1.46	666	-6.2281	-3.0104
BTP3	40.7	4733	3.34	757	-5.8306	-3.0645
STP1	71.5	-2440	1.72	705	-6.0037	-2.8781

**Table S11.** Calculations in acetonitrile

	$\mu$ (D)	$\beta_{zzz,0}$ ( $10^{-30}$ esu)	$\beta_{zzz,0}/$ JRD1 $\beta_{zzz,0}$ in CHCl <sub>3</sub>	$\lambda_{\max}$ (nm)	HOMO (eV)	LUMO (eV)
EZFTC	28	1134	0.80	568	-6.2303	-2.6986
JRD1	37.2	2161	1.52	670	-6.2227	-3.0186
BTP3	42.5	5071	3.58	767	-5.8347	-3.0782
STP1	73.1	-2304	-1.62	688	-6.0249	-2.8531

**Figure S23.** Trends in hyperpolarizability with dielectric constant.

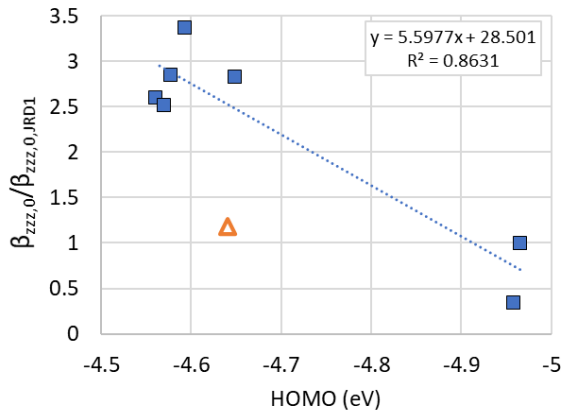


**Figure S24a.** Experimental  $\beta_{zzz,0}/\beta_{zzz,0,JRD1}$  for BTP3, BTP5, BTP7, BTH1, BTF1, JRD1, and EZFTC. STP1 (triangle) not included in the fit.

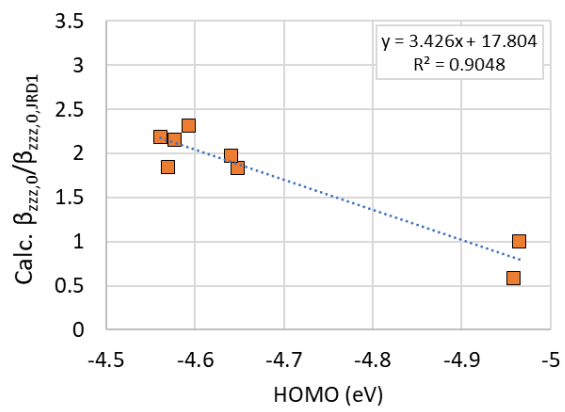


**Figure S24b.** Calculated  $\beta_{zzz,0}/\beta_{zzz,0,JRD1}$  for BTP3, BTP5, BTP7, BTH1, BTF1, STP1, JRD1, and EZFTC.

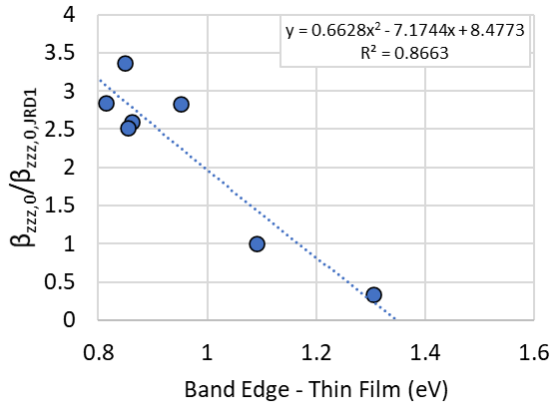


**Figure S25a.** Experimental  $\beta_{zzz,0}/\beta_{zzz,0,JRD1}$  for BTP3, BTP5, BTP7, BTH1, BTF1, JRD1, and EZFTC.

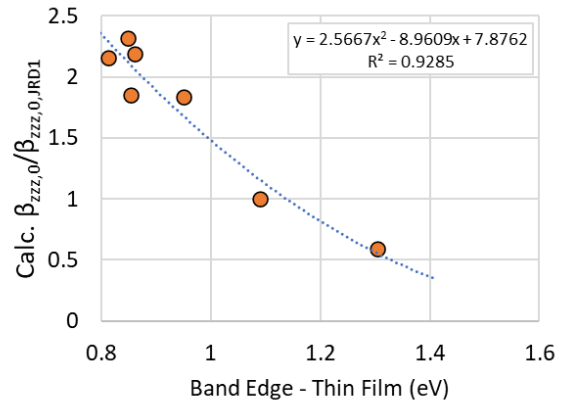


**Figure S25b.** Calculated  $\beta_{zzz,0}/\beta_{zzz,0,JRD1}$  for BTP3, BTP5, BTP7, BTH1, BTF1, JRD1, and EZFTC.

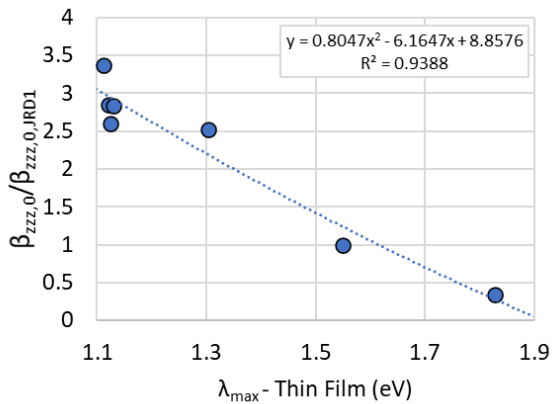


**Figure S26a.** Experimental  $\beta_{zzz,0}/\beta_{zzz,0,JRD1}$  for BTP3, BTP5, BTP7, BTH1, BTF1, JRD1, and EZFTC.

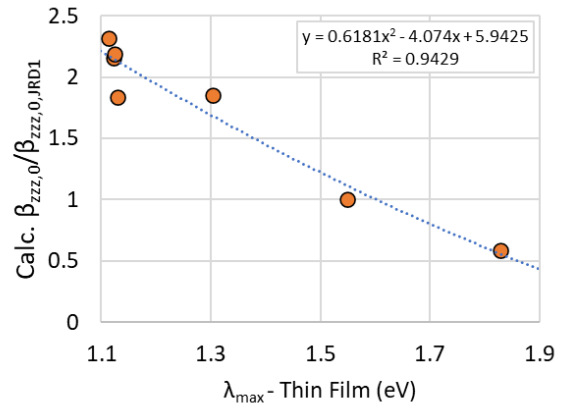


**Figure S26b.** Calculated  $\beta_{zzz,0}/\beta_{zzz,0,JRD1}$  for BTP3, BTP5, BTP7, BTH1, BTF1, JRD1, and EZFTC.

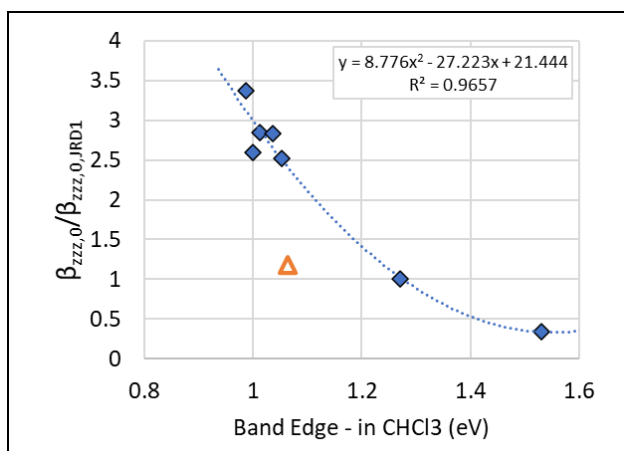


**Figure S27a.** Experimental  $\beta_{zzz,0}/\beta_{zzz,0,JRD1}$  for BTP3, BTP5, BTP7, BTH1, BTF1, JRD1, and EZFTC. STP1 (triangle) not included in the fit.

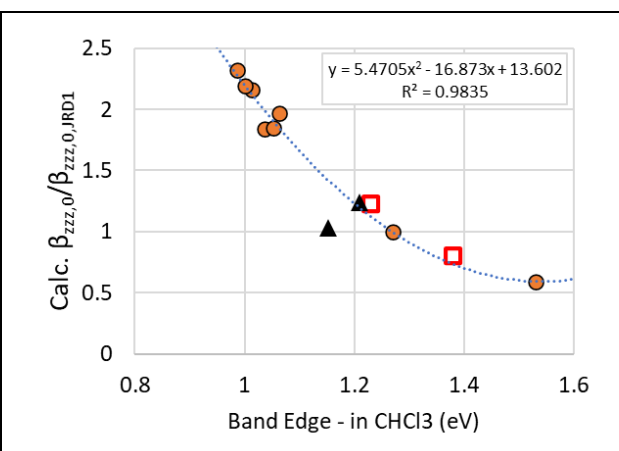


**Figure S27b.** Calculated  $\beta_{zzz,0}/\beta_{zzz,0,JRD1}$  for BTP3, BTP5, BTP7, BTH1, BTF1, STP1, JRD1, and EZFTC. JAD-B and YLD-156 (red squares) and Molecule 3, and ZH-1 (black triangles) not included in the fit.

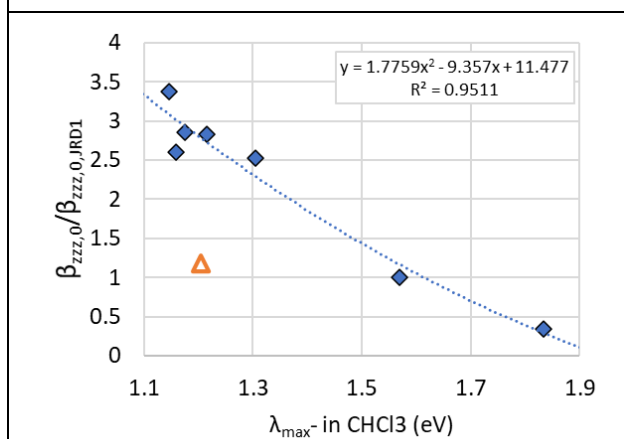


**Figure S28a.** Experimental  $\beta_{zzz,0}/\beta_{zzz,0,JRD1}$  for BTP3, BTP5, BTP7, BTH1, BTF1, JRD1, and EZFTC. STP1 (triangle) not included in the fit.

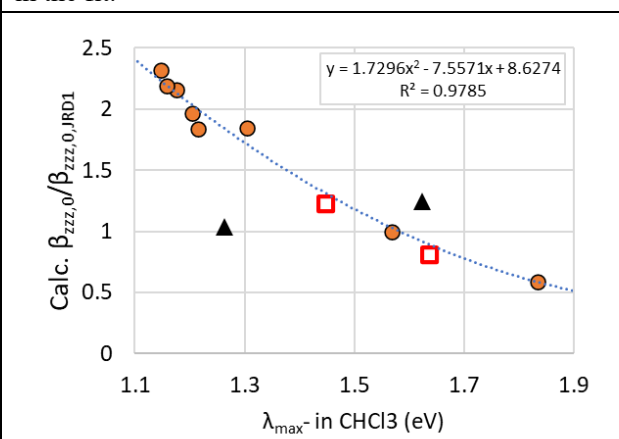


**Figure S28b.** Calculated  $\beta_{zzz,0}/\beta_{zzz,0,JRD1}$  for BTP3, BTP5, BTP7, BTH1, BTF1, STP1, JRD1, and EZFTC. JAD-B and YLD-156 (red squares) and Molecule 3, and ZH-1 (black triangles) not included in the fit.

The relationship between experimental or calculated  $\beta_{zzz,0}/\beta_{zzz,0,JRD1}$  and HOMO (determined by cyclic voltammetry) or spectroscopic properties are shown in Figures S23-S27 for the new chromophores introduced in this paper and comparative chromophores JRD1 and EZFTC. While there is in general a good correlation between  $\beta_{zzz,0}/\beta_{zzz,0,JRD1}$  and HOMO energy level ( $R^2 = 0.86$  and  $0.90$  for experimental and calculated  $\beta_{zzz,0}/\beta_{zzz,0,JRD1}$ , respectively), there are really two clusters of data reflecting the stronger BTP-type donors and the weaker dialkylaminophenyl donors of JRD1 and EZFTC. Figures S24-S27 compare  $\beta_{zzz,0}/\beta_{zzz,0,JRD1}$  with the long wavelength band edge or wavelength of maximum absorbance,  $\lambda_{max}$ , in solution or thin film. The thin film band edge (band gap) is generally preferred for correlating electrochemical properties, and the  $R^2$  correlation

with  $\beta_{zzz,0}/\beta_{zzz,0,JRD1}$  is quite good ( $R^2 = 0.87$  experimental and 0.93 calculated  $\beta_{zzz,0}/\beta_{zzz,0,JRD1}$ ). However, the correlation is even better with thin film  $\lambda_{max}$ , chloroform solution band edge, and chloroform solution  $\lambda_{max}$  (0.93-0.97 experimental and 0.94-0.98 calculated  $\beta_{zzz,0}/\beta_{zzz,0,JRD1}$ ). The discovery of a strong correlation of  $\beta_{zzz,0}/\beta_{zzz,0,JRD1}$  with  $\lambda_{max}$  in chloroform for a wide range of  $\beta$  values ( $\beta_{zzz,0}/\beta_{zzz,0,JRD1}$  from 0.59-2.32) is good to see as spectroscopic data is much more plentiful than  $\beta$  measurements and  $\beta$  calculations using the same methods. This strong correlation allows us to better compare  $\beta$  of the many EO materials reported in the literature. Four literature chromophores were plotted on the calibration curve of Figure S26b with good correlation.

## 10. Cyclic Voltammetry

**Table S12.** Electrochemical properties of various chromophores determined by cyclic voltammetry.

Sample	$E_p^{red}$ (V)	$E_{onset}^{red}$ (V)	$E_a^{ox1}$ (V)	$E_c^{ox1}$ (V)	$E_{1/2}^{ox1}$ (V)	$E_{onset}^{ox1}$ (V)	$E_a^{ox2}$ (V)	$E_c^{ox2}$ (V)	$E_{1/2}^{ox2}$ (V)	$E_{onset}^{ox2}$ (V)	CV HOMO (eV)	CV LUMO (eV)	CV Band Gap (eV)	Optical Band Gap (nm)	Optical Band Gap (eV)	Optical LUMO (eV)
BTP3	-0.860	-0.783	-0.113	-0.189	-0.151	-0.223	0.259	0.184	0.221	0.158	-4.58	-4.02	0.560	1524	0.814	-3.76
BTP5	-0.874	-0.795	-0.122	-0.202	-0.162	-0.239	0.266	0.185	0.226	0.164	-4.56	-4.00	0.556	1440	0.861	-3.70
BTH1	-0.846	-0.738	-0.013	-0.089	-0.051	-0.152	0.448	0.378	0.413	0.335	-4.648	-4.06	0.586	1304	0.951	-3.70
BTF1	-0.873	-0.783	-0.119	-0.196	-0.157	-0.231	0.272	0.199	0.236	0.171	-4.57	-4.02	0.552	1452	0.854	-3.72
STP1	-0.967	-0.867	-0.039	-0.146	-0.092	-0.159	0.295	0.187	0.241	0.187	-4.64	-3.93	0.708	1406*	0.882*	-3.76*
JRD1	-0.908	-0.821	0.269	0.186	0.227	0.165					-4.96	-3.98	0.986	1138	1.09	-3.87
YLD124	-0.895	-0.765	0.296	0.156	0.226	0.163					-4.96	-4.04	0.927	1094	1.13	-3.75
EZ-FTC	-1.101	-1.022	0.2648	0.192	0.229	0.158					-4.96	-3.78	1.18	950	1.31	-3.65
<b>3</b>					0.010	-0.065 <sup>‡</sup>					-4.73			1250	0.992	-3.74
Z2					0.0025	-0.073 <sup>‡</sup>					-4.73			1080*	1.15*	-3.58*
Z2-3F					0.0167	-0.059 <sup>‡</sup>					-4.74			1219*	1.02*	-3.72*
ZH-1					0.023	-0.053 <sup>‡</sup>					-4.75			1149*	1.08*	-3.67*
DLD164	-0.824	-0.730	0.304	0.204	0.254	0.184					-4.98	-4.07	0.914	1024	1.21	-3.77
YLD156	-0.874	-0.775	0.368	0.262	0.315	0.229					-5.03	-4.03	1.00	994	1.25	-3.78
JAD-B	-0.886	-0.800	0.130	0.034	0.082	0.041					-4.84	-4.00	0.840	1234	1.00	-3.84

<sup>‡</sup> Onset potential was estimated by shifting  $E_{1/2}$  by 0.0755 V, which was the average difference between  $E_{1/2}$  and  $E_{onset}$  for BTP3, BTP5, BTH1, BTF1, STP1, and JRD1.  $E_{1/2}$  for Z2, Z2-3F, and ZH-1 were measured in acetonitrile and referenced to  $Fc/Fc^+$ . \* The thin film optical band gap (long wavelength band edge) was estimated by using the long wavelength band edge of the main charge transfer absorbance in chloroform and the plot of calculated  $\beta_o/\beta_{o,JRD1}$  vs. band edge in chloroform (Figure S27b) to calculate  $\beta_o/\beta_{o,JRD1}$ , then use this  $\beta_o/\beta_{o,JRD1}$  value and the calibration curve of  $\beta_o/\beta_{o,JRD1}$  vs. thin film band edge (Figure S25b) to evaluate the thin film band edge.

Cyclic voltammetry was carried out at mM chromophore concentrations in dichloromethane solvent with 0.1 M tetrabutylammonium hexafluorophosphate electrolyte immediately after bubbling nitrogen through the solution for 5 minutes. The working electrode was a glassy carbon disc electrode, and the counter electrode was a platinum wire. The reference electrode was 0.01 M Ag/Ag<sup>+</sup> in acetonitrile with 0.1 M tetrabutylammonium hexafluorophosphate electrolyte, but electrode potentials were referenced relative to ferrocene/ferrocenium E<sub>1/2</sub> in dichloromethane. Values are averages of 2-3 measurements. E<sub>1/2</sub><sup>ox</sup> is the oxidative half-wave potential. E<sub>a</sub><sup>ox</sup> is the anodic oxidative peak potential. E<sub>c</sub><sup>ox</sup> is the cathodic oxidative peak potential. E<sub>onset</sub><sup>ox1</sup> is the onset potential of the first oxidation. E<sub>onset</sub><sup>ox2</sup> is the onset potential of the second oxidation. E<sub>p</sub><sup>red</sup> is the cathodic reductive peak potential (the reduction is not reversible). E<sub>onset</sub><sup>red</sup> is the onset potential of the reduction. HOMO (CV) = -4.8 - (E<sub>onset</sub><sup>ox</sup>[chromophore] - E<sub>1/2</sub>[ferrocene]) eV. LUMO (CV) = -4.8 - (E<sub>onset</sub><sup>red</sup>[chromophore] - E<sub>1/2</sub>[ferrocene]) eV. LUMO (optical) = HOMO (CV) + Band gap (optical). Band gap (CV) = LUMO (CV) - HOMO (CV). Optical band gap was measured at the long wavelength band edge of the main charge transfer band of a thin film absorbance spectrum. The scan rate was 50 mV/s. Scans started at -0.4 to -0.2 V (vs Fc/Fc<sup>+</sup>), scanned anodically, then cathodically, then anodically to near the starting potential.

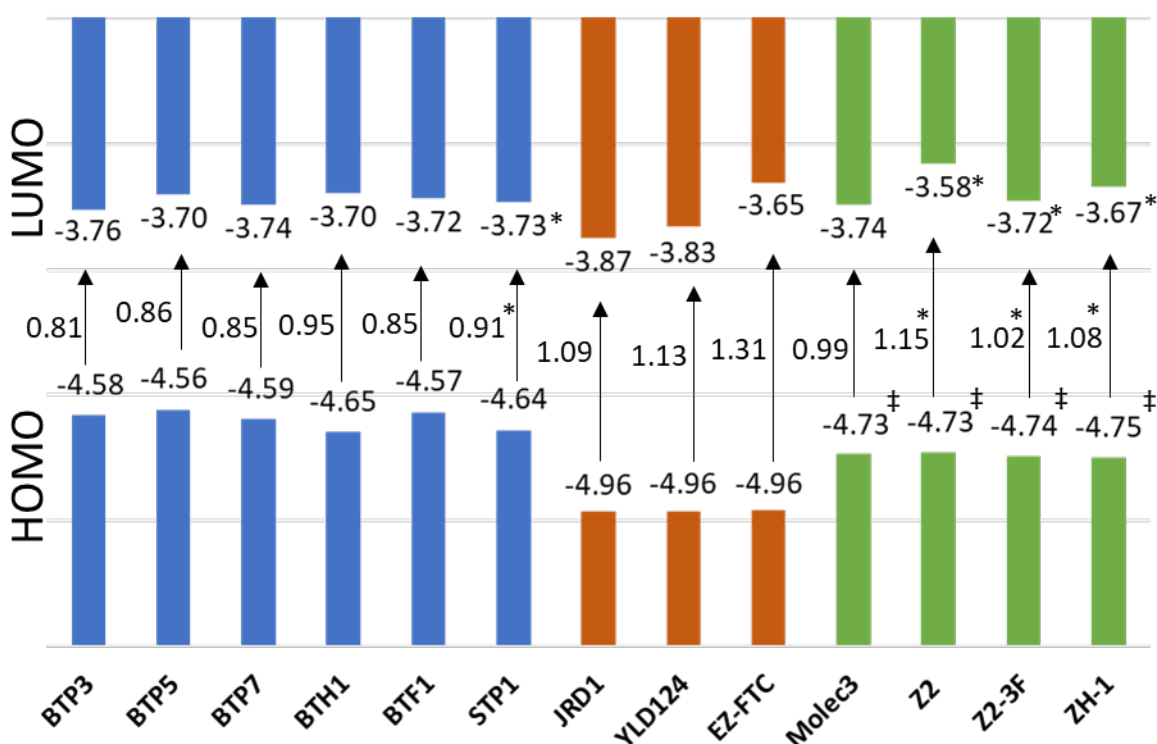


**Figure S29.** HOMO, band gap, and LUMO energy levels (in eV) measured as described above and reported in Table S12. See footnotes to Table S5 for explanations of \* and ‡ symbols.

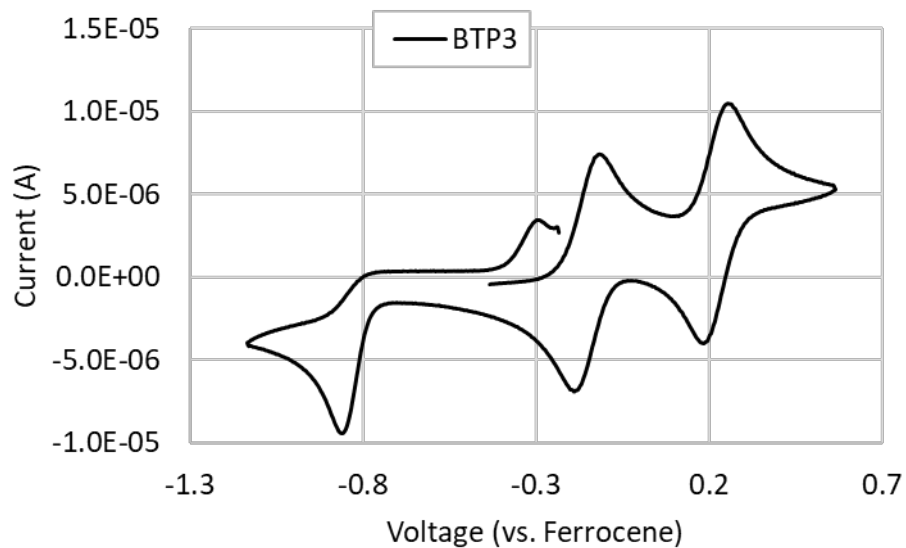


**Figure S30.** Cyclic voltammogram of BTP3 in methylene chloride.

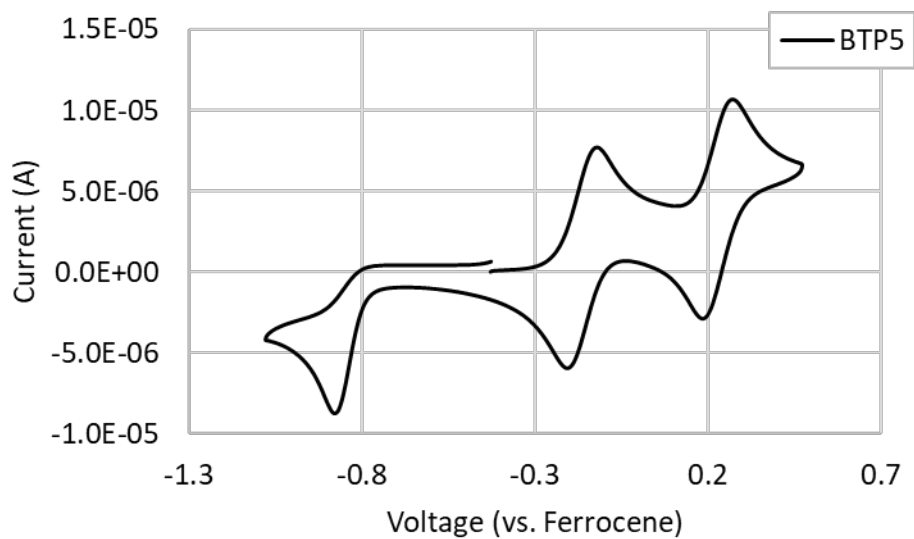


**Figure S31.** Cyclic voltammogram of BTP5 in methylene chloride.

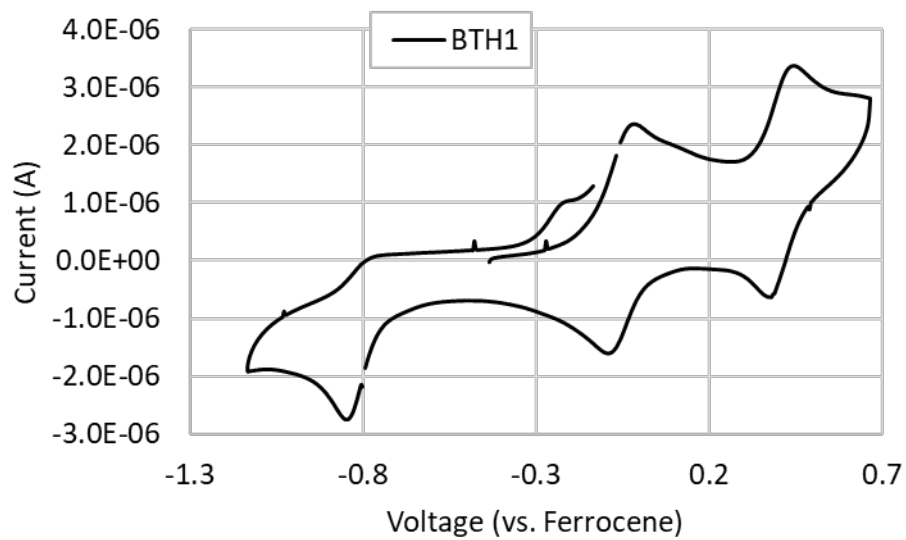


**Figure S32.** Cyclic voltammogram of BTH1 in methylene chloride.

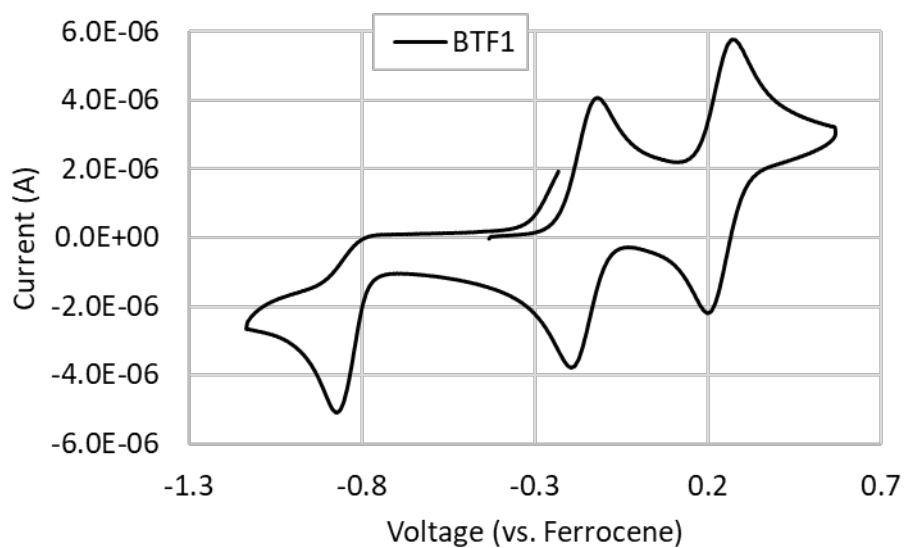


**Figure S33.** Cyclic voltammogram of BTF1 in methylene chloride.

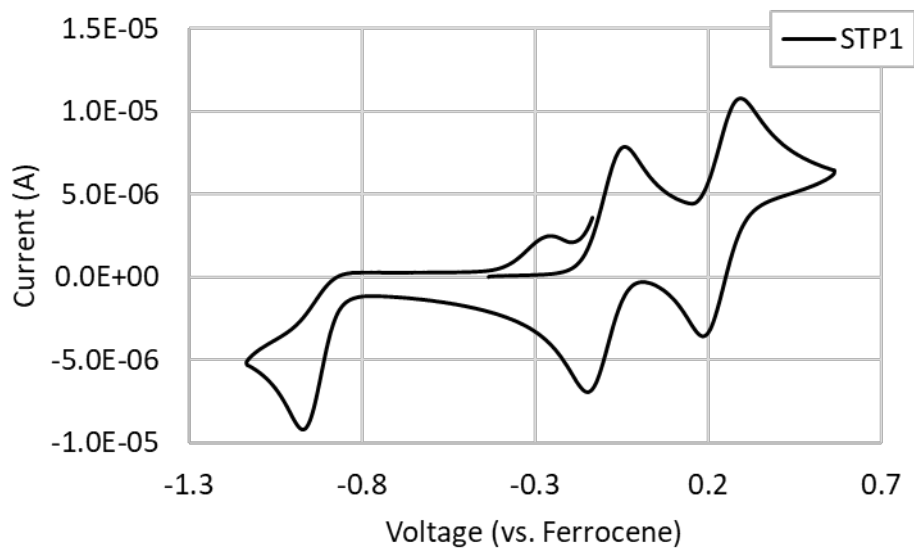


**Figure S34.** Cyclic voltammogram of STP1 in methylene chloride.

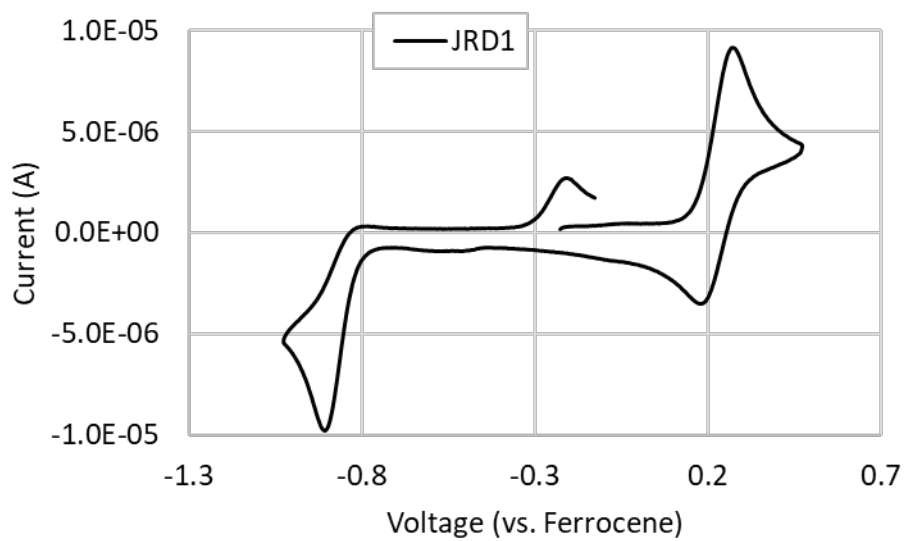


**Figure S35.** Cyclic voltammogram of JRD1 in methylene chloride.

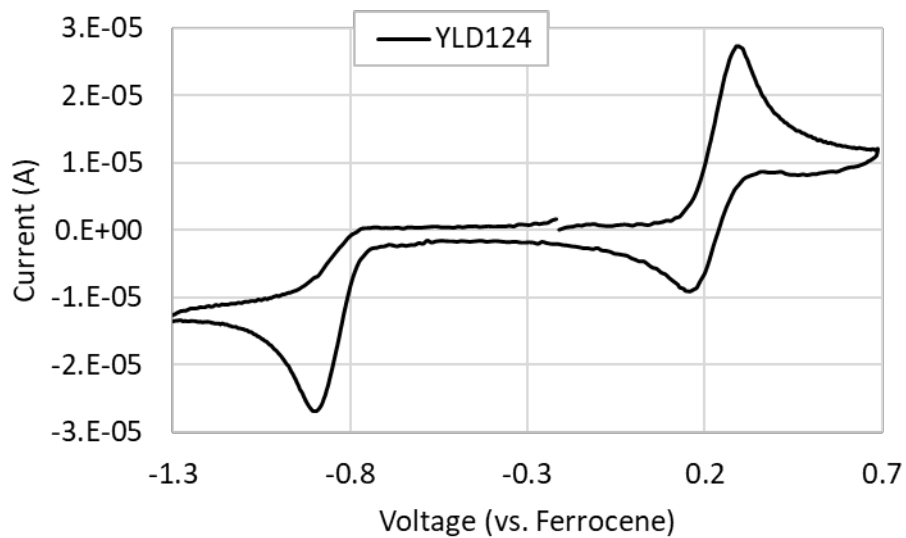


**Figure S36.** Cyclic voltammogram of YLD124 in methylene chloride.

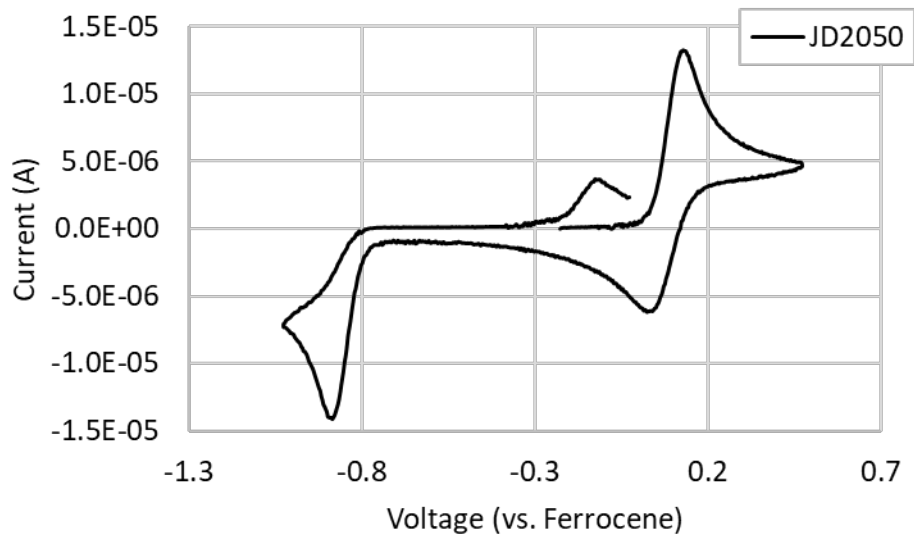


**Figure S37.** Cyclic voltammogram of JAD-B (also known as JD2050) in methylene chloride.

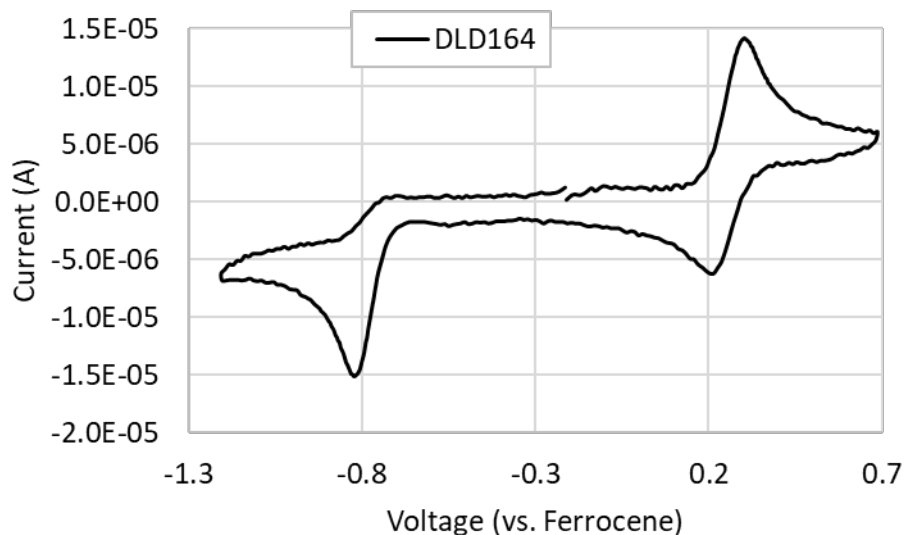


**Figure S38.** Cyclic voltammogram of DLD164 in methylene chloride.

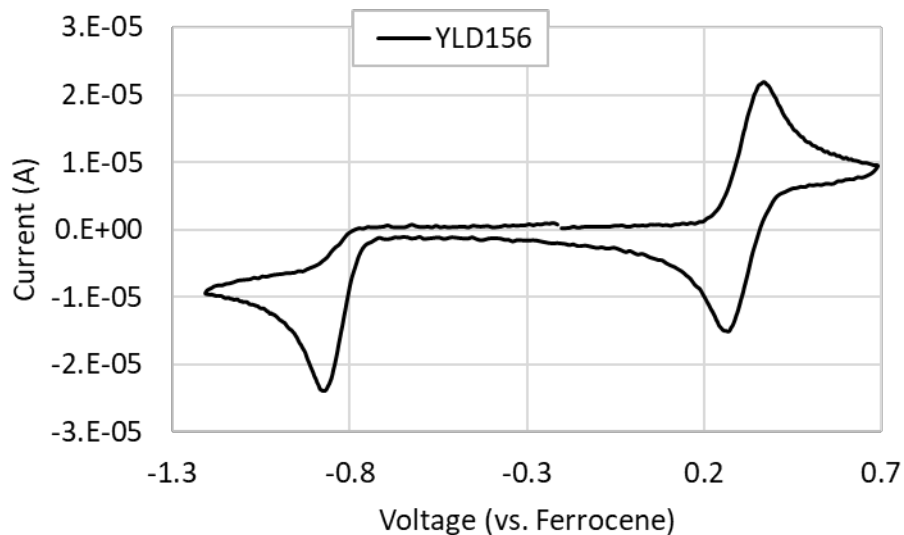


**Figure S39.** Cyclic voltammogram of YLD156 in methylene chloride.

## 11. FTIR Spectroscopy

Sample preparation for FTIR: Chromophore solutions of approximately  $10^{-3}$ – $10^{-4}$  M were prepared (in toluene, tetrahydrofuran, dichloromethane, or acetone), and then a few drops of the solution was sandwiched between two potassium bromide discs. The sample was measured by transmission FTIR (4 or 16 scans). The discs were re-positioned in the beam and re-analyzed or the potassium bromide discs were rubbed to allow some solvent to evaporate (to increase the intensity of chromophore peaks) and re-analyzed. Wavenumbers of the chromophore CN-stretch for each replicate are shown in the Table below. Spectra of solvent blanks and two representative examples of chromophore in solvent (along with an inset showing the CN-stretch region) are shown in the Figures below.

**Table S13.** Wavenumbers ( $\text{cm}^{-1}$ ) of chromophore CN stretch in various solvents.

Sample #	JRD1				BTP7			
	Toluene	THF	$\text{CH}_2\text{Cl}_2$	Acetone	Toluene	THF	$\text{CH}_2\text{Cl}_2$	Acetone
1	2227.75	2227.25	2228.25	2227.75	2229	2226	2227	2210
2	2227.5	2227.75	2228.25	2227.5	2229	2226	2227	2210
3	2227.75		2228	2227.5	2228	2226	2226	2210
4	2229		2228	2225	2228	2226	2226	2210
5	2229		2227.75		2228		2226	
6	2228.5				2228			
Average:	<b>2228.25</b>	<b>2227.5</b>	<b>2228.05</b>	<b>2226.94</b>	<b>2228.33</b>	<b>2226</b>	<b>2226.4</b>	<b>2210</b>
dielectric constant	2.4	7.6	9.1	20.7	2.4	7.6	9.1	20.7
$(\epsilon-1)/(\epsilon+2)$	0.3149	0.6875	0.7297	0.8678	0.3149	0.6875	0.7297	0.8678

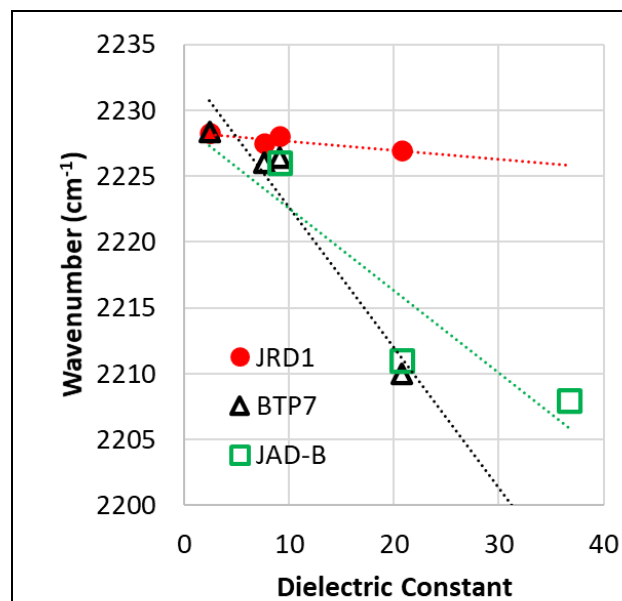


**Figure S40.** Plot of CN stretch wavenumber vs. dielectric constant,  $\epsilon$  (for structure and data on JAD-B, see Figure S18 and reference 24)<sup>24</sup>.

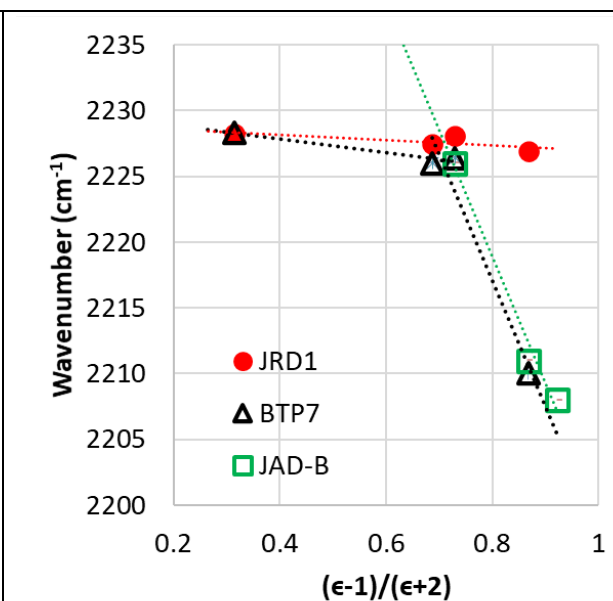


**Figure S41.** Plot of CN stretch wavenumber vs.  $(\epsilon-1)/(\epsilon+2)$  (solvent dielectric on the Reichardt scale).

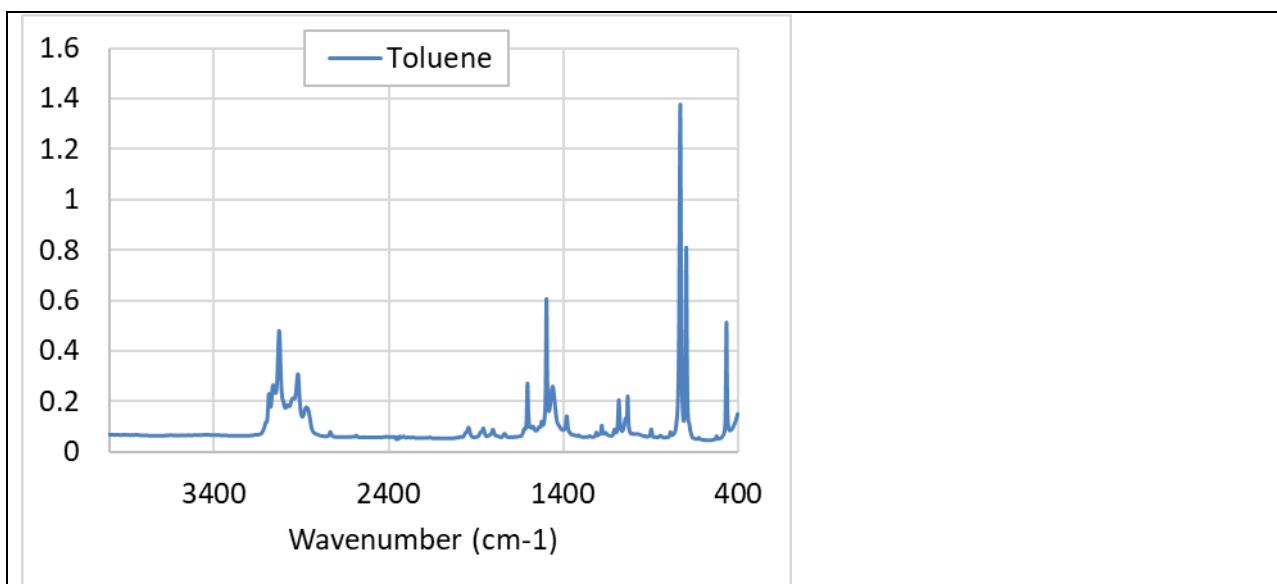


**Figure S42.** FTIR spectrum of toluene.

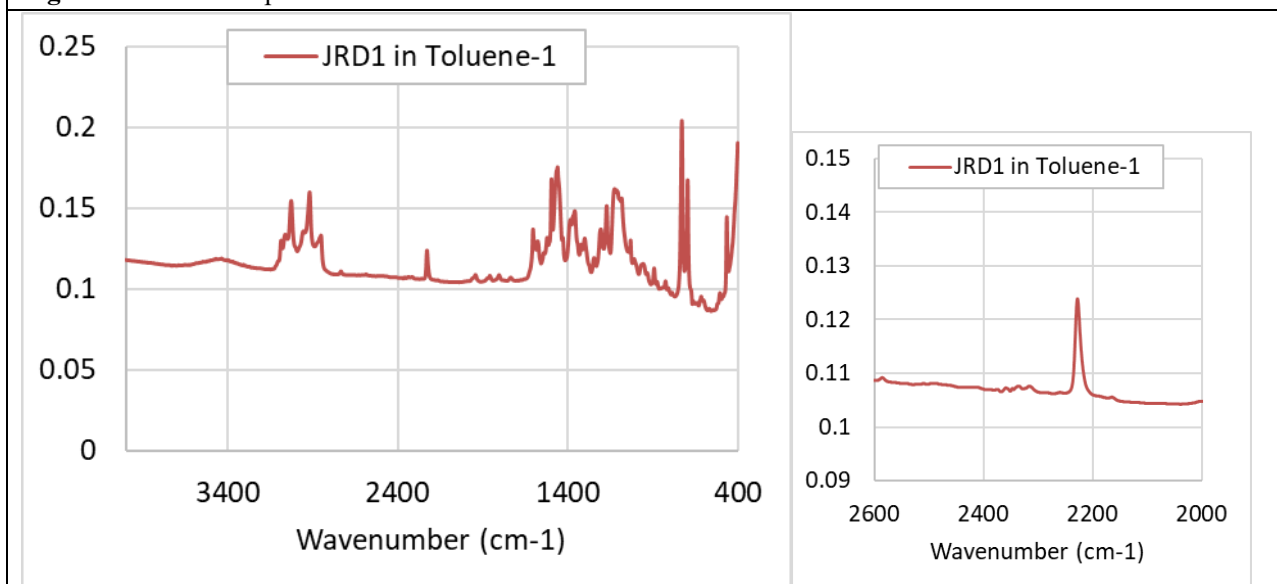


**Figure S43.** FTIR spectrum of JRD1 in toluene at  $\sim 10^{-3}$  M; full spectrum (left), zoomed in (right).

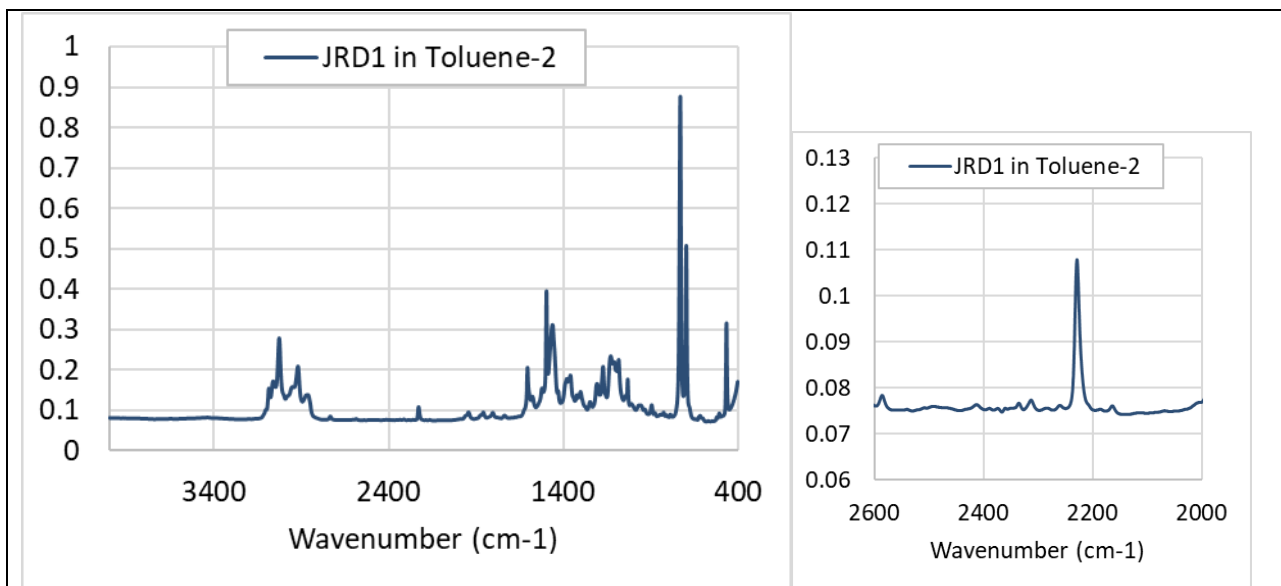


**Figure S44.** FTIR spectrum of JRD1 in toluene at a  $\sim 10^{-4}$  M; full spectrum (left), zoomed in (right).

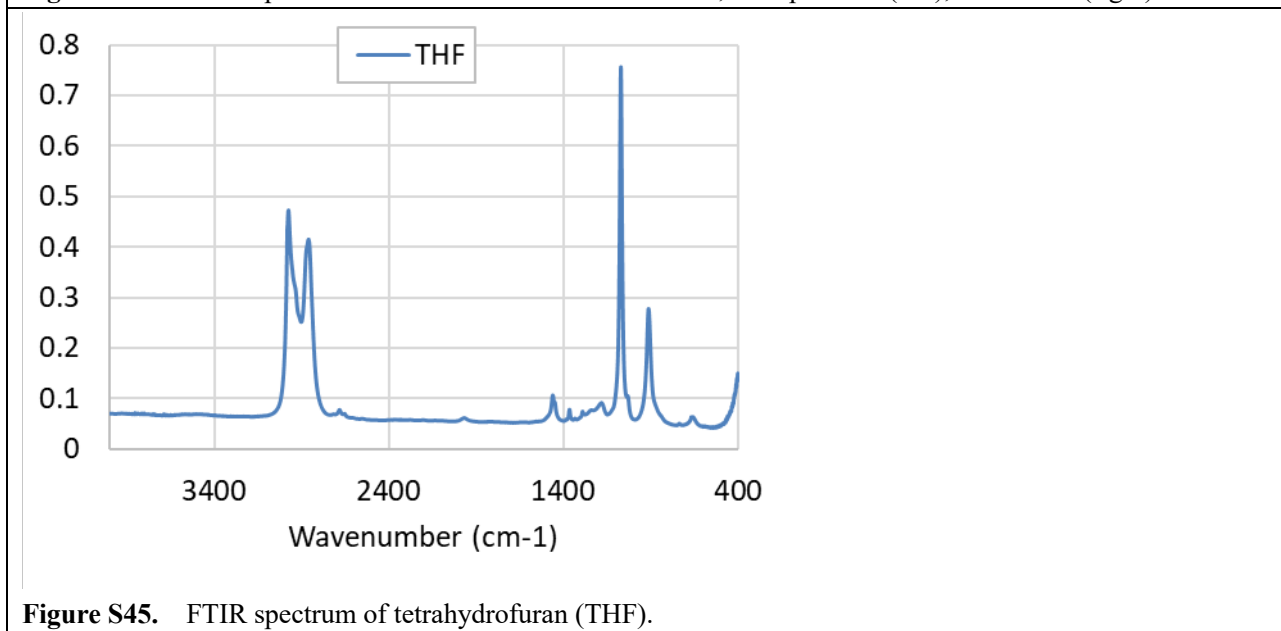


**Figure S45.** FTIR spectrum of tetrahydrofuran (THF).

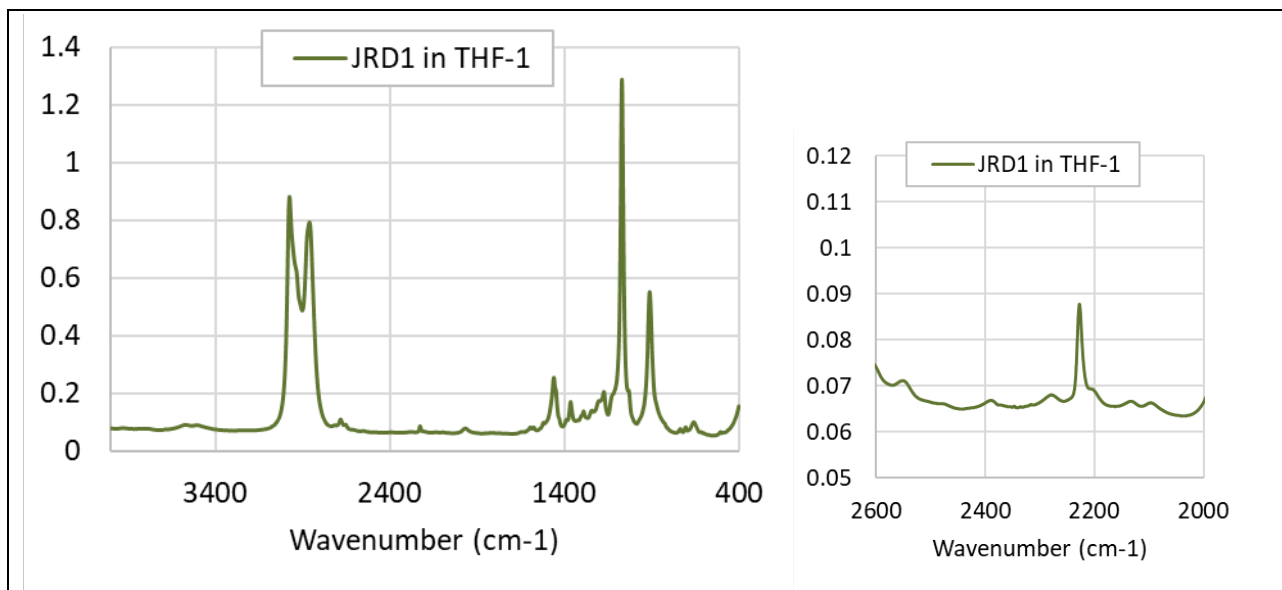


**Figure S46.** FTIR spectrum of JRD1 in THF at  $\sim 10^{-4}$  M; full spectrum (left), zoomed in (right).

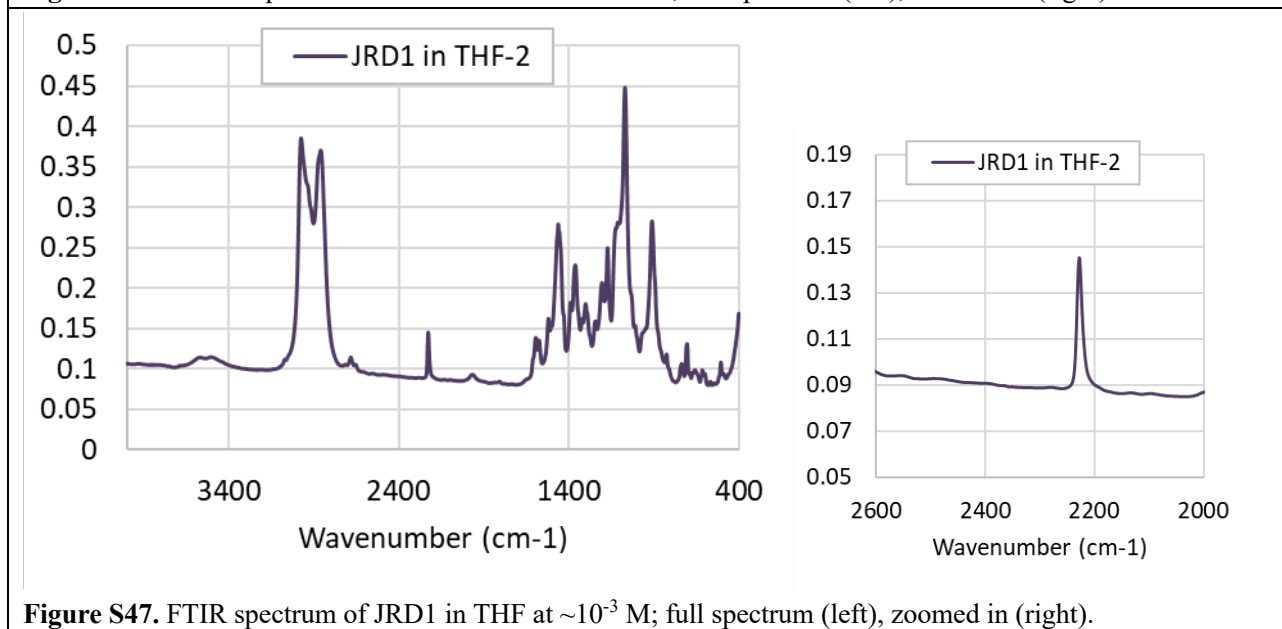


**Figure S47.** FTIR spectrum of JRD1 in THF at  $\sim 10^{-3}$  M; full spectrum (left), zoomed in (right).

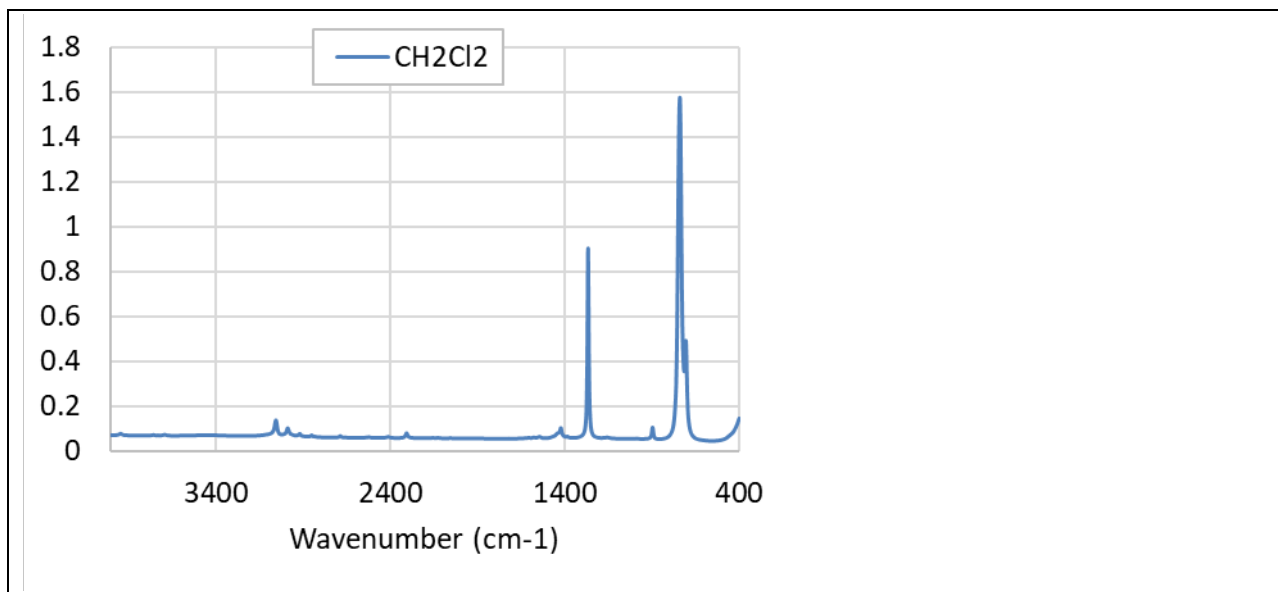


**Figure S48.** FTIR spectrum of dichloromethane (CH<sub>2</sub>Cl<sub>2</sub>).

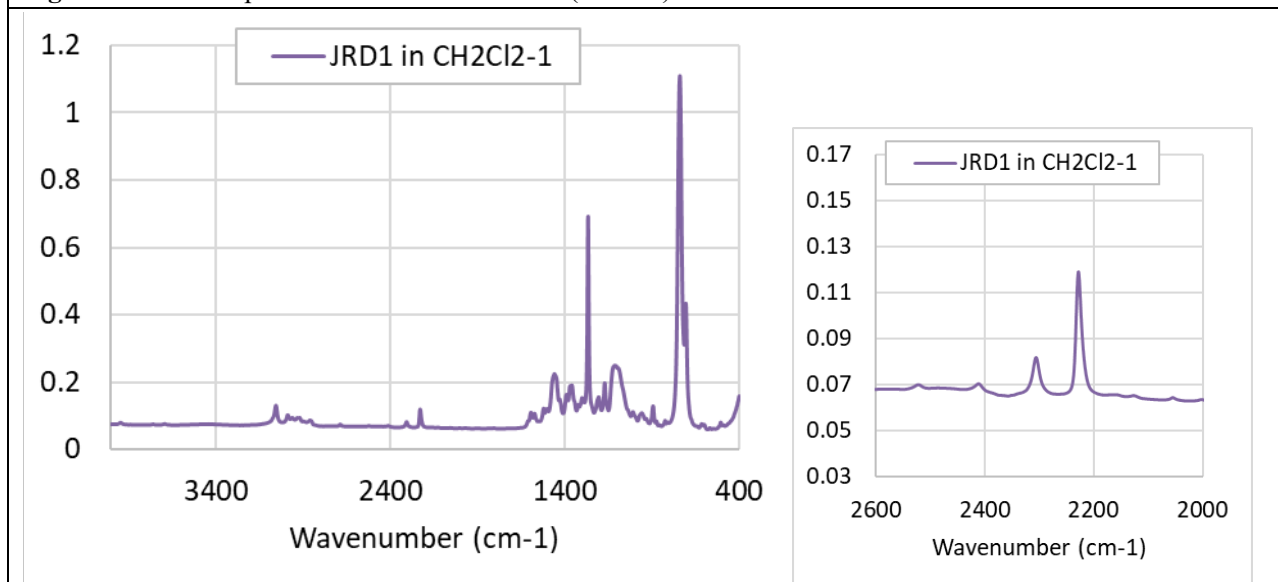


**Figure S49.** FTIR spectrum of JRD1 in CH<sub>2</sub>Cl<sub>2</sub> at ~10<sup>-4</sup> M; full spectrum (left), zoomed in (right). The small peak at 2306 cm<sup>-1</sup> corresponds to solvent.

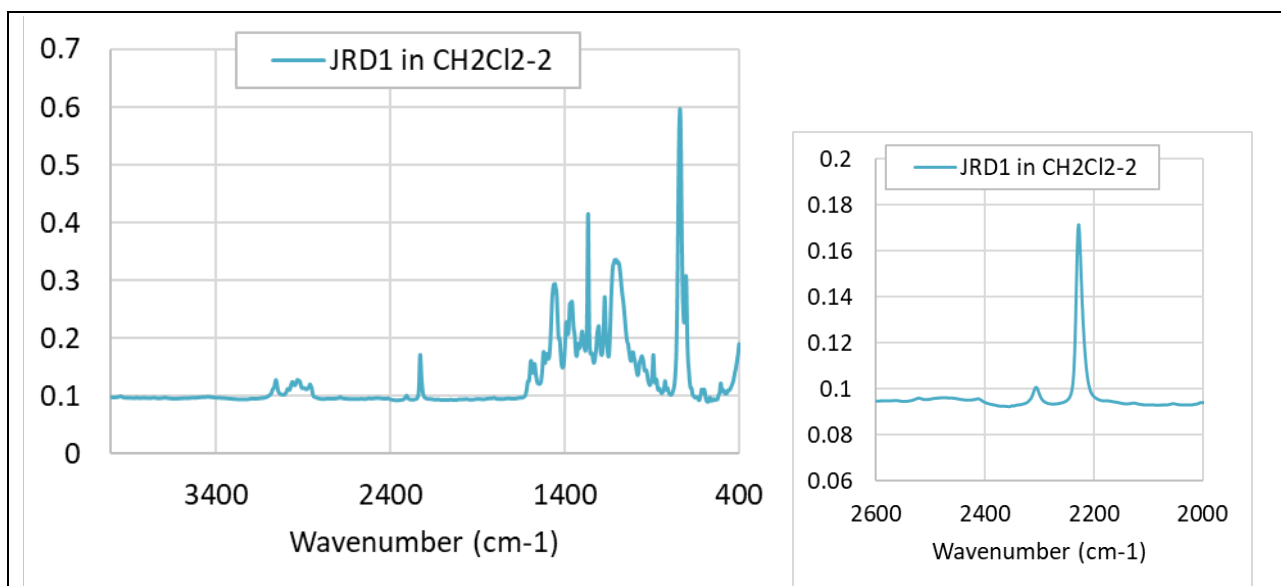


**Figure S50.** FTIR spectrum of JRD1 in CH<sub>2</sub>Cl<sub>2</sub> at  $\sim 10^{-3}$  M, full spectrum (left), zoomed in (right). The small peak at 2306 cm<sup>-1</sup> corresponds to solvent.

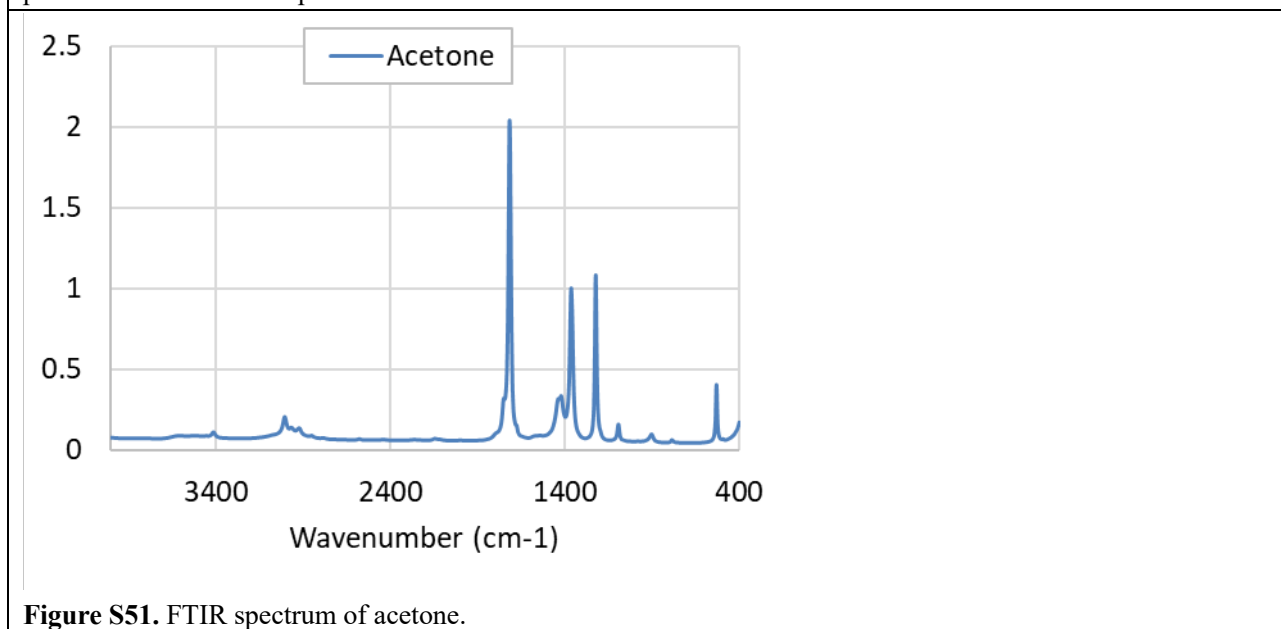


**Figure S51.** FTIR spectrum of acetone.

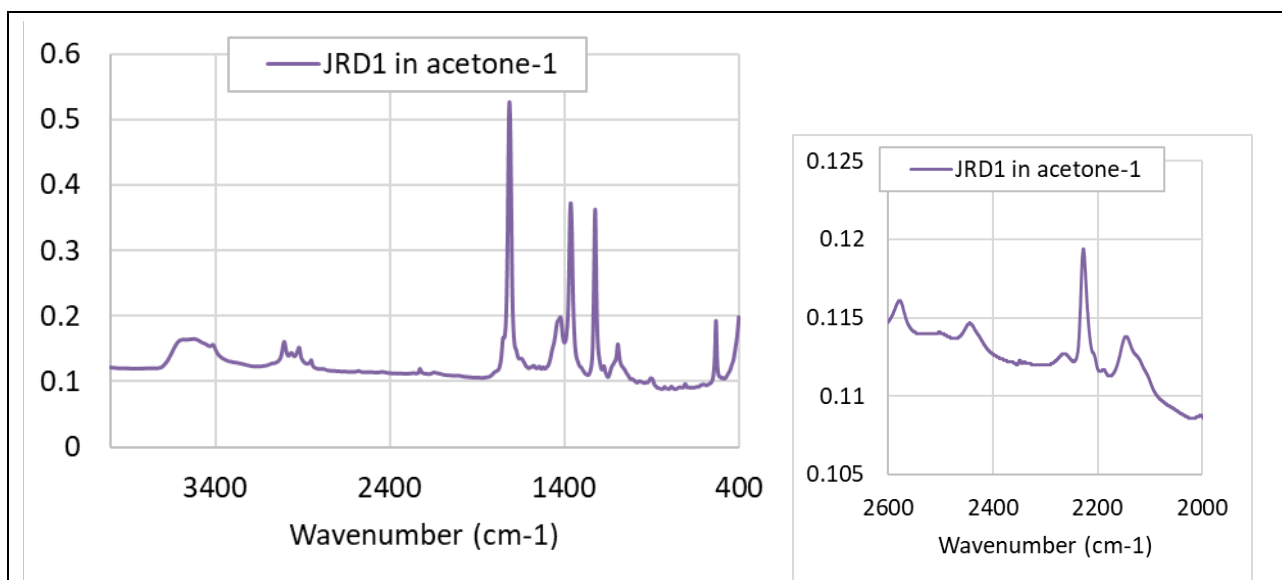


**Figure S52.** FTIR spectrum of JRD1 in acetone at  $10^{-4}$  M; full spectrum (left), zoomed in (right). All of the peaks besides the main one at  $\sim 2227$  cm<sup>-1</sup> correspond to solvent.

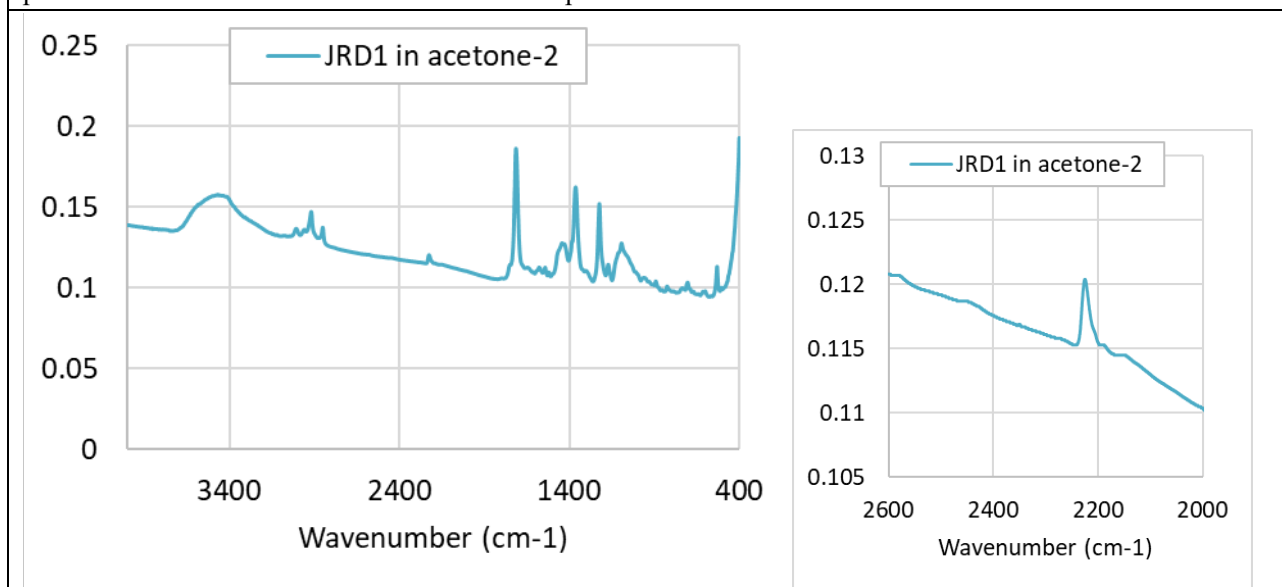


**Figure S53.** FTIR spectrum of JRD1 in acetone at  $\sim 10^{-4}$  M; full spectrum (left), zoomed in (right).

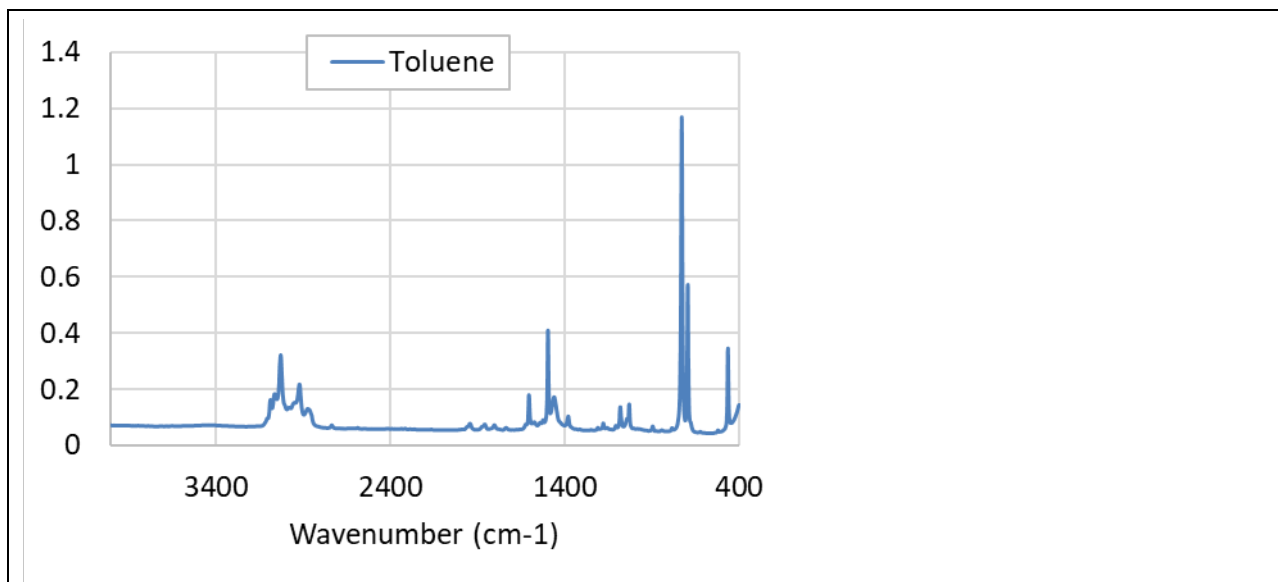


Figure S54. FTIR spectrum of toluene.

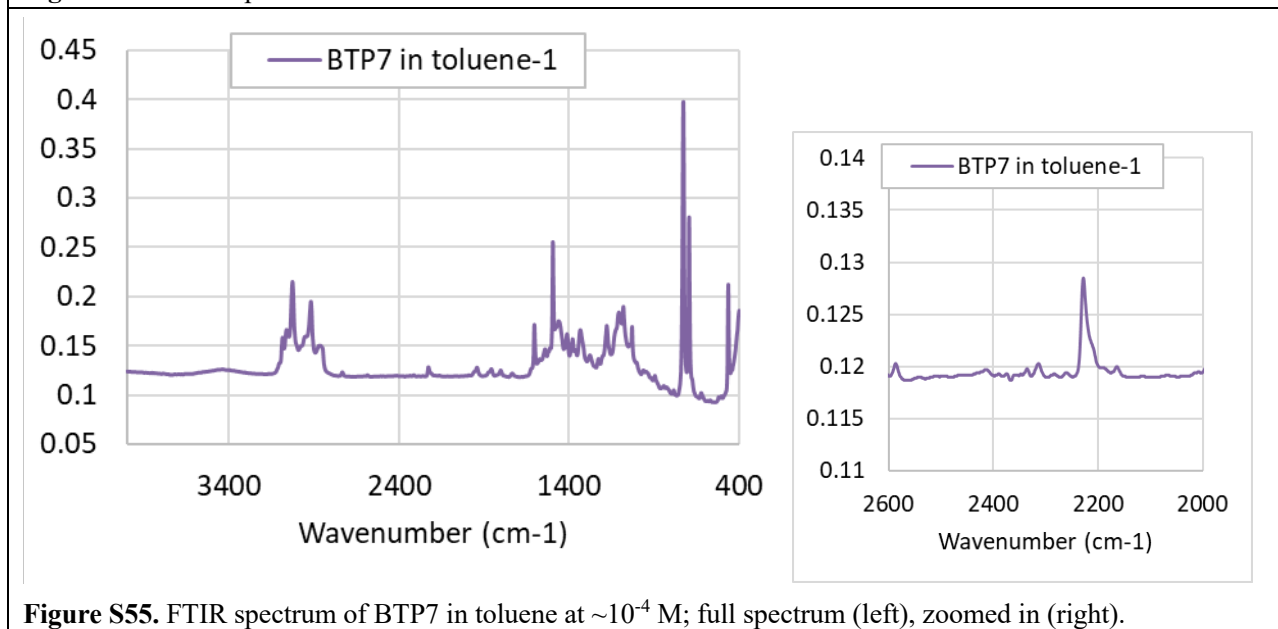
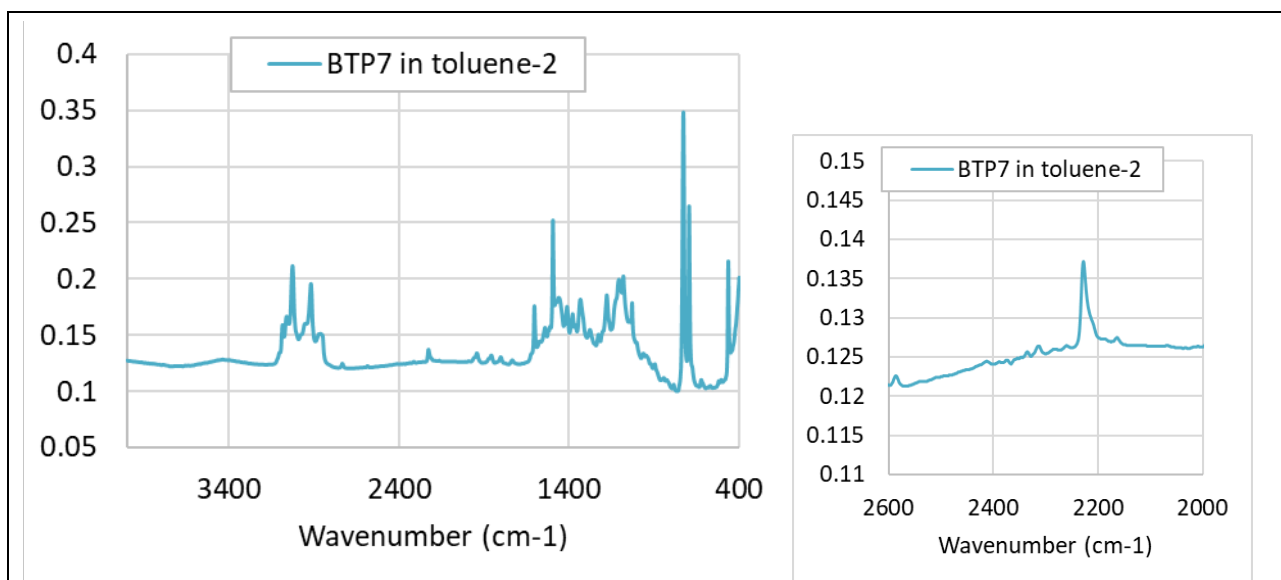
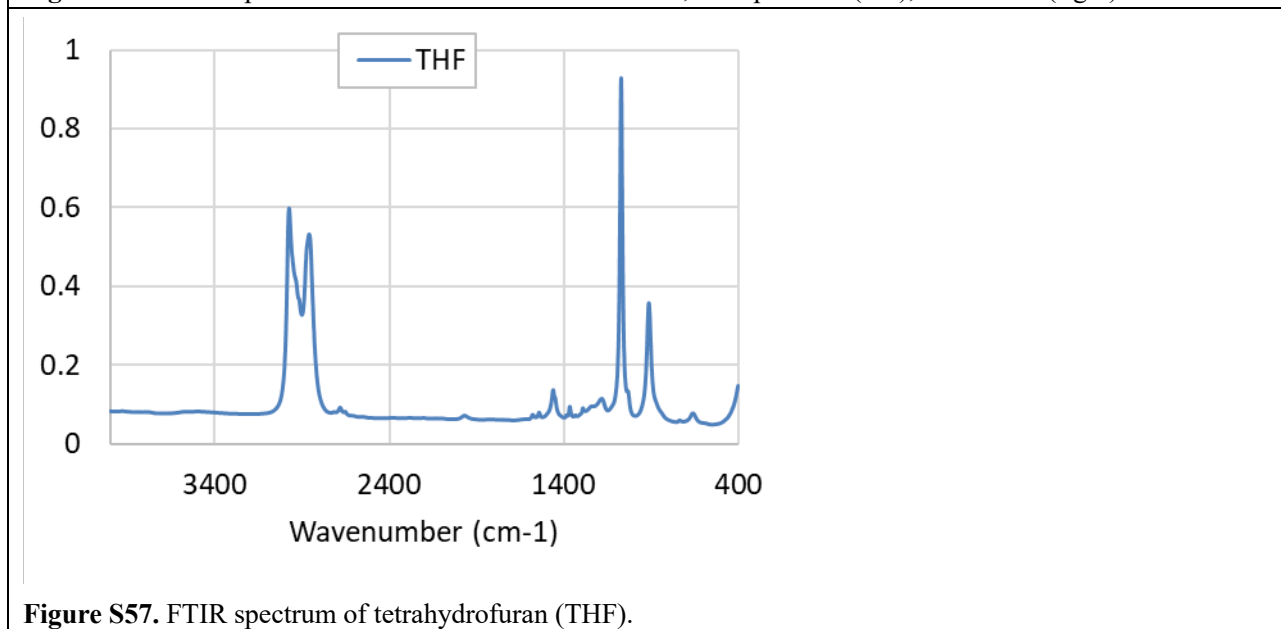


Figure S55. FTIR spectrum of BTP7 in toluene at  $\sim 10^{-4}$  M; full spectrum (left), zoomed in (right).



**Figure S56.** FTIR spectrum of BTP7 in toluene at  $\sim 10^{-4}$  M; full spectrum (left), zoomed in (right).



**Figure S57.** FTIR spectrum of tetrahydrofuran (THF).

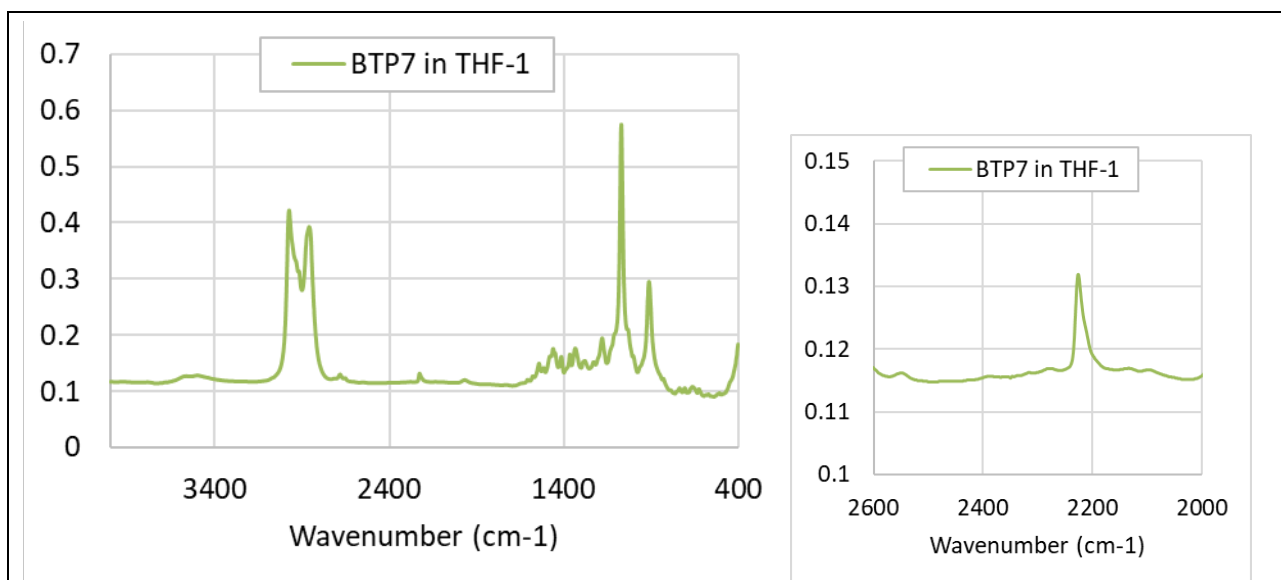


**Figure S58.** FTIR spectrum of BTP7 in THF at  $\sim 10^{-4}$  M ; full spectrum (left), zoomed in (right).

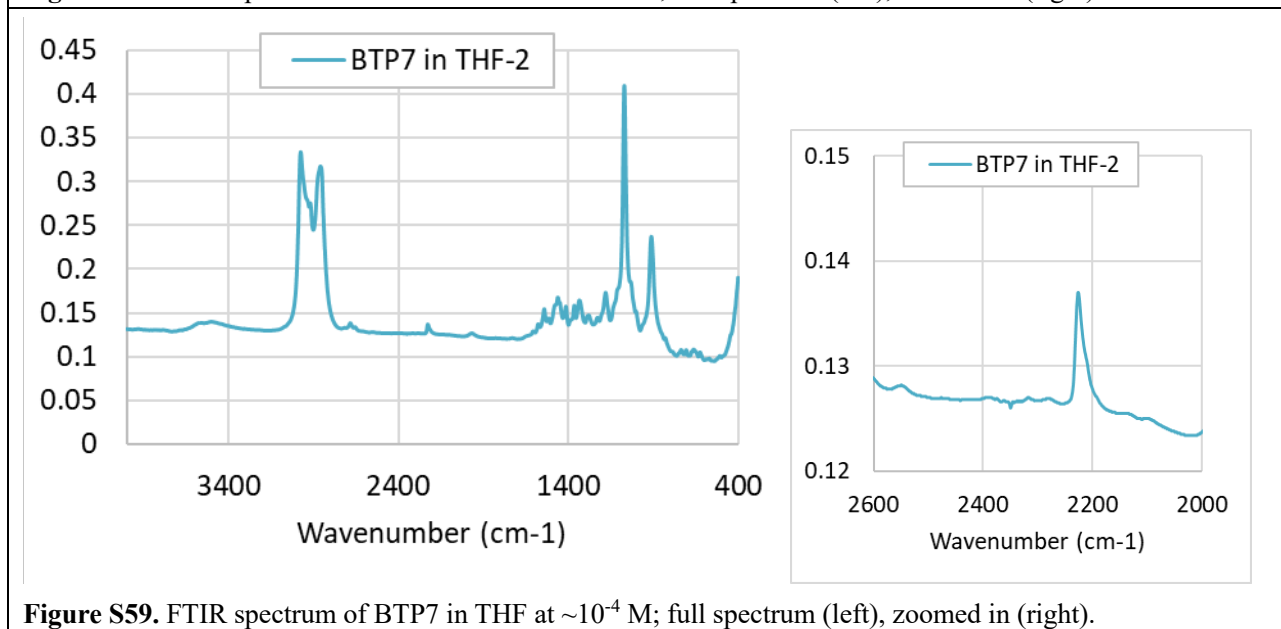


**Figure S59.** FTIR spectrum of BTP7 in THF at  $\sim 10^{-4}$  M; full spectrum (left), zoomed in (right).

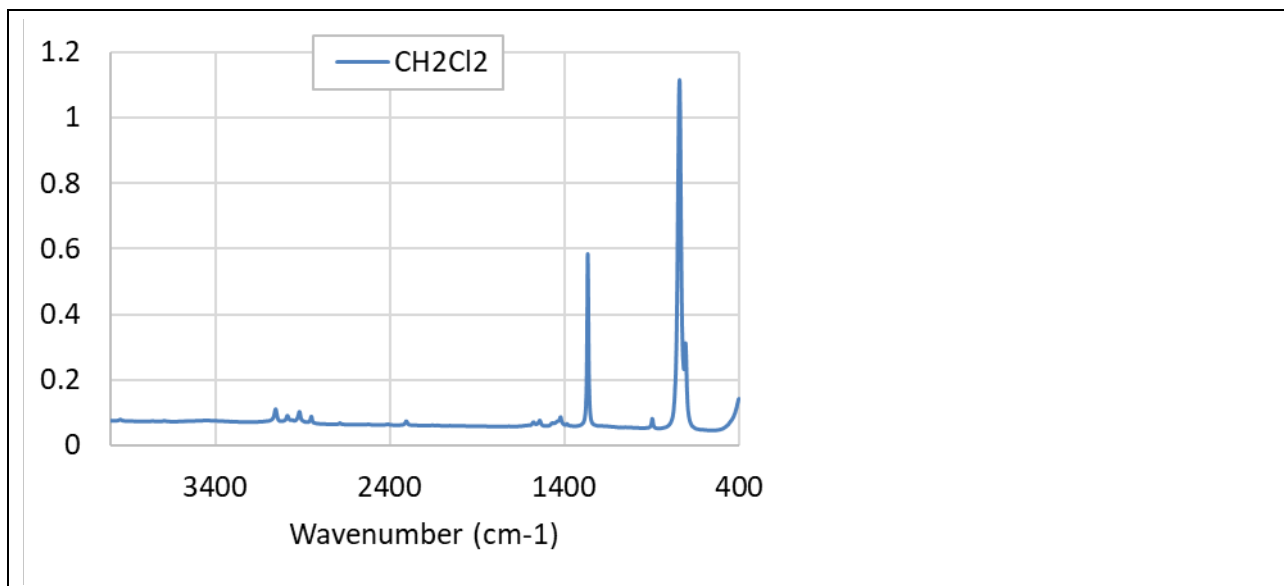


**Figure S60.** FTIR spectrum of dichloromethane ( $\text{CH}_2\text{Cl}_2$ ).

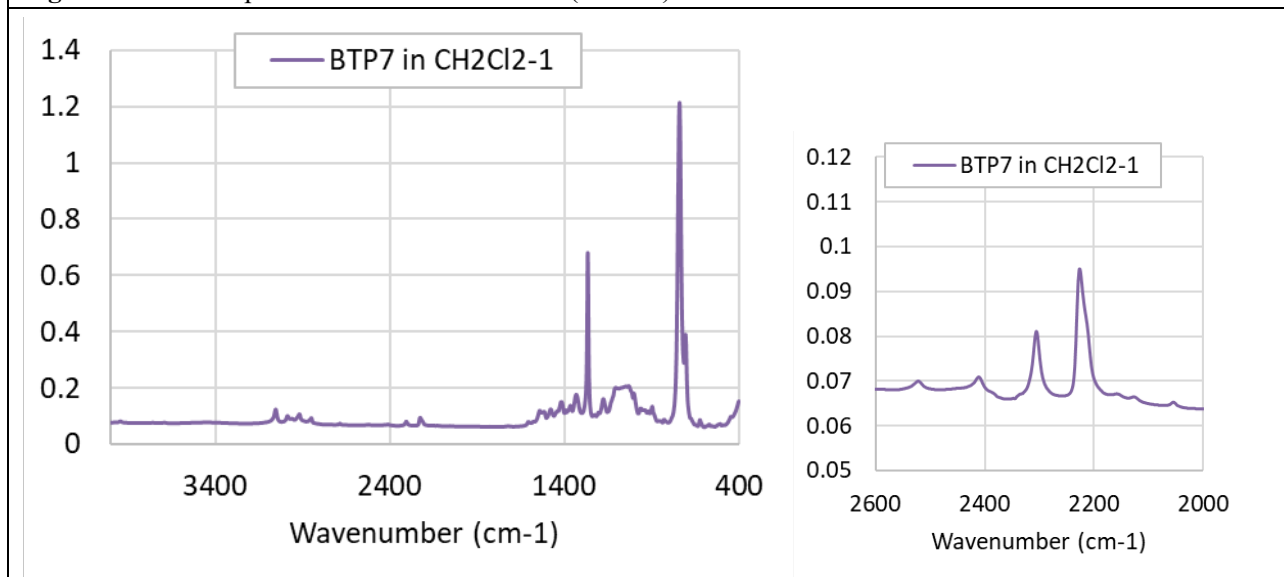


**Figure S61.** FTIR spectrum of BTP7 in  $\text{CH}_2\text{Cl}_2$  at  $\sim 10^{-4}$  M; full spectrum (left), zoomed in (right). The smaller peak at  $2306\text{ cm}^{-1}$  corresponds to solvent.

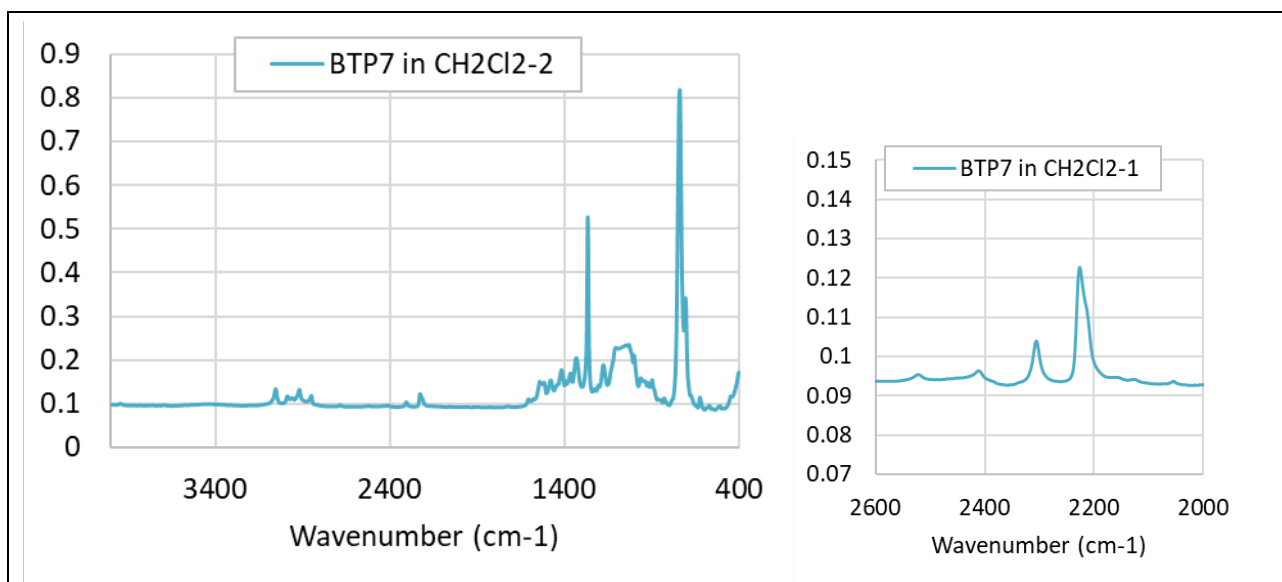


**Figure S62.** FTIR spectrum of BTP7 in CH<sub>2</sub>Cl<sub>2</sub>  $\sim 10^{-4}$  M; full spectrum (left), zoomed in (right). The smaller peak at 2306 cm<sup>-1</sup> corresponds to solvent.

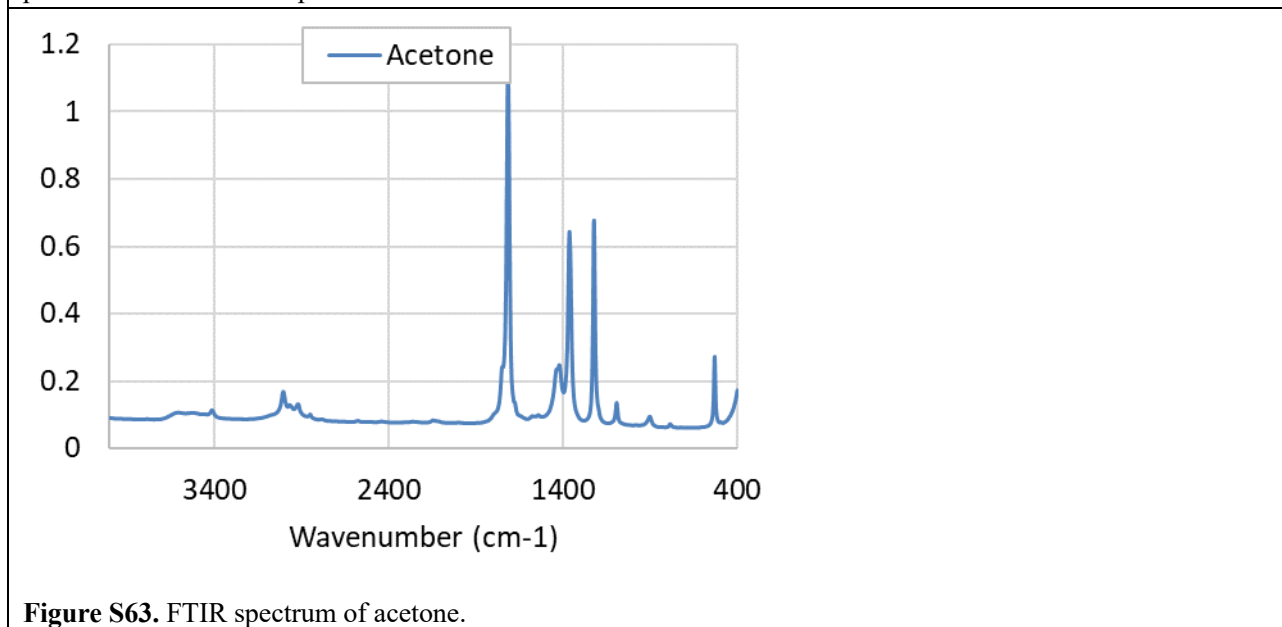


**Figure S63.** FTIR spectrum of acetone.

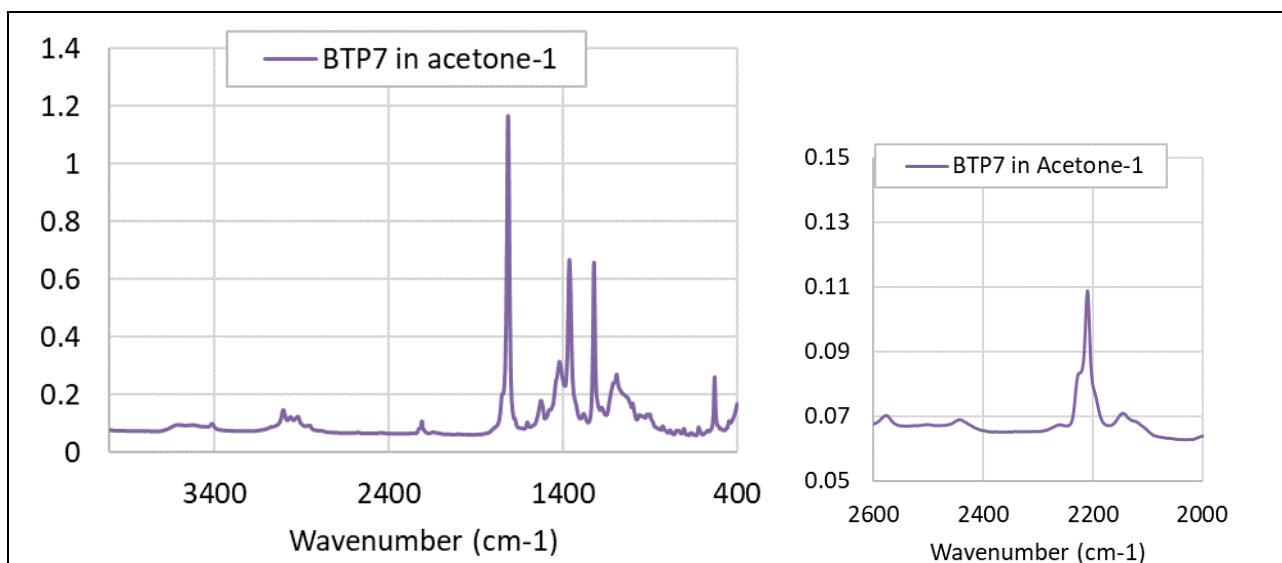


**Figure S64.** FTIR spectrum of BTP7 in acetone at  $\sim 10^{-4}$  M; full spectrum (left), zoomed in (right).

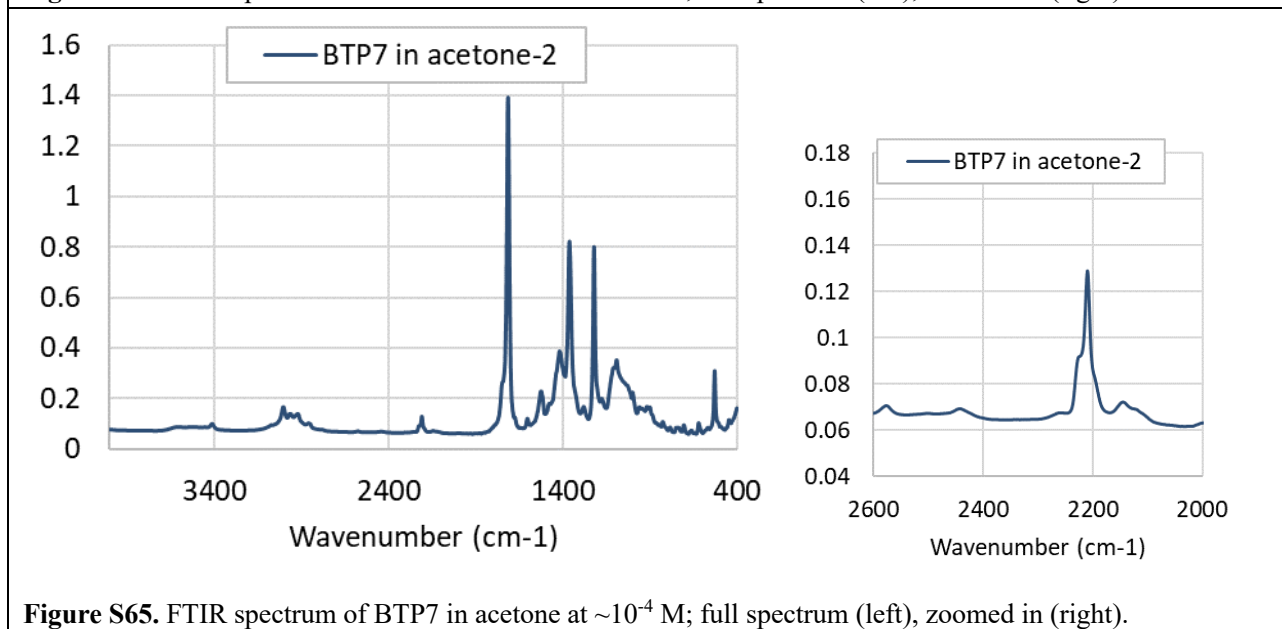


**Figure S65.** FTIR spectrum of BTP7 in acetone at  $\sim 10^{-4}$  M; full spectrum (left), zoomed in (right).

A similar comparison was performed for DFT predictions of the infrared spectra for STP1 and BTP3 in different solvents. A clear qualitative shift was observed for STP1 (Figure S66, left), while a lesser shift was observed for BTP3 (Figure S66, right). The discrepancy between the computational and experimental BTP results for IR solvatochromism, along with solvatochromism-related shifts in hyperpolarizability, likely results from an underestimation of the reaction field strength in the calculations; however, the STP1 results clearly show two distinct families of peaks for NGS and ZGS that are consistent with the hyperpolarizability results.

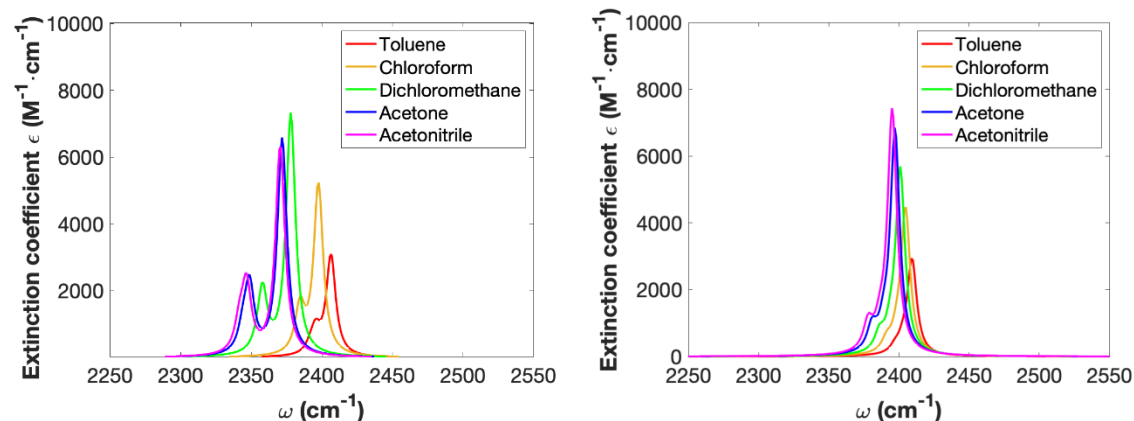


**Figure S66.** Computational IR comparison for STP1 (left) and BTP3 (right).

## References

- Bhunias, S.; Kumar, S. V.; Ma, D. N, N' -Bisoxalamides Enhance the Catalytic Activity in Cu-Catalyzed Coupling of (Hetero)Aryl Bromides with Anilines and Secondary Amines. *J. Org. Chem.* **2017**, *82* (23), 12603-12612.
- Pratt, D. A.; DiLabio, G. A.; Valgimigli, L.; Pedulli, G. F.; Ingold, K. U. Substituent Effects on the Bond Dissociation Enthalpies of Aromatic Amines. *J. Am. Chem. Soc.* **2002**, *124* (37), 11085-11092.
- Teng, C. C.; Man, H. T. Simple Reflection Technique for Measuring the Electrooptic Coefficient of Poled Polymers. *Appl. Phys. Lett.* **1990**, *56* (18), 1734-1736.
- Shuto, Y.; Amano, M. Reflection measurement technique of electro - optic coefficients in lithium niobate crystals and poled polymer films. *J. Appl. Phys.* **1995**, *77* (9), 4632-4638.
- Jin, W.; Johnston, P. V.; Elder, D. L.; Tillack, A. F.; Olbricht, B. C.; Song, J.; Reid, P. J.; Xu, R.; Robinson, B. H.; Dalton, L. R. Benzocyclobutene barrier layer for suppressing conductance in nonlinear optical devices during electric field poling. *Appl. Phys. Lett.* **2014**, *104* (104), 243304-243304-5.
- Cheng, Y.-J.; Luo, J.; Hau, S.; Bale, D. H.; Kim, T.-D.; Shi, Z.; Lao, D. B.; Tucker, N. M.; Tian, Y.; Dalton, L. R.; Reid, P. J.; Jen, A. K.-Y. Large Electro-optic Activity and Enhanced Thermal Stability from Diarylaminophenyl-Containing High- $\beta$  Nonlinear Optical Chromophores. *Chem. Mater.* **2007**, *19* (5), 1154-1163.
- Cheng, Y. J.; Luo, J. D.; Huang, S.; Zhou, X. H.; Shi, Z. W.; Kim, T. D.; Bale, D. H.; Takahashi, S.; Yick, A.; Polishak, B. M.; Jang, S. H.; Dalton, L. R.; Reid, P. J.; Steier, W. H.; Jen, A. K.-Y. Donor-acceptor thiolated polyenic chromophores exhibiting large optical nonlinearity and excellent photostability. *Chem. Mater.* **2008**, *20* (15), 5047-5054.
- Piao, X.; Zhang, X.; Inoue, S.; Yokoyama, S.; Aoki, I.; Miki, H.; Otomo, A.; Tazawa, H. Enhancement of electro-optic activity by introduction of a benzyloxy group to conventional donor- $\pi$ -acceptor molecules. *Org. Electron.* **2011**, *12* (6), 1093-1097.
- Luo, J.; Cheng, Y.-J.; Kim, T.-D.; Hau, S.; Jang, S.-H.; Shi, Z.; Zhou, X.-H.; Jen, A. K.-Y. Facile synthesis of highly efficient phenyltetraene-based nonlinear optical chromophores for electrooptics. *Org. Lett.* **2006**, *8* (7), 1387-1390.
- Kim, T. D.; Luo, J. D.; Cheng, Y. J.; Shi, Z. W.; Hau, S.; Jang, S. H.; Zhou, X. H.; Tian, Y.; Polishak, B.; Huang, S.; Ma, H.; Dalton, L. R.; Jen, A. K.-Y. Binary chromophore systems in nonlinear optical dendrimers and polymers for large electrooptic activities. *J. Phys. Chem. C* **2008**, *112* (21), 8091-8098.
- Zhou, X.-H.; Luo, J.; Davies, J. A.; Huang, S.; Jen, A. K.-Y. Push-pull tetraene chromophores derived from dialkylaminophenyl, tetrahydroquinolinyl and julolidinyl moieties: optimization of second-order optical nonlinearity

- by fine-tuning the strength of electron-donating groups. *J. Mater. Chem.* **2012**, *22* (32), 16390-16398.
12. Zhang, H.; Huo, F.; Liu, F.; Chen, Z.; Liu, J.; Bo, S.; Zhen, Z.; Qiu, L. Synthesis and characterization of two novel second-order nonlinear optical chromophores based on julolidine donors with excellent electro-optic activity. *RSC Adv.* **2016**, *6* (102), 99743-99751.
  13. Campo, J.; Desmet, F.; Wenseleers, W.; Goovaerts, E. Highly sensitive setup for tunable wavelength hyper-Rayleigh scattering with parallel detection and calibration data for various solvents. *Opt. Express.* **2009**, *17* (6), 4587-4604.
  14. Campo, J.; Wenseleers, W.; Hales, J. M.; Makarov, N. S.; Perry, J. W. Practical Model for First Hyperpolarizability Dispersion Accounting for Both Homogeneous and Inhomogeneous Broadening Effects. *J. Phys. Chem. Lett.* **2012**, *3* (16), 2248-52.
  15. Xu, H. J.; Liu, F. G.; Elder, D. L.; Johnson, L. E.; de Coene, Y.; Clays, K.; Robinson, B. H.; Dalton, L. R. Ultrahigh Electro-Optic Coefficients, High Index of Refraction, and Long-Term Stability from Diels-Alder Cross-Linkable Binary Molecular Glasses. *Chem. Mater.* **2020**, *32* (4), 1408-1421.
  16. Kaatz, P.; Donley, E. A.; Shelton, D. P. A comparison of molecular hyperpolarizabilities from gas and liquid phase measurements. *J. Chem. Phys.* **1998**, *108* (3), 849-856.
  17. Bale, D. H. *Nonlinear optical materials characterization studies employing photostability, hyper-Rayleigh scattering, and electric field induced second harmonic generation techniques*. Thesis (Ph. D.)--University of Washington: 2008.
  18. Budy, S. M.; Suresh, S.; Spraul, B. K.; Smith, D. W. High-temperature chromophores and perfluorocyclobutyl copolymers for electro-optic applications. *J. Phys. Chem. C* **2008**, *112* (21), 8099-8104.
  19. Kim, T. D.; Kang, J. W.; Luo, J. D.; Jang, S. H.; Ka, J. W.; Tucker, N.; Benedict, J. B.; Dalton, L. R.; Gray, T.; Overney, R. M.; Park, D. H.; Herman, W. N.; Jen, A. K.-Y. Ultralarge and thermally stable electro-optic activities from supramolecular self-assembled molecular glasses. *J. Am. Chem. Soc.* **2007**, *129* (3), 488-489.
  20. Meyers, F.; Marder, S. R.; Pierce, B. M.; Bredas, J. L. Electric-Field Modulated Nonlinear-Optical Properties of Donor-Acceptor Polyenes - Sum-over-States Investigation of the Relationship between Molecular Polarizabilities ( $\alpha$ ,  $\beta$ , and  $\gamma$ ) and Bond-Length Alternation. *J. Am. Chem. Soc.* **1994**, *116* (23), 10703-10714.
  21. Frisch, M.; Trucks, G.; Schlegel, H. B.; Scuseria, G. E.; Robb, M. A.; Cheeseman, J. R.; Scalmani, G.; Barone, V.; Mennucci, B.; Petersson, G. gaussian 09, Revision d. 01, Gaussian. Inc., Wallingford CT **2009**, 201.
  22. Zhao, Y.; Truhlar, D. G. The M06 suite of density functionals for main group thermochemistry, thermochemical kinetics, noncovalent interactions, excited states, and transition elements: two new functionals and systematic testing of four M06-class functionals and 12 other functionals. *Theor. Chem. Acc.* **2008**, *120* (1), 215-241.
  23. Johnson, L. E.; Dalton, L. R.; Robinson, B. H. Optimizing calculations of electronic excitations and relative hyperpolarizabilities of electrooptic chromophores. *Acc. Chem. Res.* **2014**, *47* (11), 3258-65.